Fatigue Properties of Nickel-Base Superalloy at Elevated Temperatures

（Ｎｉ基超合金の高温疲労特性に関する研究）

Qiang CHEN

Kagoshima University

December 20, 1999

Fatigue Properties of Nickel-Base Superalloy at Elevated Temperatures

Qiang CHEN

要　　旨

本論文は「Fatigue Properties of Nickel-base Superalloy at Elevated Temperatures」（Ni基超合金の高温疲労特性に関する研究）と題し，７章から構成されている．

第１章では，Ni基超合金の特徴，分類，そして優れた各種特性に関連した広範な用途と実用的重要性について記述している．そして，これまでの本合金の機械的性質に関する研究の成果特に疲労特性に関する現状を説明し，材料開発と強度設計さらに保守の点から本研究の位置付けと目的を明確にしている．

第２章では，室温大気中で回転曲げ疲労試験を行い，本合金の高温疲労特性を検討する際の基礎となる室温での疲労特性について調べ，本合金の平滑材の疲労限度は微小き裂の伝ぱ限界で決まること，有限寿命域においては全寿命のほとんどが１mm 以下の微小き裂の伝ぱ寿命で占められ，疲労限度だけでなく破断する際も微小き裂の伝ぱが重要であることを指摘している．

第３章では，まず本合金の疲労強度が高温環境下で上昇する特異な現象を示すことを明らかにし，高温下における微小き裂の発生及びその伝ぱの詳細な観察を通じて，高温環境の影響を素材の機械的性質の変化と高温酸化の点から検討し，そのメカニズムの解明を行っている．

第４章では，本合金のき裂伝ぱ抵抗の温度依存性について調べ，温度の上昇に伴いき裂伝ぱ抵抗は低下することを明らかにしている．また，高温での微小き裂伝ぱの評価さらに疲労寿命の予測に微小き裂伝ぱ則が有効であることを示している．

第５章は，切欠材の疲労限度に及ぼす温度の影響を，き裂発生限界に対する疲労限度とき裂伝ぱ限界に対する疲労限度にわけて調べたものであり，高温における本合金の切欠感度は線形切欠力学で評価できることを明らかにしている．

第６章では，本合金は難削材の一つであること，そのような難削材に対してＣＢＮ加工が有効であること，さらに実際に機械加工のままで使用されることを考慮し，疲労強度特に高温での疲労強度に及ぼすＣＢＮ研削加工の影響を硬さと材質の変化，表面粗さおよび残留応力の点から検討している．

第７章では，以上の各章で得られた結論を要約している．

To people whose love helps me.

CONTENTS

		Page
Chapter 1	**Introduction**	1
1.1	A Brief Knowledge of Nickel-Base Superalloys	1
1.2	A Review of the Previous Studies on Inconel 718	2
1.3	Objectives	4
1.4	Contents of the thesis	5
	Reference	6
Chapter 2	**Fatigue Properties at Room Temperature**	8
2.1	Introduction	8
2.2	Material and Experimental Procedures	9
2.3	Results and Discussion	13
2.3.1	S-N Curves	13
2.3.2	Initiation and Propagation Mechanism of a Small Fatigue Crack	13
2.3.3	Significance of the Fatigue Limit at Room Temperature	13
2.3.4	Small Crack Growth Behavior	22
2.3.5	Fatigue Life Prediction Based on the Small Crack Growth Law	26
2.4	Conclusions	29
	Reference	30
Chapter 3	**Initiation and Early Growth Behavior of a Small Fatigue Crack at Elevated Temperatures**	31
3.1	Introduction	31
3.2	Material and Experimental Procedures	32
3.3	Experimental Results	35
3.3.1	Fatigue Strength at Elevated Temperatures	35
3.3.2	Initiation and Early Growth Behavior of a Small Fatigue Crack at Elevated Temperatures	35
3.3.3	Significance of Fatigue Limit at Elevated Temperatures	41
3.3.4	Stress Dependence of Small Crack Initiation and its Early Growth	46
3.4	Discussion	51
3.4.1	Effect of Temperature on the Crack Initiation	51
3.4.2	Effect of Temperature on the Early Crack Growth	55
3.5	Conclusions	58
	Reference	59
Chapter 4	**Fatigue Crack Growth Resistance at Elevated Temperatures**	60
4.1	Introduction	60
4.2	Experimental Procedures	60
4.3	Results and Discussion	62
4.3.1	S-N Curves	62
4.3.2	Small Crack Growth Rate at Elevated Temperatures	62

4.3.3 Fatigue Life Prediction at Elevated Temperatures 72
4.3.4 Fatigue Crack Growth Resistance at Elevated Temperatures 77
4.4 Conclusions 79
Reference 80

Chapter 5 Notch Sensitivity at Elevated Temperatures 81

5.1 Introduction 81
5.2 Material and Experimental Procedures 81
5.3 Results and Discussion 85
5.3.1 S-N Curves 85
5.3.2 Significance of Fatigue Limit in Notched Specimens 85
5.3.3 Evaluation of Notch Sensitivity Based on the Linear Notch Mechanics 85
5.4 Conclusions 96
Reference 97

Chapter 6 Influence of CBN Grinding on the Fatigue Strength 98

6.1 Introduction 98
6.2 Material and Experimental Procedures 98
6.3 Results and Discussion 99
6.3.1 Fatigue Strength at Room Temperature 99
6.3.2 Fatigue Strength at Elevated Temperatures 99
6.3.3 Significance of Fatigue Limit in CBN Ground Specimens 99
6.3.4 Discussion 104
6.4 Conclusions 111
Reference 112

Chapter 7 Summary 113

Acknowledgements 116

Chapter 1 Introduction

1.1 A brief knowledge of nickel-base superalloys

Superalloys is a term appeared shortly after World War Two to describe a group of heat-resistant alloys developed for high temperature services such as the use in turbosupercharger and aircraft-turbine engines. In addition to high strength at high temperature, superalloys also exhibit excellent oxidation and corrosion resistance.

There are many types of superalloys including iron-base, cobalt-base and nickel-base superalloys. Some of superalloys contain chromium for resistance to oxidation and corrosion and some contain other elements for strength at high temperature. Superalloys can be strengthened in different ways such as solid-solution strengthening, precipitation hardening and oxide-dispersion strengthening. The high temperature applications of superalloys are extensive, including components for aircraft, chemical-plant equipments as well as nuclear power plant equipments. The increasing significance of superalloys in today's commerce is typified by the fact that the percentage of the parts made of superalloys in the total weight of an aircraft turbojet engine has risen several times during these 40 years comparing to that (approximately 10%) in 1950s.

Nickel-base superalloys are the most widely used alloys of all the classes of superalloys and can be generally classified into two types: one is the solid-solution strengthened nickel-base superalloys and the other is the precipitation hardened nickel-base superalloys. The nickel-base superalloys were first developed in the middle of 1940s by International Nickel Co. (U.S.A.) and Mond Nickel Co. (U.K.) separately, for the purpose of producing more cheaper alloys providing them with high strength comparable to the nichrome alloy, which was the only alloy then possessing good elongation, ductility and oxidation resistance at high temperature up to 1100°C. Since then, many new alloys have been developed and the properties of the alloys have been improved greatly. The main alloying elements used in the various formulations of nickel-base superalloys and the effects of these additives are readily available in the literature[1].

Inconel 718 is a precipitation hardened nickel-base superalloy[2] that maintains a stable microstructure, corrosion resistance property and high strength up to 650°C. Due to these outstanding characteristics and other mechanical properties, Inconel 718 has found extensive applications in the modern nuclear and aerospace industries such as the use in the critical structural components of jet engine, rocket engine as well as gas turbine engine of nuclear power generation[3],[4], in which the high strain-stressed, erosive and/or corrosive conditions of components are quite common and in many cases components have to be employed for prolonged periods of design life. Therefore, the creep property and fatigue behavior of the alloy, especially at elevated temperature, is necessary to be clarified and any variable that might alter the properties of Inconel 718 must be accounted for.

1.2 A review of the previous studies on Inconel 718

In the past several decades, a great deal of attention has been drawn to the creep and low cycle fatigue behavior of Inconel 718. Some researchers intended to explore the optimum heat treatment conditions which consist of a solution treating and a two-stage aging, in order to obtain the best combination of mechanical properties and creep and fatigue properties such as ductility, tensile strength, fracture toughness and crack growth resistance at elevated temperature, through controlling the microstructural variables, e.g. grain and precipitate sizes, grain boundary structure and matrix precipitate morphology[5]-[11].

For instance, it was observed that the coarse-grained specimen exhibits shorter low cycle fatigue life than the fine-grained one, despite the slower crack growth rates it has[12],[13]. A similar study revealed the effect of grain size on the near-threshold crack growth rate and ΔK_{th} (threshold value of stress intensity factor range), it was found that increasing the grain size results in a decrease of crack growth rate and an increase of ΔK_{th} due to the intensified roughness-induced crack closure at greater grain sizes[14],[15]. The morphology and volume fraction of γ' and γ" precipitates play important role in determining the strength of Inconel 718 and finer precipitates lead to slower long crack growth rate and longer low cycle fatigue life[13],[16]. It is interesting to note that the coarsening of γ" precipitate particles are able to alter the mechanism of dislocation motion from one involving the shearing of precipitate particles to that of bypassing by the Orowan process[17],[18].

The crack growth process of Inconel 718 is affected appreciably by the testing conditions, i.e. stress ratio R ($R= \sigma_{max}/\sigma_{min}$, where σ_{max} and σ_{min} are the maximum and minimum stress amplitudes respectively), loading frequency, wave shape, holding time, temperature and environment (e.g. the presence of hydrogen). The detailed results are readily available in the literatures[1], [19], [20], in which the interactive influence of each of these operating parameters on the crack growth rate was correlated with the nature of the crack tip zone.

Besides providing fundamental information related to the behavior of a material, the creep and low cycle fatigue data may be applied to predict the life of engineering components which subjected to a similar straining history as simulated in a laboratory. Moreover, in many applications, components have to be in service for extended lifetime, therefore, a knowledge of the material behavior beyond the normal design service exposures as well as the establishment of the residual life evaluation method are urgently required in practice. In the middle of 1980s, the concept of damage tolerance design was developed which allows the existence of flaws or defects with a size corresponding to the detecting limit of the nondestructive inspection technique in structural components when they enter into service. These flaws or defects are then assumed to act as propagating cracks and their rates of propagation are established on the basis of fracture mechanics principles, using the experimental crack growth rate data. This approach, which extends the useful life in existing components by retaining them in service until a crack has indeed been detected, replaces the previous design method which is based on the statistical data of creep-fatigue experiments in which a component that had some useful lifetime remaining to crack initiation was retired from service. Clearly, the safe use of this approach depends on two factors: the ability to predict accurately crack growth rate and the reliability of nondestructive inspection

technique. For this purpose, numerous life assessment models and nondestructive detection methods[21]-[27] were reported for elevated temperature components, yet no method has been widely accepted as a design code for high temperature application because each model or method was only capable of predicting life in a certain range of testing conditions.

In 1975, Pearson[28] discovered that small fatigue cracks grow faster than and below the threshold ΔK of long cracks under nominally equivalent cyclic stress intensities, since then the importance of the small crack growth behavior have been emphasized in many literatures[29],[30]. For instance, it has been found in many metals that the substantial fraction of fatigue life in a plain specimen is occupied by the growth life of small cracks, especially the cracks smaller than 1~2 mm[31]-[33], meaning that the assessment of crack growth rate for small cracks takes a significant role in the life prediction of materials. Meanwhile, the validity of applying the linear elastic fracture mechanics, which concerns the growth of long cracks under the condition of small scale yielding, to describe the growth behavior of small cracks is questioned because high stress levels are necessary to propagate small cracks, such that the condition of small scale yielding is exceeded. Therefore, the evaluation based on the elastic-plastic fracture mechanics must be used. For Inconel 718, the majority of previous studies in small crack growth pertains to creep and low cycle fatigue testing, in which small crack growth rate was evaluated in terms of either the range of effective stress intensity factor ΔK_{eff} or the range of J integral ΔJ in an attempt to consolidate the growth rate of small cracks with that of long cracks[19],[20],[34],[35]. However, in the case of high cycle fatigue, the initiation and propagation behavior of small cracks is not clear, though it is essential to the life prediction of members being used in their prolonged period of service or approaching to the end of design life.

Because Inconel 718 is used extensively in nuclear and aerospace industries, the accurate fatigue test data is necessary to meet the needs of design for reactors and engines, where safety is extremely important. On the other hand, the great progress in modern manufacturing techniques makes the design criteria and techniques used for high technology structures changed and increased in complexity, in order to satisfy the increasing requirements of nuclear and aerospace industries. For example, the design of gas turbine engines may be one of the most difficult design from the viewpoint of structure design and life prediction. Besides the high temperature in service, gas turbine engines have complex shapes accompanied with numerous stress concentrations. These stress concentrations will induce local yielding, lead to the initiation of microcracks and reduce the fatigue strength of materials considerably. Consequently, the deteriorative effect of stress concentrations on the fatigue strength, or the notch sensitivity must be investigated, especially at elevated temperature[3].

Despite some exceptions, most of fatigue cracks initiate from the surface of materials. Therefore, the surface sensitive mechanical properties such as creep, fatigue, and stress corrosion cracking are easy to be influenced by the conditions of machined surfaces. It was reported[36] that machining not only produces specified dimensions, tolerances and surface roughness but also generates residual stress and plastic deformation in the surface region, initiates surface and subsurface cracks and forms surface cavities. Moreover, the components in service are generally employed in machined condition, hence a knowledge of the influence of surface integrity on the fatigue strength of machined components will provide very valuable information for determining the service life of machined components. On the other hand, however, Inconel 718 is one of the

difficult-to-machine materials because it is extremely hard and has a tendency to clog and gum up the grinding wheel during grinding due to its low thermal conductivity. This will manifest in higher forces and heat generation and in turn accelerate the wheel wear rate and worsen the surface integrity. For this reason, many previous researches gathered in the machining efficiency and method, surface integrity including surface roughness and residual stress, and tools and tool wear[37)-(40)], but less attention has been attracted to the influence of machining on the fatigue strength of Inconel 718[41)].

Recently, Cubic Boron Nitride (CBN) wheels have been frequently used to grind the materials like Inconel 718 which is difficult to machine using conventional machining tools. CBN abrasive have superior physical properties to the conventional abrasive in terms of its hardness (only second to the diamond) and ultra high thermal conductivity. It has been reported that with the help of high-efficiency deep grinding technique, several hundred times of removal rate can be reached as that by conventional grinding technology, accompanied with low grinding wheel wear, low surface temperature as well as high compressive residual stress arose in the surface region[42)], the latter is more interesting because the compressive residual stress existed in the surface layer is considered to be favorable to the improvement of fatigue strength. By these reasons, a large amount of components made of Inconel 718 are grinding finished before putting into use, the knowledge of the influence of CBN grinding on the fatigue strength of Inconel 718, especially the fatigue strength at elevated temperatures, is very important and essential to the machine designers.

1.3 Objectives

Since the first application of nickel-base superalloys, almost fifty years have been passed during which great deal of efforts have been made in order to improve the physical properties and the creep and fatigue strengths of the alloys and to extend their applications in modern industries. In the case of Inconel 718, as mentioned in the above review, a large amounts of studies were carried out focused on the creep and low cycle fatigue behavior of the alloy, but the data of high cycle fatigue behavior is far not enough and many problems were left unclear.

Therefore, in the present thesis, rotating bending fatigue tests were carried out for Inconel 718 at room and elevated temperatures in order to clarify the following problems:

(1) Fatigue properties at room temperature

(2) Effect of temperature on the initiation and early propagation of small cracks

(3) Evaluation of fatigue crack growth rate and fatigue crack growth resistance at elevated temperatures

(4) Strength prediction for the notched specimens and the notch sensitivity at elevated temperatures

(5) Influence of CBN grinding on the fatigue strength at elevated temperatures.

1.4 Contents of the dissertation

The dissertation is composed of seven chapters and the concise description of the content of each chapter are as follows.

Chapter 1 is an introduction which contains a brief knowledge of the physical characteristics and engineering applications of nickel-base superalloys, a review of the previous researches and a description of the objectives and features of the dissertation.

The fatigue properties at room temperature is investigated in chapter 2. The initiation and growth behavior of small cracks are observed directly under a scanning electron microscope (SEM) or under a optical microscope using the plastic replica method. The significance of the fatigue limit in a plain specimen is discussed according to the result of successive observation of small cracks. The crack growth rate of small cracks and the fatigue life of plain specimens are evaluated on the basis of the small crack growth law.

In chapter 3, the fatigue strength at elevated temperatures is investigated and the influence of temperature on the fatigue strength is examined in terms of the crack initiation, the early growth of small cracks and the crack arresting phenomenon at the fatigue limit of the plain specimen. Then, the results are discussed from the interaction between the softening of matrix and the surface oxidation of specimen at elevated temperatures.

The fatigue crack growth resistance at elevated temperatures is clarified in chapter 4 by using the specimen with a small blind hole (0.3 mm in diameter and depth). The crack growth rates at elevated temperatures are assessed either by the Paris' law or by the small crack growth law and the limiting stress levels for the applicability of each law are proposed. The change of the fatigue crack growth resistance with the increase of temperature is elucidated depending on the small crack growth law with the consideration of the decrease of static strength of the alloy.

In chapter 5, the fatigue strength of notched specimen is investigated at room and elevated temperatures using the 60 degree V-grooved specimens which have different notch radius and notch depth. The notch sensitivity of the alloy is evaluated in terms of the notch sensitivity at the fatigue limit for crack initiation and that for crack growth respectively, based on the linear notch mechanics. The results are discussed from the viewpoint of the effect of temperature.

Chapter 6 concerns the fatigue strength of CBN ground specimen. The effect of CBN grinding is investigated by comparing the fatigue strength of CBN ground specimens with those of electro-polished and emery paper polished specimens. The results are discussed from the viewpoints of residual stress, surface roughness and work-hardening in the surface region of specimens.

Chapter 7 is a summary presenting the principle conclusions obtained in this dissertation.

References

(1) Garimella, L., et al., *JOM*, Vol. 49, No. 7, (1997), pp. 67-71.

(2) Eiselstein, H.L., (The International Nickel Company), *United States Patent Office* **3.046.108**, 1962.

(3) Korth, G.E. & Smolik, G.R., "Status report of physical and mechanical test data of alloy 718", *TREE-***1254** (1978), pp. 1-81.

(4) Hasegawa, E., et al., *Trans. Jpn Soc. Mech. Eng.*, (in Japanese), **61**-588, A (1995), pp. 1695-1700.

(5) Mills, W. J., *Trans. ASME, J. of Eng. Mat. and Tech.*, **102** (1980), pp. 118-126.

(6) Raymond, E.L., *Trans. Met. Soc. AIME*, **239** (1967), pp. 1415-1422.

(7) Muller, J.F. & Donachie, M.F., *Metall. Trans. A*, **6A** (1975), pp. 2221-2277.

(8) Wilson, D.J., *Trans. ASME, J. of Eng. Mat. and Tech.*, **95** (1973), pp. 112-123.

(9) Merrick, H.F., *Metall. Trans. A*, **7A** (1976), pp. 505-514.

(10) Thamburaj, R. et al., Tokyo, Japan, *JSME/ASME*, 1986, pp. 275-282.

(11) Koul, A.K. et al., *Proc. of Superalloys 1988* (Ed. by Reichman, S., et al., The Metallurgical Society), 1988, pp. 3-12.

(12) Denta, T., et al., *Metall. Trans. A*, **23**A (1992), pp. 519-526.

(13) Krueger, D.D., et al., *Metall. Trans. A*, **18**A (1987), pp. 1431-1449.

(14) Kim, S. & Knott, K.F., *Fracture & Strength '90 Key Engng. Mater.*, **51** (1991), pp. 209-214.

(15) King, J.E., *Met. Sci.*, **16** (1982), pp. 345-357.

(16) Schwarzkopf, E.A., Ph.D. dissertation, Columbia University (1989).

(17) Pedron, J.PP. & Pineau, A., *Mater. Sci. Eng.*, **56** (1982), pp. 143-155.

(18) Zheng, D. & Ghonem, H., *Metall. Trans. A*, **23**A (1992), pp. 3169-3171.

(19) Ghonem, H., et al., *Fatigue Fract. Engng Mater. Struc.*, Vol. **16**, No. 5 (1993), pp. 565-576.

(20) Ghonem, H., et al., *Fatigue Fract. Engng Mater. Struc.*, Vol. **16**, No. 6 (1993), pp. 577-590.

(21) Goswami, T., *J. of High Temperature Materials and Processes*, Vol. **15**, No. 1-2 (1996), pp. 91-96.

(22) Kim, K.S., et al., *Proc. of Int. Sympp. on Mater. Ageing and Component Life Extension* (Ed. by V. Bicego, A. Nitta and R. Viswanathan), 1995, Vol. **1**, pp. 25-36.

(23) Rosenberger, A., et al., *Proc. of Superalloys 1992* (Ed. by S.D. Antolovich et al., The Metallurgical Society), 1992, pp. 737-746.

(24) Nicholas, T., et al., *Int. J. of Fatigue*, **41** (1989), pp. 157-176.

(25) Boyce, L., *Proc. of AIAA/SAE/ASME/ASEE 28th Joint Propulsion Conf. and Exhibit,* 1992, pp. 1-10.

(26) Hasegawa, E., et al., *Trans. Jpn Soc. Mech. Eng.*, (in Japanese), **61**-588, A (1995), pp. 1701-1706.

(27) Kumazaki, S., et al., *Trans. Jpn Soc. Mech. Eng.*, (in Japanese), **63**-611, A (1997), pp. 1481-1488.

(28) Pearson, S., *Engng Fract. Mech.*, **7** (1975), pp. 235-247.

(29) Miller, K.J., *Fat. Fract. Eng. Mat. Struc.*, 10 (2) (1987), pp. 75-92.

(30) Miller, K.J., *Fat. Fract. Eng. Mat. Struc.*, 10 (2) (1987), pp. 93-113.

(31) Nisitani, H. & Kawagoishi, N., *Trans. Jpn Soc. Mech. Eng.*, (in Japanese), **49**-440, A (1983), pp. 431-

440.

(32) Nisitani, H. & Kawagoishi, N., *Trans. Jpn Soc. Mech. Eng.*, (in Japanese), **50**-450, A (1984), pp. 277-282.

(33) Nisitani, H. & Goto, M., *Trans. Jpn Soc. Mech. Eng.*, (in Japanese), **50**-453, A (1984), pp. 1090-1096.

(34) Rosenberger, A. H. & Ghonem, H., *Fatigue Fract. Engng Mater. Struc.*, Vol. **15**, No. 11 (1993), pp. 1125-1139.

(35) Reddy, S.C. & Fatemi, A., *Advances in fatigue lifetime predictive techniques, ASTM STP 1122* (Ed. M.R.Mitchell and R.W. Landgraf), 1992, pp. 276-289.

(36) Ishigawa, T. & Kumar, K.V., *J. Japan Society of Precision Engineering*, (in Japanese), **58** (1992), pp. 597-600.

(37) Sadat, A.B., et al., *ASME PED*, **40** (1989), pp. 9-17.

(38) Ezugwu, E.Q., et al., *Lubrication Engineering*, **47** (1991), pp. 751-757.

(39) Komanduri, R. & Schroeder, T.A., *ASME PED*, **35** (1984), pp. 287-307.

(40) Kumagai, N., *J. Japan Society of Precision Engineering*, (in Japanese), **58** (1992), pp. 12-15.

(41) Korth, G.E., *U.S. DOE Reports*, *EGG*-**2105**, 1981, pp. 1-21.

(42) Tonshoff, H.K. et al., *Tool Engineer* (in Japanese), **31** (1987), pp. 81-89.

Chapter 2 Fatigue Properties at Room Temperature

2.1 Introduction

The increasing demands of machine designs such as high strength, excellant corrosion properties and good creep and fatigue resistance at high temperature have led to the rapid development of various new kinds of heat-resistant materials. Hence, the studies of the strength characteristics of these materials as well as the influences of environmental variables have been often reported[(1)–(3)].

Nickel-base superalloys, as mentioned in chapter 1, are widely used in the aerospace and nuclear industries because of their high strengths at high temperature and other excellent mechanical properties, to replace the conventional heat-resistant materials, e.g., the stainless steels. Therefore, many studies[(4)-(9)] have been performed by focusing on the metallurgical design of the alloys, and recently the studies of the creep properties and low cycle fatigue behavior of the alloys have been increased as well. Nevertheless, very little has been known or published about the high cycle fatigue strength properties of nickel-base superalloys at both elevated and room temperatures.

In this chapter, rotating bending fatigue tests are carried out in order to investigate the fatigue properties of nickel-base superalloy Inconel 718 at room temperature, because the fatigue properties at room temperature is necessary not only in the machine designs but also for the comprehension of the fatigue properties of the alloy at elevated temperatures. The initiation and propagation behavior of a small fatigue crack will be observed successively and the fatigue properties of Inconel 718 will be examined in terms of the fatigue limit, the behavior of the small fatigue crack and the resistance to fatigue crack growth.

2.2 Material and experimental procedures

The material used was a rolled round bar (13 mm in diameter) of Inconel 718 whose chemical composition is shown in Table 2.1. The material was solution treated at 982°C for 1 h, water quenched, then aged at 720°C for 8 h, furnace cooled to 621°C and aged at 621°C for other 8 h followed by air cooling. The mechanical properties at room temperature and the microstructure after heat treatment are presented in Table 2.2 and Fig. 2.1, respectively. The average grain size is about 9 μm.

Figure 2.2 shows the shape and dimensions of specimens. Fig. 2.2 (a) shows the plain specimen. To localize the crack initiation site, the mid-surface of specimens was partially notched (5 mm at radius and 0.2 mm in depth) with silica carbide papers or blindly drilled (0.3 mm both at diameter and in depth) by using a high speed precision bench drill. The details of the partial notch and the small blind hole are shown in Fig. 2.2 (a) and (b), respectively. The specimens with a partial notch were used to examine the initiation and early growth behavior of a small fatigue crack. The fatigue limits (the limiting stresses for specimens not to fracture after the stress repetitions of 10^7 cycles) of plain and partially notched specimens were 490 and 450 MPa, respectively. This means that the decrease of the fatigue strength due to the partial notch was less than 10 %, or in other words, the strength reduction factor, K_f , is close to unity. Hence, the behavior of a small fatigue crack in partially notched specimens can be used to simulate that in plain ones and partially notched specimens will be mentioned as plain specimens, hereafter. While those with a blind hole will be mentioned as drilled specimens and used to evaluate the small crack growth resistance in the alloy.

Prior to fatigue testing, all the specimens were electropolished to remove the worked surface layer by about 40 μm in diameter for plain specimens and 20 μm for drilled ones. The observation of fatigue surface damage and the measurement of crack length were conducted directly under Scanning Electron Microscope (SEM) or under an optical microscope using the plastic replica technique. The crack length, l, was measured along the circumferential direction on the surface including the 0.3 mm diameter of the hole in the case of drilled specimens. The stress value referred to is the nominal stress amplitude, σ_a, at the minimum cross section by ignoring the existence of the partial notch and the hole.

The fatiue tests were carried out at room temperature in air using an Ono-type rotating bending fatigue machine with a capacity of 15 N·m operating at a frequency of 50 Hz.

Table 2.1 Chemical composition

(wt. %)

C	Si	Mn	P	S	Ni	Cr	Mo	Co	Cu	Al	Ti	Fe	B	Nb+Ta
0.03	0.05	0.06	0.008	0.002	Bal.	18.5	3.08	0.27	0.02	0.55	0.96	19.18	0.004	5.03

Table 2.2 Mechanical properties at room temperature

0.2% proof stress $\sigma_{0.2}$ (MPa)	Tensile strength σ_B (MPa)	True breaking stress σ_T (MPa)	Reduction of area ψ (%)
1320	1461	2320	70

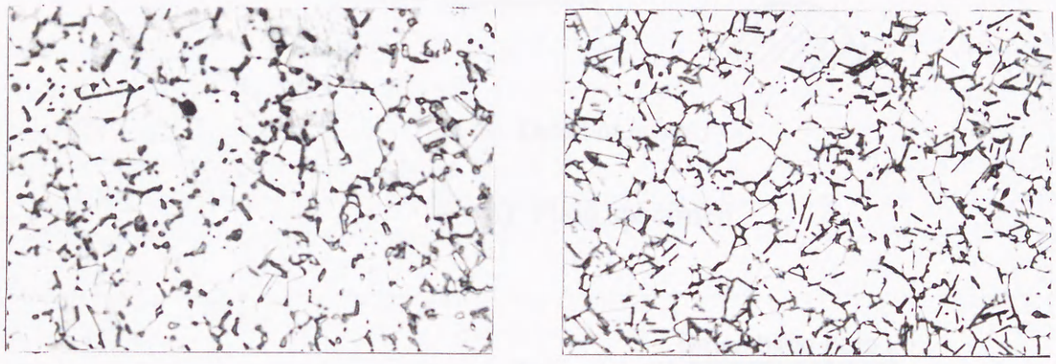

(a) Longitudinal section

(b) Cross section

Fig. 2.1 Microstructure of Inconel 718.

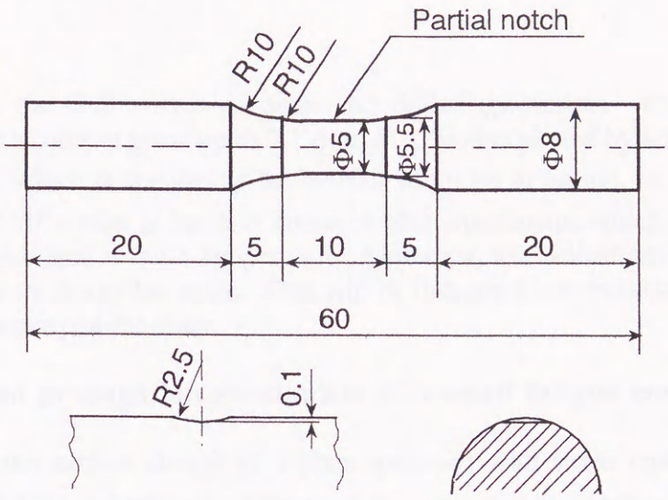

Detail of notch

(a) Plain specimen

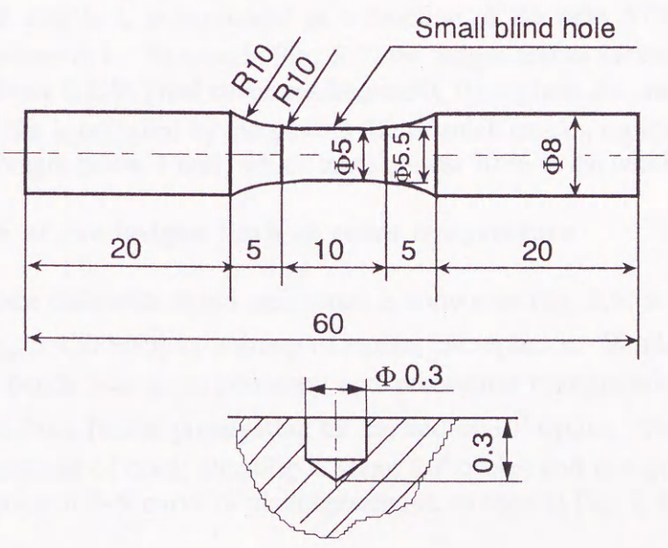

Detail of hole

(b) Drilled specimen

Fig. 2.2 Shape and dimensions of (a) plain and (b) drilled specimens (in mm).

2.3 Results and discussion

2.3.1 *S-N* curves

Figure 2.3 shows the *S-N* curves of plain and drilled specimens. In the case of plain specimens, the life for a crack to grow up to 0.1 mm, $N_{0.1}$, is also plotted by dotted line in addition to the fatigue life, N_f, which is denoted as the number of cycles to failure. A knee point appears around the number of 10^6 cycles in the *S-N* curve of plain specimens, which means that Inconel 718 has a definite fatigue limit at room temperature. Moreover, the inclinations of two *S-N* curves in the finite life region are nearly the same. This will be discussed later because it is related to the small crack growth property of the alloy.

2.3.2 Initiation and propagation mechanism of a small fatigue crack

Figure 2.4 shows the surface change of a plain specimen with stress repetitions under high stress level, σ_a = 750 MPa, which caused the final fracture of plain specimens. In the case of Inconel 718, a fatigue crack usually initiates from the surface slip bands near grain boundaries, this can be seen more clearly from the SEM microphoto in Fig. 2.5, in which the typical morphology of fatigue crack initiation at room temperature is presented. After growing up to some length, the crack propagates transgranularly with the steady formation of striations (Fig. 2.6).

Figure 2.7 shows the crack growth curves of plain specimens at room temperature, in which the logarithm of crack length, l, is expressed as a function of the ratio N/N_f, where N is the number of cycles correlated to l. As seen in Fig. 2.7, the fatigue cracks initiates in the early stage of stress repetitions (about $0.2\,N_f$) and coalesces frequently throughout the crack growth process. A great part of fatigue life is occupied by the growth life of small cracks, especially the growth life of small cracks in the length below 1 mm, which takes almost 70 % in the whole fatigue life.

2.3.3 Significance of the fatigue limit at room temperature

The change of surface state with stress repetitions is shown in Fig. 2.8, at the fatigue limit of plain specimen σ_{W0} (σ_{W0} = 450 MPa) by a group of replica microphotos. Similarly, a fatigue crack initiates from the slip bands near grain boundary and propagates transgranularly up to about 21 μm, there it is arrested from further propagating till the end of 10^7 cycles. The number of cycles related to the commencement of crack arresting is about 10^6 cycles and in a good correspondence to the life at the knee point in *S-N* curve of plain specimens, as seen in Fig. 2.3.

However, when the specimen is stressed up to higher stress level, e.g., $\sigma_{W0} \rightarrow$ 750 MPa (Fig. 2.9), the arrested small crack propagates again and leads to the final fracture of the specimen. This shows that the arrested small crack in Fig. 2.8 is the major crack in the specimen. The crack growth curves of the major crack under the stress levels of the fatigue limit σ_{W0} = 450 MPa and the higher stress σ_a = 750 MPa, is shown in Fig. 2.10.

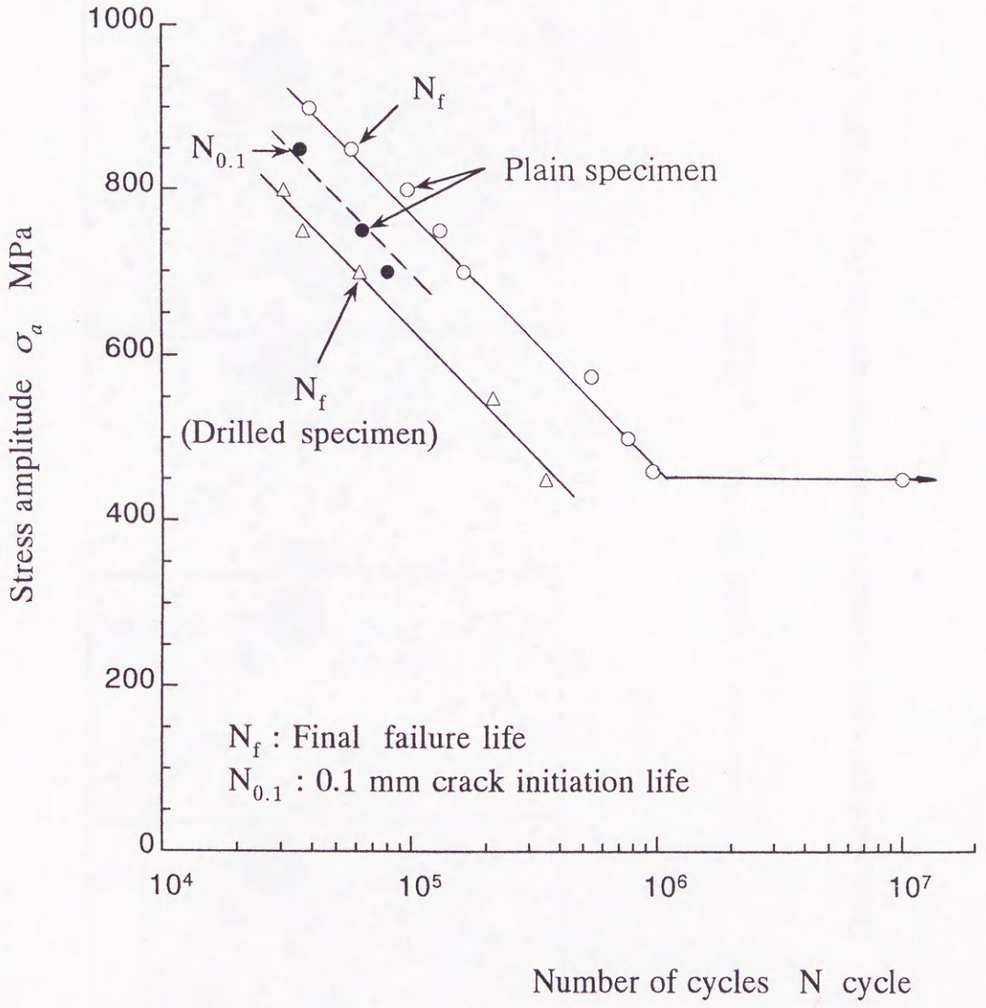

Figure 2.3 *S-N* curves of plain and drilled specimens.

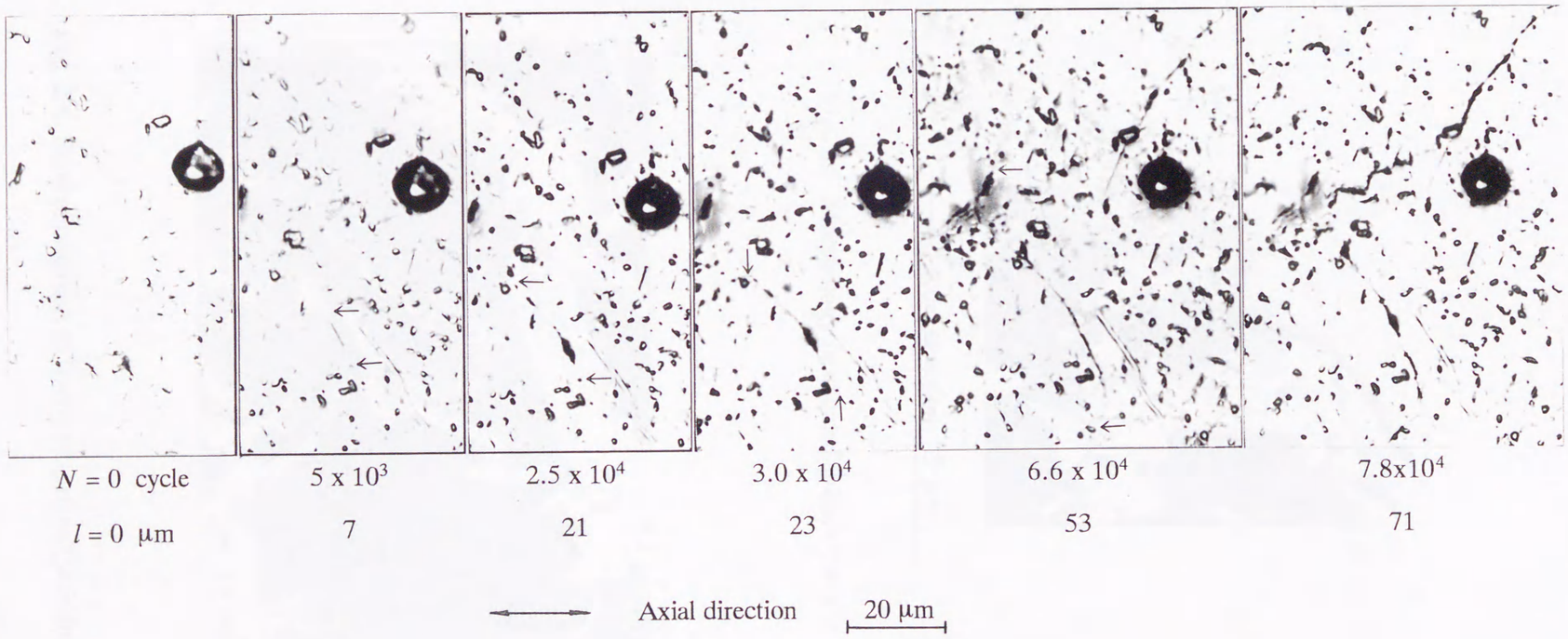

Fig. 2.4 Change in surface state of specimen with stress repetition (σ_a = 750 MPa, N_f = 1.12 x 10^5).

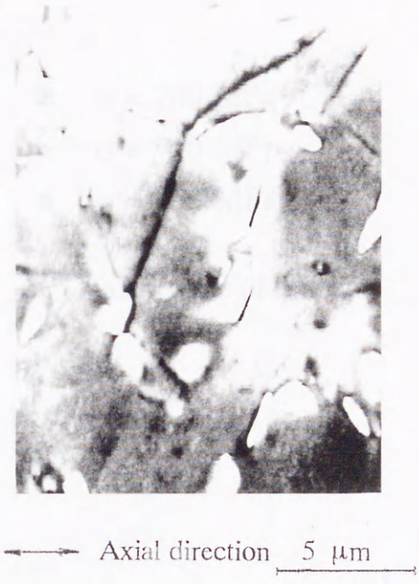

Fig. 2.5 Morphology of initiated surface crack.

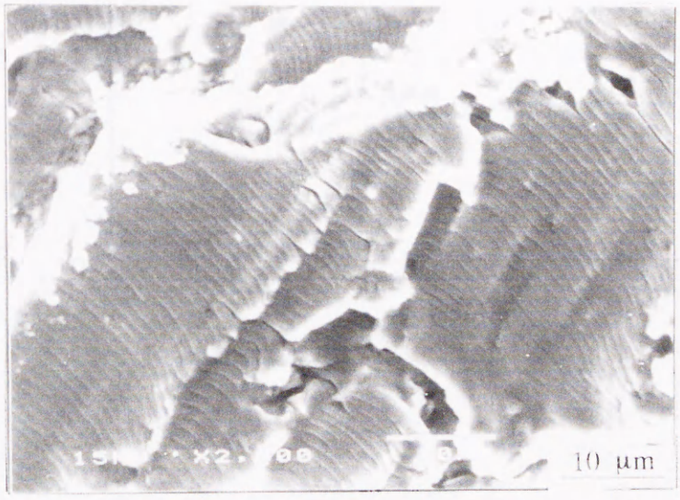

Fig. 2.6 SEM photograph of fractured surface (Striations).

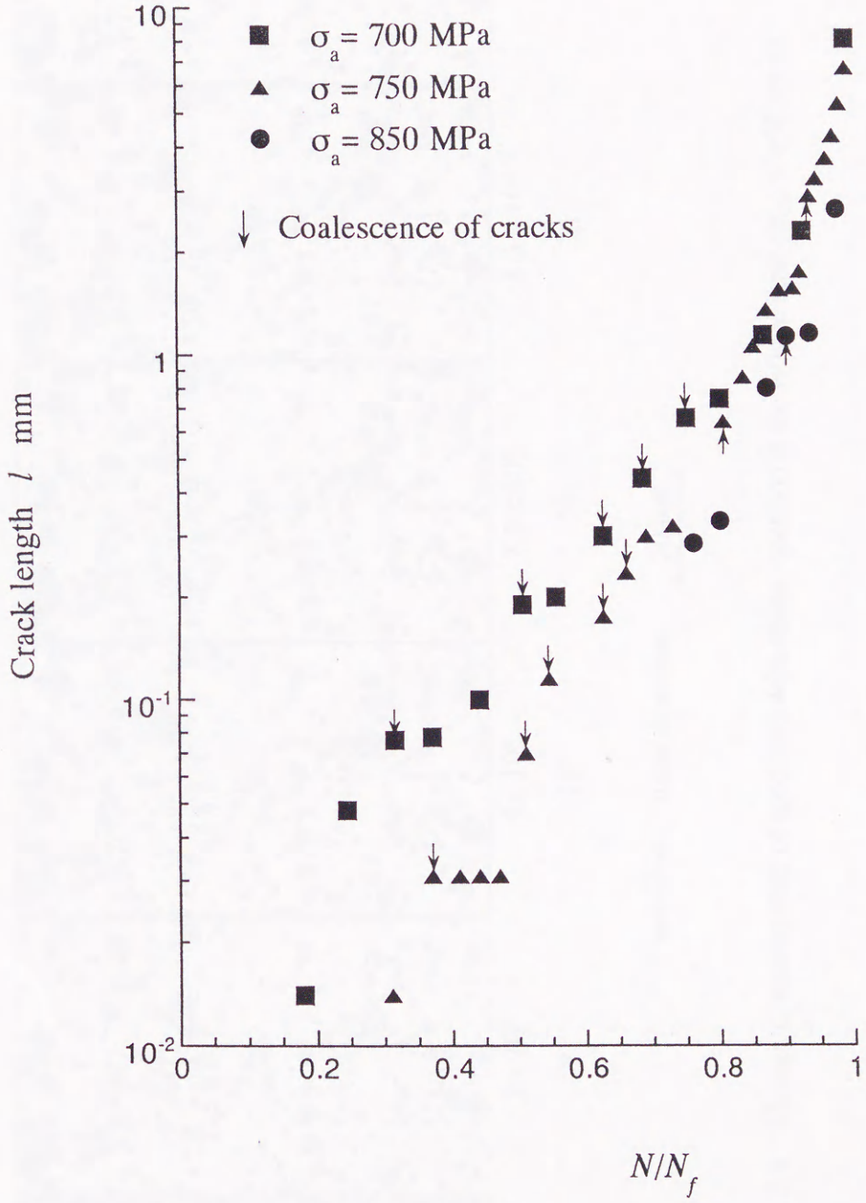

Fig. 2.7 Crack growth curves.

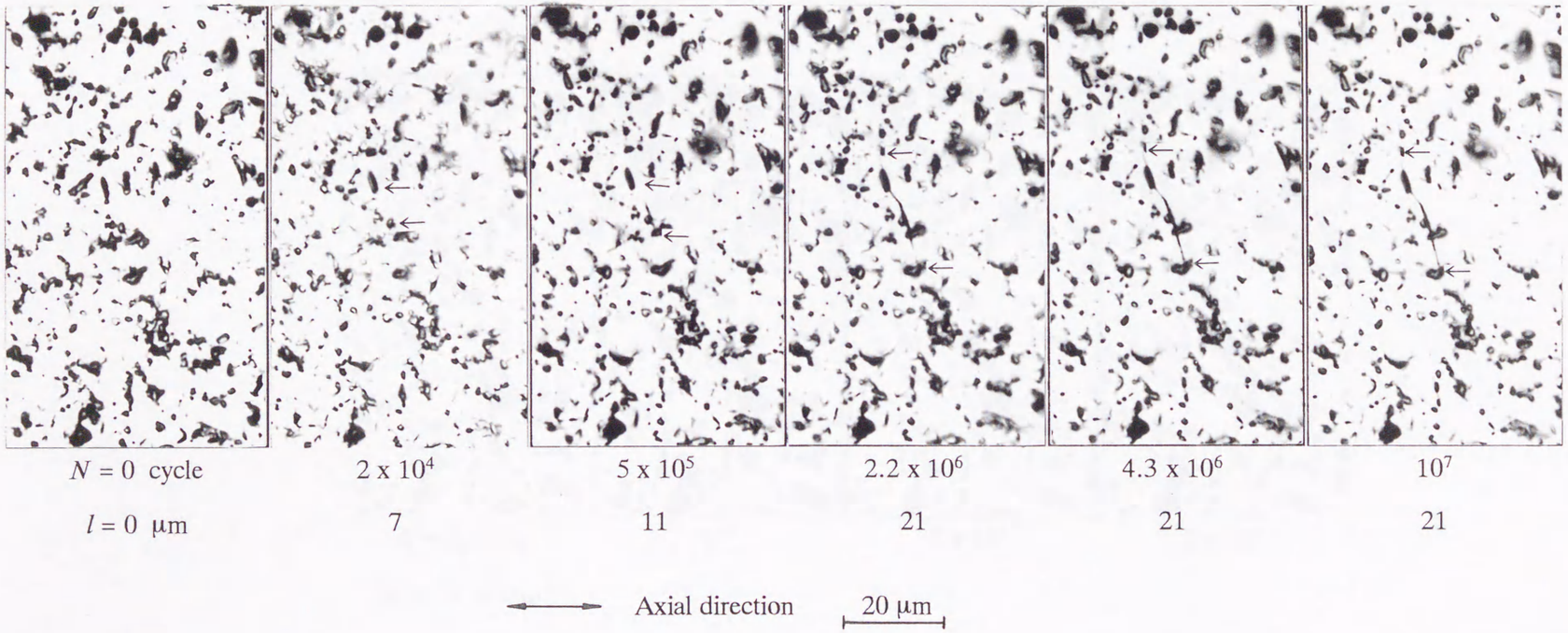

Fig. 2.8 Change in surface state of specimen with stress repetition at the fatigue limit (σ_{w0} = 450 MPa).

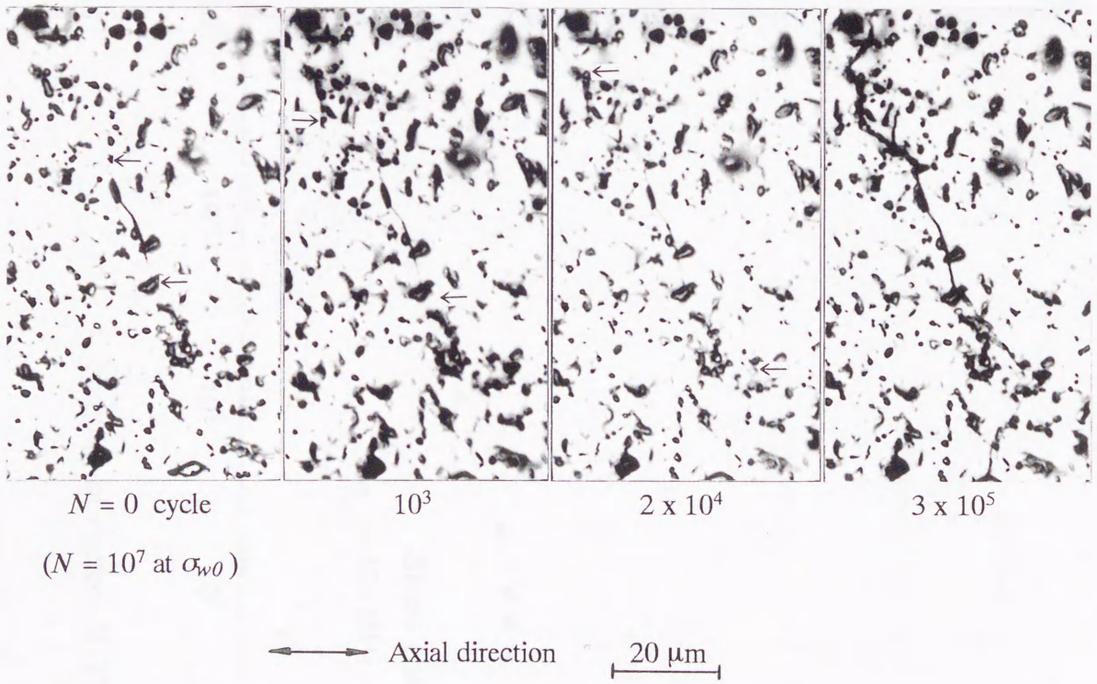

Fig. 2.9 Growth behavior of arrested crack in Fig. 2.8 under high stress ($\sigma_{w0} \rightarrow 450$ MPa).

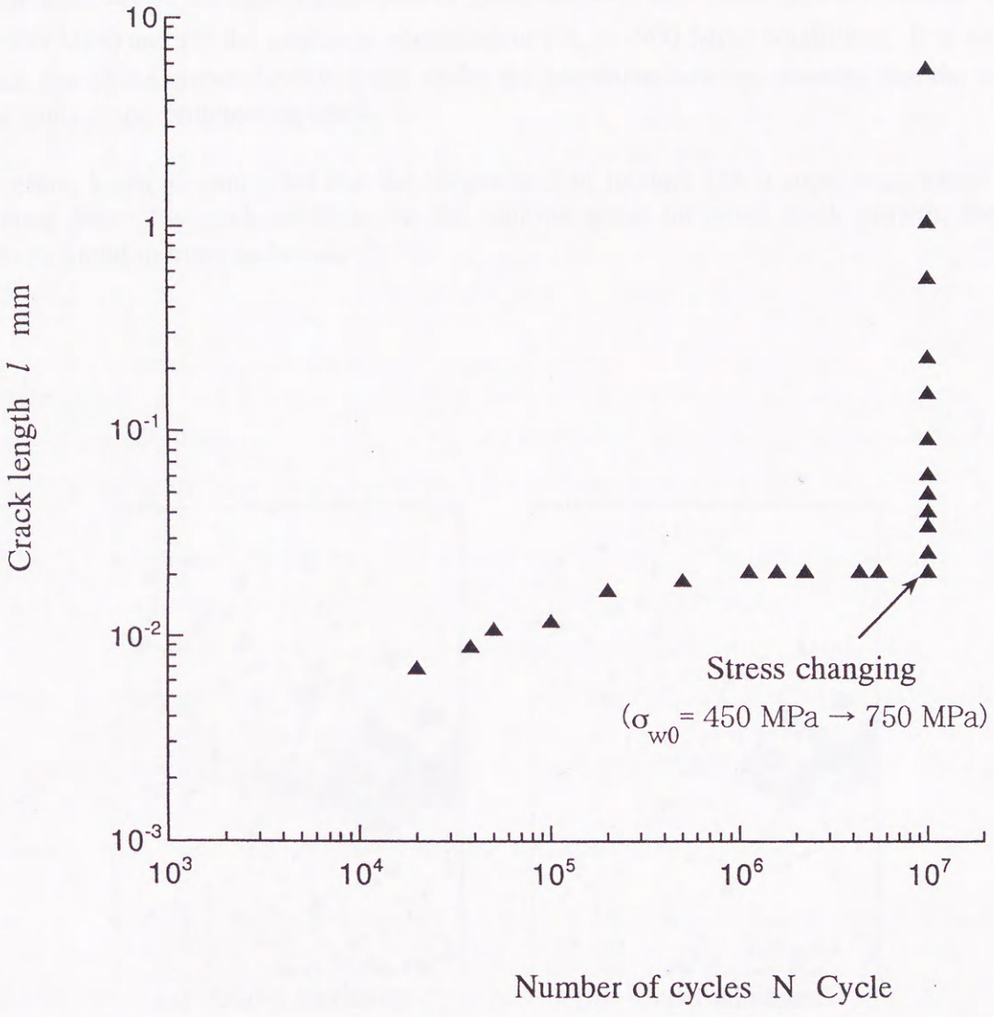

Fig. 2.10 Crack growth curves of the major crack in Figs. 2.8 and 2.9.

To confirm that the arrested crack in Fig. 2.8 is not slip bands but a non-propagating crack, the opening and closure phenomena of a similar arrested crack is investigated under static over stress condition (e.g., σ_a = 900 MPa) using another specimen prepared under the stress level of the fatigue limit at room temperature after the stress repetitions of 10^7 cycles.

Figure 2.11 shows the replica microphotos of the arrested crack under (a) the maximum tension (σ_{max}= 900 MPa) and (b) the minimum compression (σ_{min}= –900 MPa) conditions. It is seen that the crack tips of the arrested crack opens under the maximum tension, meaning that the arrested crack is really a non-propagating crack.

Therefore, it can be concluded that the fatigue limit of Inconel 718 at room temperature is not the limiting stress for crack initiation but the limiting stress for small crack growth, the same property as found in irons and steels[10],[11].

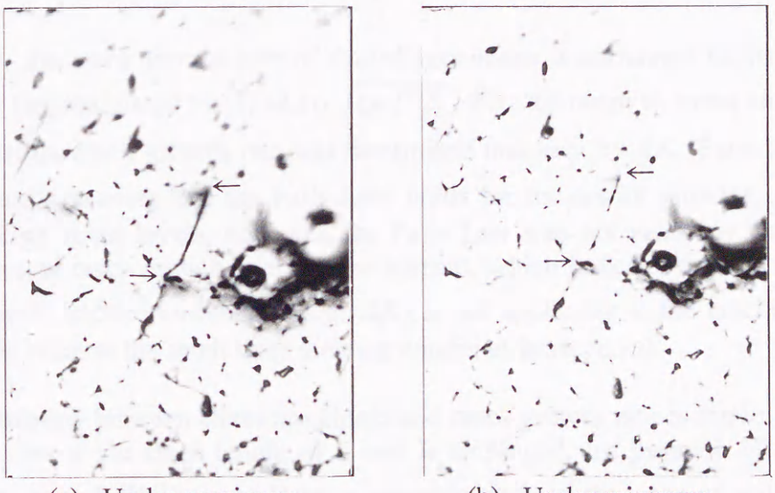

Fig. 2.11 Opening and closure states of a non-propagating crack at room temperature.

2.3.4 Small crack growth behavior

As above mentioned that in the finite fatigue life region, most of the fatigue life in a plain specimen was occupied by the growth life of cracks smaller than 1 mm. This fact and that the fatigue limit is determined by the limiting stress for crack growth imply that the propagation behavior of small cracks takes a very important role in the life prediction and strength evaluation of Inconel 718.

Figure 2.12 shows the relationship of crack growth rate, dl/dN, with crack length, l, in the case of drilled specimen. Some results of plain specimens are plotted in Fig. 2.12, either. It can be seen that the crack growth curves of both specimens coincide well with each other in the regime dominated by mechanical factors, in which the growth behavior of a small fatigue crack is less influenced by the microstructure of materials. This means that the steady crack growth behavior of a small fatigue crack in plain specimens can be estimated from that in drilled ones. Furthermore, in the *log-log* diagram, this relation can be linearly approximated under all the stress levels.

However, the inclinations of the approximated lines took two different values according to the stress levels, that is, under high stress levels the value is nearly 1 and the crack growth rate is proportional to crack length, $dl/dN \propto l$; while under low stress levels the value is about 2 and the crack growth rate is nearly proportional to the square of crack length, $dl/dN \propto l^2$.

In Fig. 2.13, the crack growth rate of drilled specimens is correlated to the stress intensity factor range ΔK (approximated by $(2/\pi)\Delta\sigma\sqrt{(\pi l/2)}$, $\Delta\sigma$: the range of stress amplitude). Under low stress levels, the crack growth rate was determined uniquely by ΔK (Paris Law[12], $dl/dN \propto \Delta K^m$, m: constant), meaning that the Paris Law holds for the cracks growing under low stress levels. Under high stress levels, however, the Paris Law was not valid any longer because the stress dependence of crack growth rate was recognized, which indicates that the evaluation based on the linear elastic fracture mechanics (e.g. ΔK) is not applicable to the cracks growing under high stress levels because the small scale yielding condition is exceeded.

The *log-log* relation between stress amplitude and crack growth rate is shown in Fig. 2.14, in which only the data at the crack length of 1 mm is employed, for instance. It is clear that the relation between σ_a and dl/dN can be linearly approximated and the slope of approximated line is about 5. Similar relation is available for any other cracks in the range of crack lengths from 0.5 mm to 1~2 mm in which the relation of $dl/dN \propto l$ holds, growing under high stress levels.

The results in Figs. 2.12 and 2.14 can be summarized as follows: for cracks growing under high stress levels, the crack growth rate can be determined by the term of $\sigma_a{}^n l$, or in other words, the crack growth rate can be evaluated by the following small crack growth law[13].

$$dl/dN = C\sigma_a{}^n l \qquad (n \approx 5) \qquad (2\text{–}1)$$

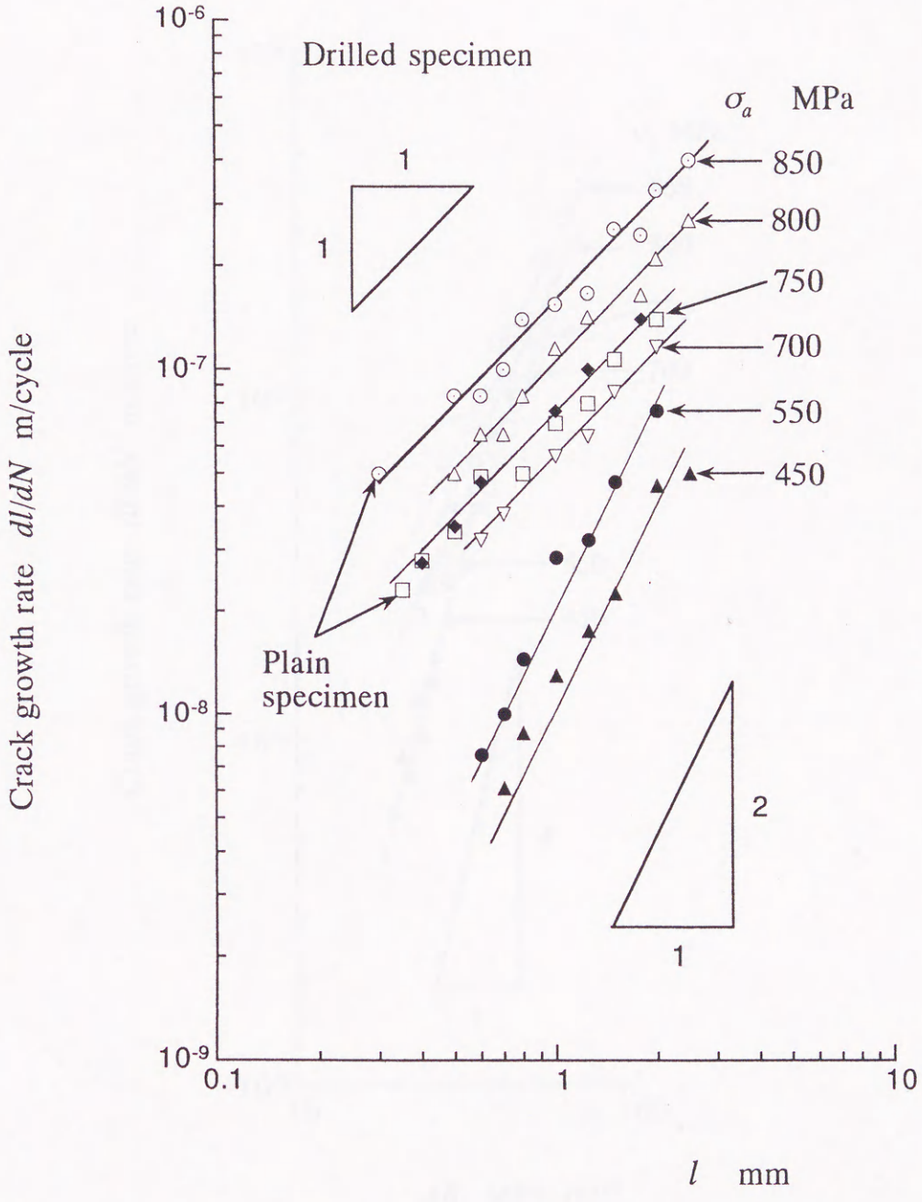

Fig. 2.12 dl/dN versus l .

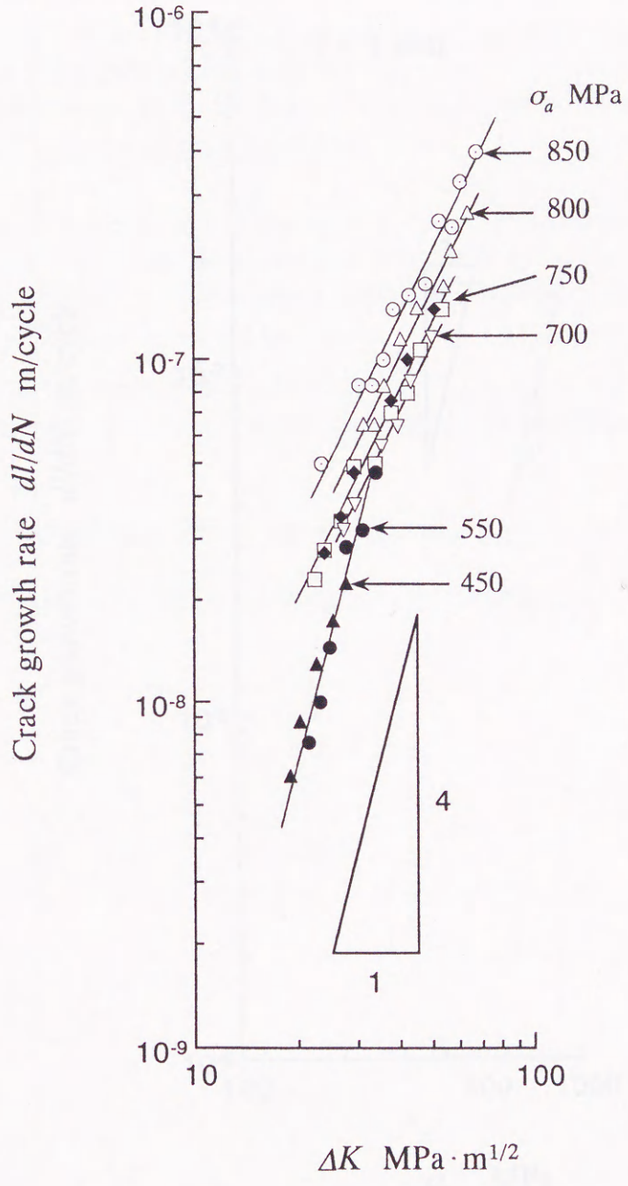

Fig. 2.13 *dl/dN* versus ΔK.

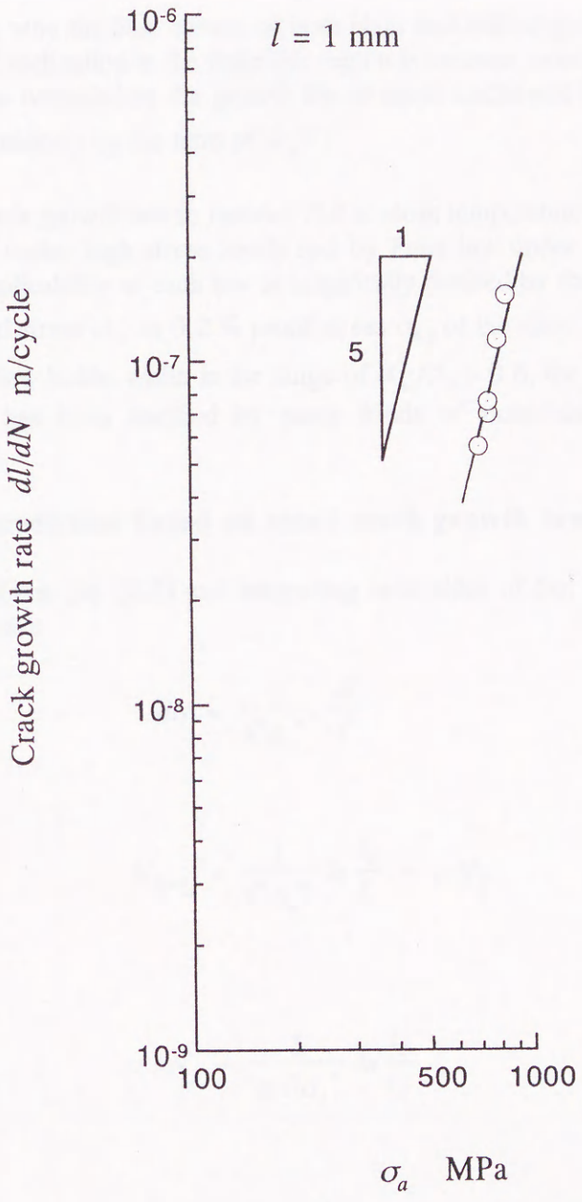

Fig. 2.14 dl/dN versus σ_a.

where C and n are constants. As seen from Fig. 2.15, the crack growth rate is determined uniquely by the term of $\sigma_a^5 l$.

Therefore, the reason why the *S-N* curves of both plain and drilled specimens (Fig. 2.3) took almost the same value of inclination in the finite life region is because most of fatigue life in a plain or a drilled specimen was occupied by the growth life of small cracks and the growth rate of small cracks was determined uniquely by the term of $\sigma_a^5 l$.

Consequently, the crack growth rate in Inconel 718 at room temperature can be predicted by the small crack growth law under high stress levels and by Paris law under low stress levels. The limiting stress for the applicability of each law is empirically decided by the ratio of nominal stress amplitude σ_a to the yield stress σ_s or 0.2 % proof stress $\sigma_{0.2}$ of the alloy. That is, in the range of $\sigma_a/\sigma_s < 0.5$, the Paris law holds; while in the range of $\sigma_a/\sigma_s > 0.6$, the small crack growth law is valid, a result that has been testified by many kinds of materials under various testing conditions[13], [14].

2.3.5 Fatigue life prediction based on small crack growth law

By rewriting Eq. (2.1) as Eq. (2.2) and integrating both sides of Eq. (2.2) with respect to N and l, respectively, we have

$$dN = \frac{1}{C\sigma_a^{\,n}} \frac{dl}{l} \tag{2-2}$$

$$N_{l_1 \to l_2} = \frac{1}{C\sigma_a^{\,n}} ln\frac{l_2}{l_1} = \alpha N_f \tag{2-3}$$

or

$$N_f = \frac{1}{\alpha C\sigma_a^{\,n}} ln\frac{l_2}{l_1} \tag{2-4}$$

where α is the ratio of the crack growth life $N_{l_1 \to l_2}$ from the length of l_1 to l_2, to the fatigue life N_f, and C and n are constants.

For example, in the case of plain specimen, α is about 0.70 when l_1 and l_2 are assigned as 0.01 mm and 1 mm respectively (Fig. 2.7), while C and n are constants and can be calculated using the least square method from the relations shown in Fig. 2.15 and 2.14, individually. It is known that C= 2.9537×10^{-19}, n = 5.

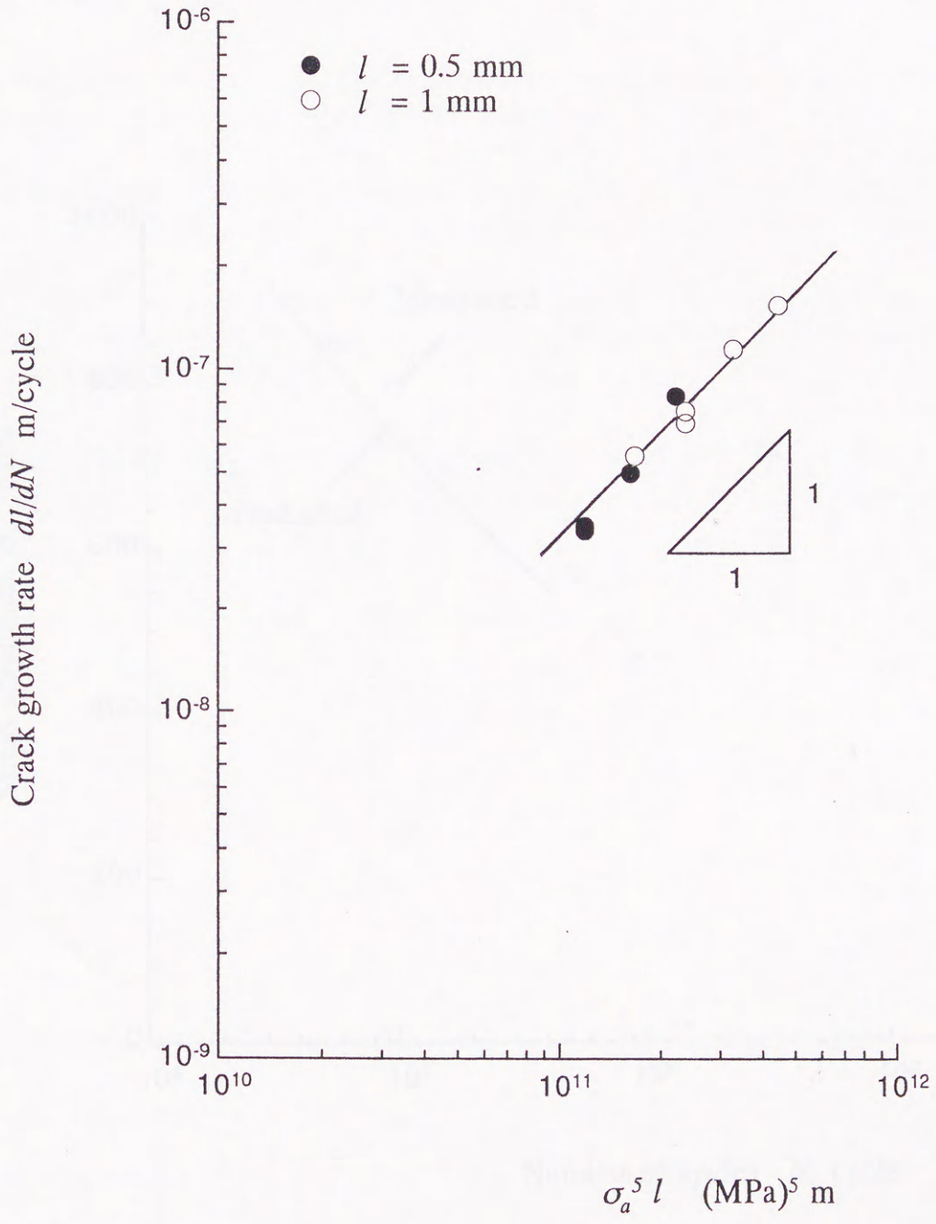

Fig. 2.15 dl/dN versus $\sigma_a^n l$.

Therefore, the life prediction for plain specimens can be easily conducted using Eq. (2.4). The predicted and measured *S–N* curves are shown in Fig. 2.16. The precision of life prediction based on small crack growth law is quite satisfied.

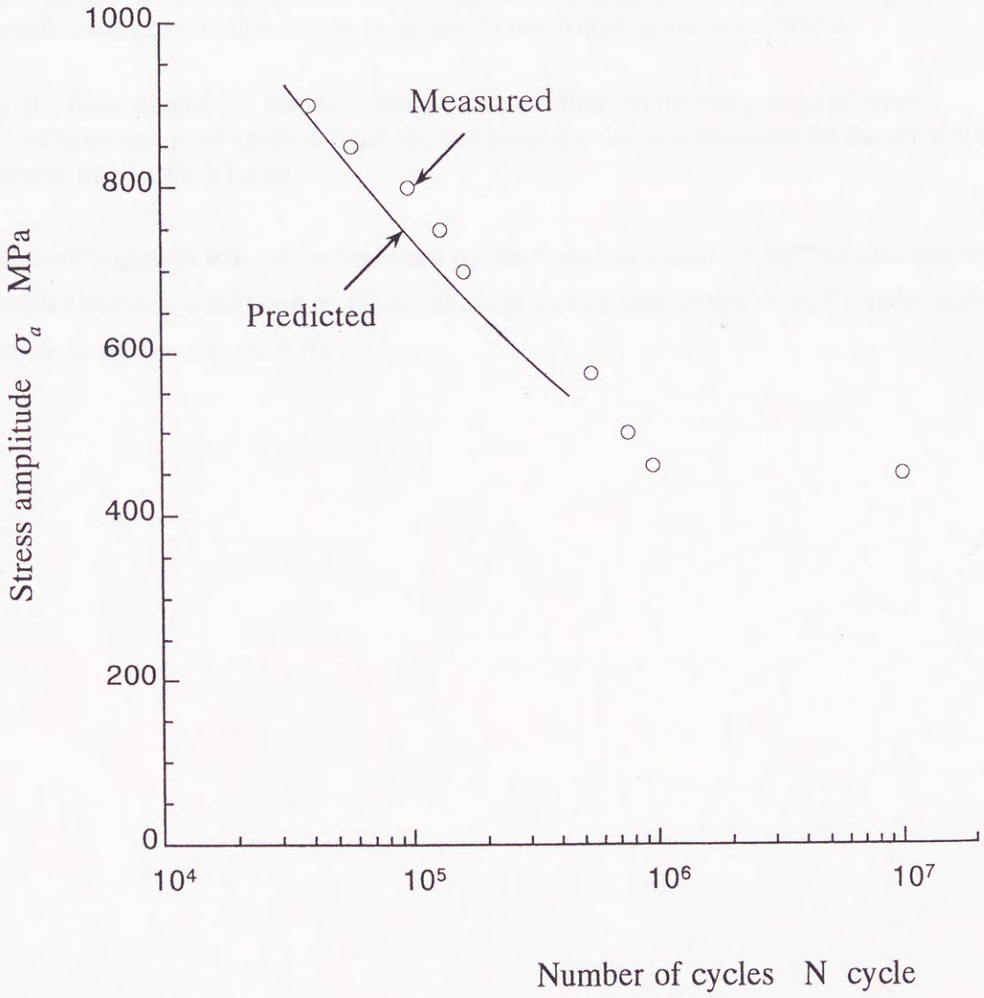

Fig. 2.16 Life prediction for plain specimens based on the small crack growth law.

2.4 Conclusions

Rotating bending fatigue tests were carried out for Inconel 718 at room temperature. The fatigue behavior of small cracks were investigated through the observation of crack initiation and crack propagation. The conclusions obtained are as follows.

(1) A fatigue crack in the plain specimens propagates transgranularly accompanied with the formation of striations after being initiated from slip bands near grain boundary.

(2) The fatigue limit of the alloy at room temperature is determined by the limiting stress for small crack growth; this feature is similar to that found in irons and steels.

(3) In the finite fatigue life region, a fatigue crack initiates in the early stage of stress repetitions and most of the fatigue life in a plain specimen is occupied by the growth life of cracks smaller than 1 mm.

(4) The crack growth rate can be evaluated by the Paris law ($dl/dN \propto \Delta K^m$) under low stress levels ($\sigma_a/\sigma_{0.2} < 0.5$) and by the small crack growth law ($dl/dN \propto \sigma_a{}^n l$) under high stress levels ($\sigma_a/\sigma_{0.2} > 0.6$).

References

(1) Samuelson, E. Et al., *JOM*, **42**-8 (1990), pp. 27-30.

(2) Hicks, P. D. & Altstetter, C.J., *Metall. Trans. A*, **214**-2 (1990), pp. 365-372.

(3) Pedron, J.P. & Pineau, A., *Mater. Sci. Eng.*, **56**-2 (1982), pp. 143-156.

(4) Ghonem, H. Et al., *Fract. Eng. Mater. Struct.*, **16** (1993), pp. 565-576.

(5) Kawagoishi, N., et al., *Trans. Jpn Soc. Mech. Eng.*, (in Japaness), **62**-596 A (1996), pp. 960-965.

(6) Matubara, M. & Nitta, A., *Trans. Jpn Soc. Mech. Eng.*, (in Japaness), **57**-540 A (1991), pp. 1726-1731.

(7) Okazaki, M., et al., *Trans. Japan Society of Materials Science*, (in Japaness), **44**-498 (1995), pp. 348-354.

(8) Smith, H.H. & Michel, D.J., *Metall. Trans.*, **17**A (1986), pp. 370-374.

(9) Ghonem, H. & Zheng, D., *Mater. Sci. Eng.*, A**150** (1992), pp. 151-160.

(10) Nisitani, H. & Nishida, S., *Trans. Jpn Soc. Mech. Eng.*, (in Japaness), **39**-321(1973), pp. 1385-1392.

(11) Yamada, K. & Kunio, T., *Trans. Jpn Soc. Mech. Eng.*, (in Japaness), **45**-393 A (1979), pp. 440-447.

(12) Paris, P.C. & Erdogan, F., *Trans. ASME. J. Basic Eng.*, **85**-4 (1963), pp. 528-534.

(13) Nisitani, H., *Mechanics of Fatigue-AMD*, **47** (1981), pp. 151-166, ASME.

(14) Nisitani, H. & Kawagoishi, N., *JSME Int. J.*, **35**-1, A (1992), pp. 1-11.

Chapter 3 Initiation and early growth behavior of a small fatigue crack at elevated temperatures

3.1 Introduction

For materials employed in the aerospace and nuclear applications, the severe operating conditions such as the heavy load, corrosive environment and high temperature are quite routine and the influence of environmental parameters on the fatigue strength of the materials as well as the behavior of a small fatigue crack in the materials is an important factor to be mastered by both the machine designers and material manufacturers.

As mentioned previously, nickel-base superalloys are usually applied as the critical components of jet engines and gas turbines and a great deal of attentions has been given to their creep properties[1], fatigue characteristics at high temperature[2]~[7] and strength estimation at corrosive environment. However, as regard the initiation of a small fatigue crack in nickel-base superalloys, many mechanisms have been reported including the transgranular or intergranular slips on the surface[8], precipitates cracking[9], shrinkage[10] as well as the interiors fracture under the oxide films at elevated temperature[11], indicating that the initiation mechanism of a small fatigue crack differs with the kinds of alloys, the stress levels and the environmental conditions. Particularly, the crack initiation becomes more complicated at elevated temperatures because the influence of surface oxidation must be taken into account[11],[12]~[14] besides the change of mechanical properties of materials. Consequently, the behavior of a small fatigue crack at elevated temperatures is necessary to be thoroughly clarified for each alloy in order to satisfy the needs of material selecting in practice.

In chapter 2, the behavior of a small fatigue crack at room temperature was investigated and some important conclusions were obtained. Continuously, in this chapter, the effect of temperature on the behavior of a small fatigue crack, especially the initiation and early growth behavior, is to be examined through rotating bending fatigue tests at the elevated temperatures of 300°C, 500°C and 600°C. Testing at room temperature is also performed for comparison. The effect of temperature will be discussed from the interaction of the softening of matrix with the increase of temperature and the oxidation on the surface of specimens at elevated temperatures. While the effect of temperature on the behavior of small crack growth in steady stage propagation will be investigated in chapter 4.

3.2 Material and experimental procedures

The material used was the same as in chapter 2. Table 3.1 shows the mechanical properties of the material at all the tested temperatures.

The observation of the fatigue behavior of small crack initiation and its early propagation, the partially notched specimens were employed (Fig. 3.1). However, the decrease of the fatigue strength owing to the partial notch was very small, in fact, the strength reduction factors at all the tested temperatures were less than 1.1 (Table 3.2), so that the partially notched specimens can be dealt with as the plain ones. The stress amplitude, σ_a, is determined by the nominal stress of net area with the existence of the partial notch ignored.

The preparation of specimens, the observation of fatigue process as well as the measurement of crack length were conducted in the same way as mentioned in chapter 2. The formation and the variation of oxide films on the specimen surface were analyzed using the Electron Spectroscopy for Chemical Analysis (ESCA) technique. For the tests performed at the elevated temperatures, the fatigue process was monitored by stopping machine at the specified intervals of stress repetitions, cooling down the specimen to take the plastic replicas, then heating up the specimen again to continue the next interval of the tests. However, the influence of the repetitious heating and cooling process on the fatigue life of specimens was almost not recognized.

The tests were carried out at room temperature and the elevated temperatures of 300°C, 500°C and 600°C using the Ono-type rotating bending fatigue testing machine for high temperature purpose with a capacity of 100 N·m operating at about 55 Hz. The stress repetitions were commenced one hour later after the established temperature on the specimen surface was reached. The temperature was detected by a thermocouple with the front of sensor fixed 3 mm apart from the specimen surface and was preserved at the precision of ± 3°C by a Proportional-Integral-Differential (PID) controller.

Table 3.1 Mechanical properties at all the temperatures

Temperature	0.2% proof stress $\sigma_{0.2}$ (MPa)	Tensile strength σ_B (MPa)	True breaking stress σ_T (MPa)	Reduction of area ψ (%)
R.T.	1320	1461	2320	70.0
300°C	1127	1335	1987	44.0
500°C	1050	1254	1734	38.4
600°C	1070	1226	1848	45.0

Table 3.2 Strength reduction factors at all the temperatures

Temperature	Fatigue limit of plain specimen σ_{w0} (MPa)	Fatigue limit of partially notched specimen σ_w (MPa)	Strength reduction factors $K_t = \sigma_{w0}/\sigma_w$
R.T.	500	460	1.09
300°C	610	600	1.02
500°C	700	680	1.03
600°C	630	610	1.03

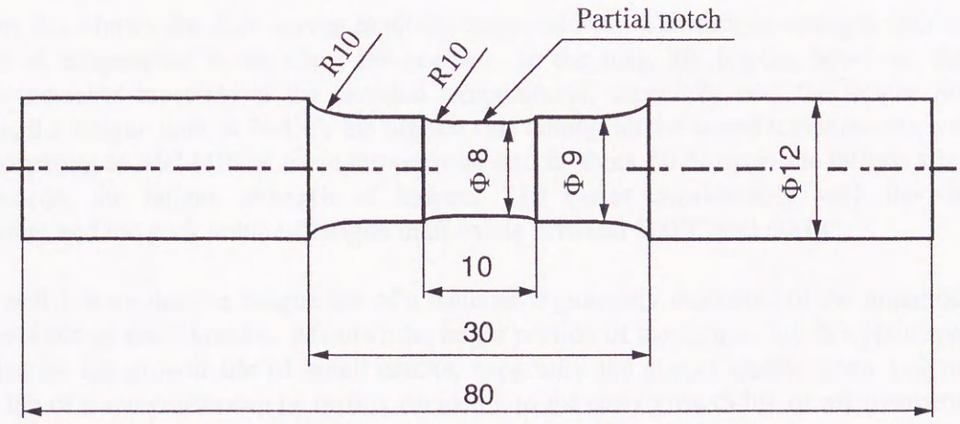

Detail of partial notch

Fig. 3.1 The shape and dimensions of partially notched specimen (in mm).

3.3 Experimental results

3.3.1 Fatigue strength at elevated temperatures

Figure 3.2 shows the *S-N* curves at all the temperatures. The fatigue strength decreases with increase of temperature in the short life region. In the long life region, however, the fatigue strength increases inversely at the elevated temperatures, especially near the fatigue limit. For example, the fatigue limit at 500°C, the highest one among all the tested temperatures, values 680 MPa comparing to 460 MPa at room temperature and is about 50 % up in the fatigue strength. In other words, the fatigue strength of Inconel 718 varies considerably with the change of temperature and the peak value of fatigue limit exists between 500°C and 600°C.

It is well known that the fatigue life of a material is generally consisted of the initiation life and the growth life of small cracks. Meanwhile, larger portion of the fatigue life in a plain specimen is controlled by the growth life of small cracks, especially the cracks smaller than 1~2 mm. The growth life of small cracks can be further divided into the early growth life of microstructural small cracks and the steady crack growth life of larger cracks. Therefore, this chapter mainly concerns the influence of temperature on the crack initiation and its early propagation. While the influence of temperature on the steady crack propagation will be discussed in chapter 4.

3.3.2 Initiation and early growth behavior of a small fatigue crack at elevated temperatures

The changes in surface state with stress repetitions at all the temperatures are compared under the same stress level of σ_a = 800 MPa, as shown in Fig. 3.3. The crack tips are indicated by arrows in Fig. 3.3, and the same below. At each temperature, a fatigue crack initiates at the early stage of stress repetitions from surface slip band near the grain boundary. The fatigue damage increases with temperature and the initiated cracks tend to propagate in the direction vertical to the stress axe at higher temperature.

However, the influence of temperature on the fracture mechanism of the alloy is not recognized because the striations on the fracture surface of specimens are observed at all the temperatures, as shown in Figs. 2.6 and 3.4. Furthermore, the stress dependence of the fracture mechanism is not recognized.

Figure 3.5 shows (a) crack growth curves and (b) crack growth rate curves at room temperature and 500°C, under the high stress level, σ_a = 700 MPa, under which the fatigue strength was increased to be higher at elevated temperature than at room temperature. Figure 3.6 shows the crack growth curves at each temperature for specimens which have very close fatigue life to the number of 4 x 10^5 cycles. The results in Figs. 3.5 and 3.6 can be summarized as the follows:

(1) The effect of temperature on the crack initiation is small though a fatigue crack tends to initiate earlier at higher temperature. However, the difference between the elevated temperatures is small.

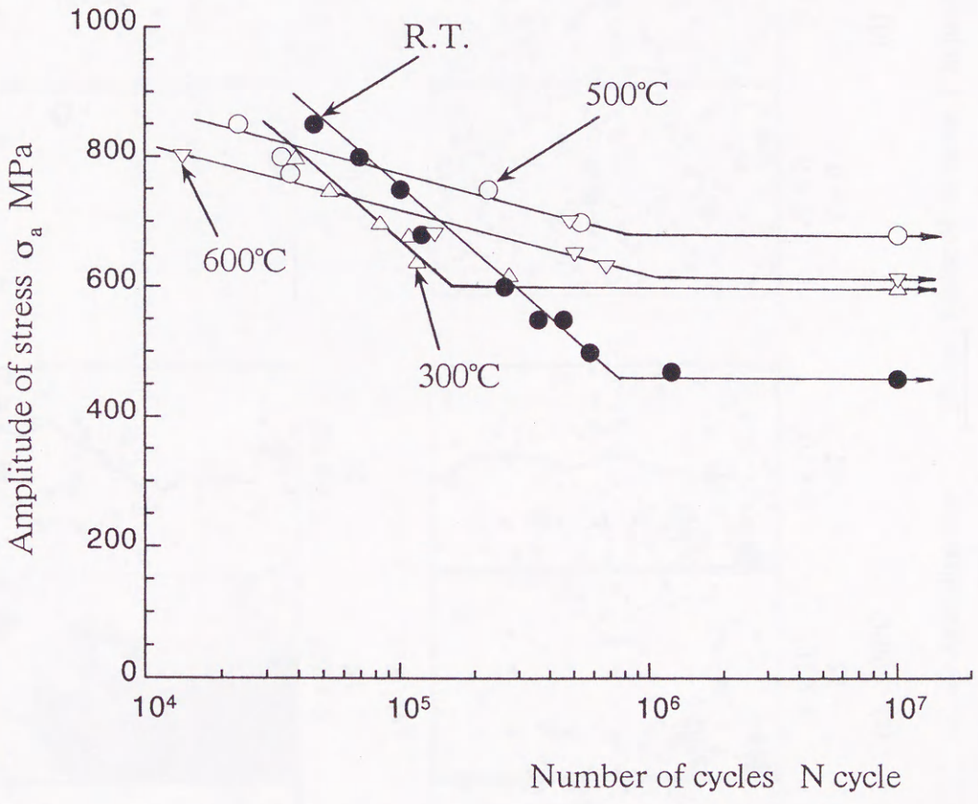

Fig. 3.2 *S-N* curves at all the temperatures.

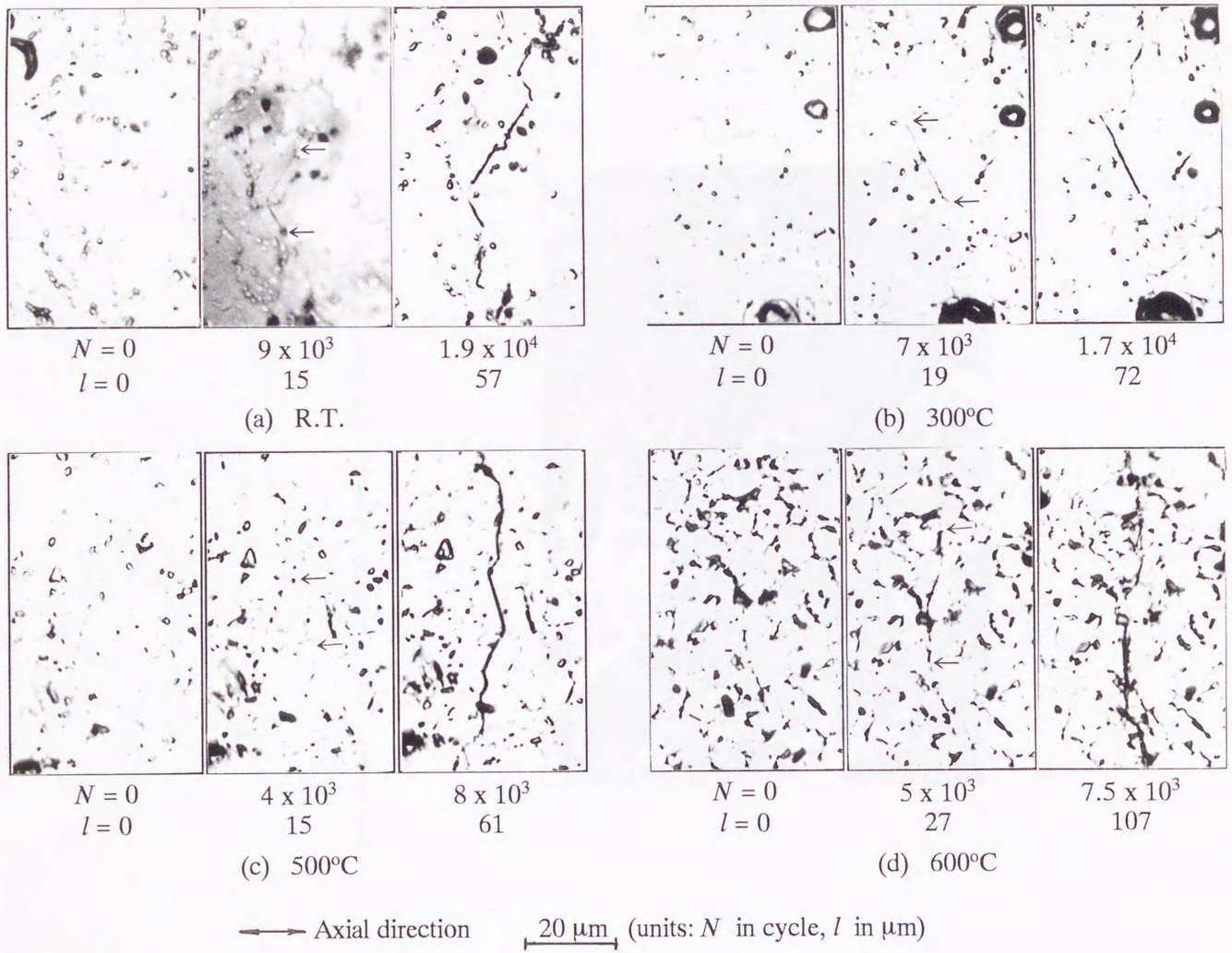

Fig. 3.3 Change in surface state of specimen with stress repetition at all the tested temperatures (σ_a = 800 MPa).

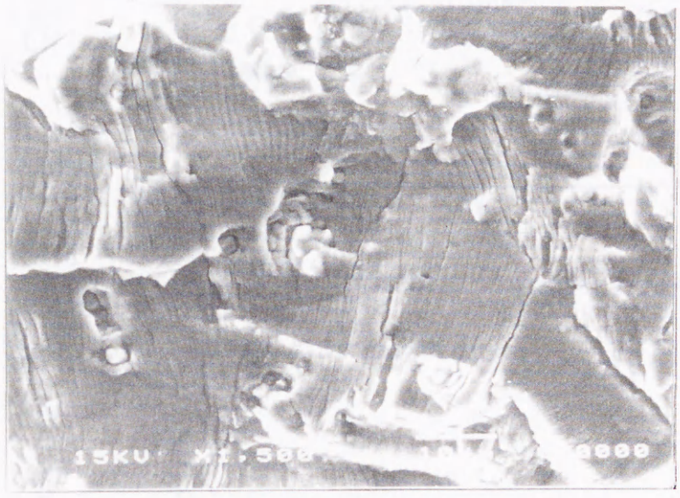

Fig. 3.4 SEM photograph of fracture surface at 500°C (Striations).

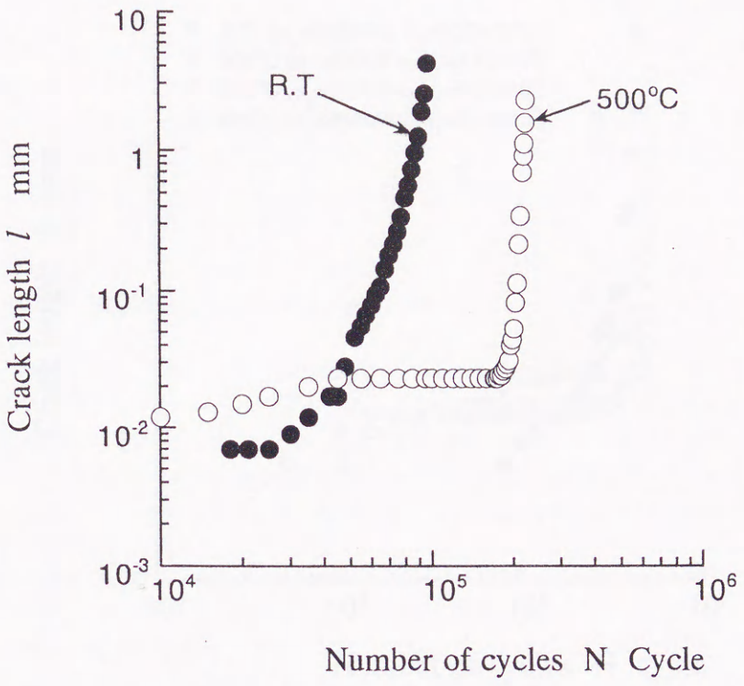

(a) Crack growth curves

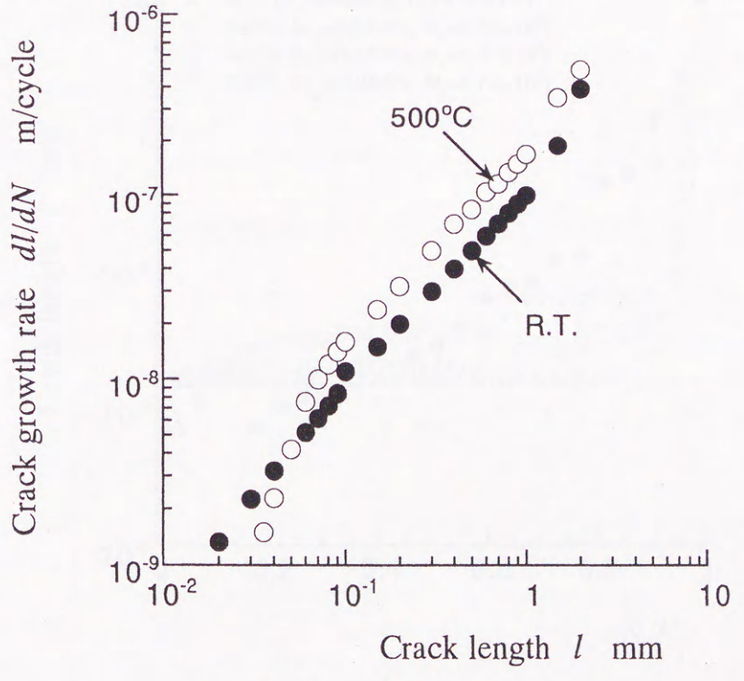

(b) Crack growth rate curves

Fig. 3.5 Comparison of the crack growth data between R.T. and 500°C (σ_a = 800 MPa).

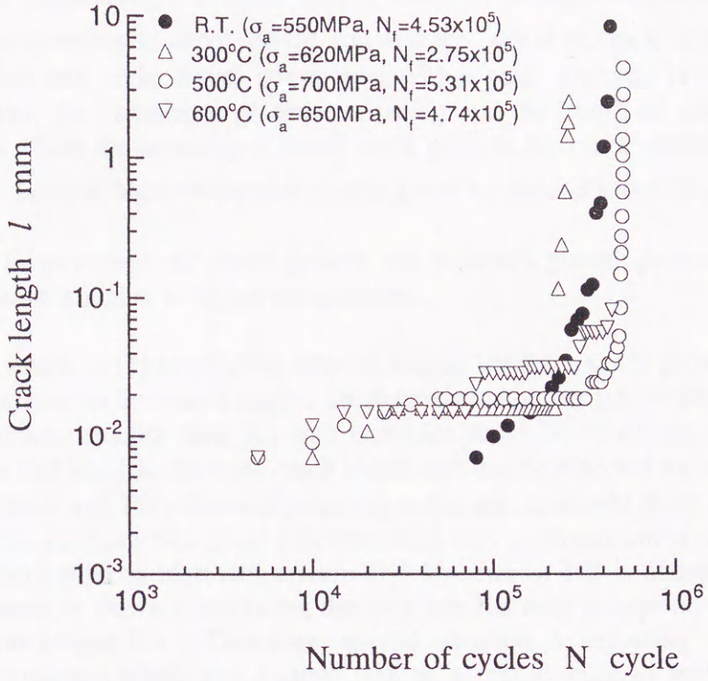

(a) $l-N$

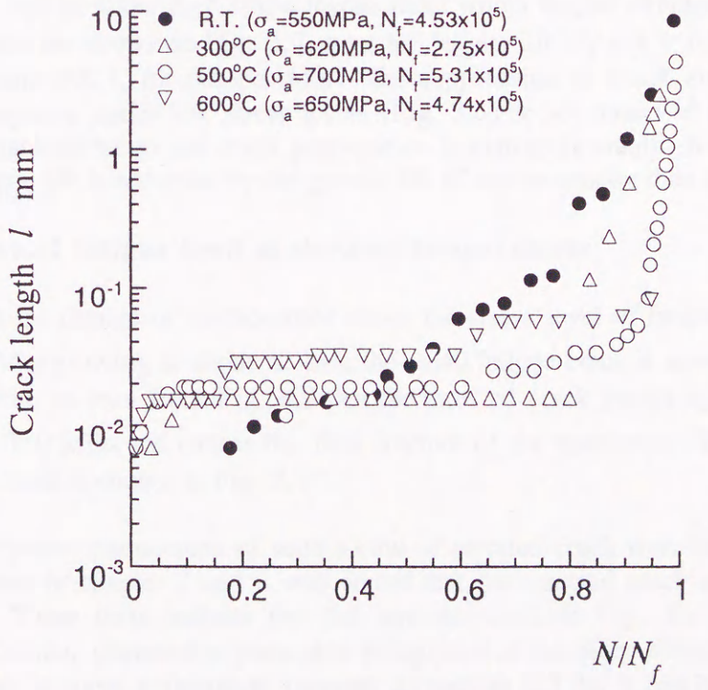

(b) $l-N/N_f$

Fig. 3.6 Crack growth curves near the fatigue life N_f = 4 x 10^5 cycles.

(2) At the elevated temperatures, a small fatigue crack is arrested temporally from further propagating after growing to about 20~30 μm and the period of crack arresting extends at higher temperature and under lower stress level with a peak observed between 500°C and 600°C. However, the commence of crack arresting and the length of arrested cracks are nearly the same. After the arresting of small crack growth, the crack continues propagation and grows more faster at higher temperature after growing beyond about 50 μm.

(3) At the elevated temperatures, the crack growth rate at steady growth process after the crack growth suppression is higher at higher temperature.

(4) Therefore, as a result of (1) to (3), the ratio of fatigue life for a crack growing through the steady growth process to the whole fatigue life decreases at higher temperature, especially the growth life of cracks smaller than 0.1 mm occupies about 90 % of the total fatigue life. Considering this fact and that the least crack length that can be detected by means of modern detecting techniques, e.g. the ultrasonic detecting technique, is merely about 0.25 mm[15], the detection of cracks or flaws which are less than 0.25 mm in dimension is nearly impossible in practical services such as high temperature and low stress, and is of less significance to find out such cracks or flaws if reminding the very less life ratio occupied by such cracks or flaws in the total fatigue life. Therefore, special attention is necessary in the design of machines and structures which use Inconel 718 as a critical material and service at high temperature environment.

The crack growth curves under high stress levels under which fatigue strength decreases with increase of temperature are shown in Fig. 3.7, near the fatigue life $N_f = 4 \times 10^4$ cycles at room temperature, 300°C and 500°C for comparison. The suppression of crack growth at elevated temperature which happens under low stress levels (Fig. 3.6) is not observed and the effect of temperature on the crack initiation and crack propagation is extremely small. It is also clear that larger amount of fatigue life is occupied by the growth life of cracks smaller than 1 mm.

3.3.3 Significance of fatigue limit at elevated temperatures

Figure 3.8 shows the change of surface state under the stress level of fatigue limit at 500°C (σ_{w0} = 680 MPa). After growing to about 23 μm, the small fatigue crack is arrested from further propagating. However, as seen from Fig. 3.9 that the arrested crack grows again under higher stress level of σ_a = 750 MPa and causes the final fracture of the specimen. The crack growth curve of the arrested crack is shown in Fig. 3.10.

The opening and closure phenomena of such a kind of arrested crack were investigated in the same way as described in chapter 2 and it was found that the arrested crack opened under the maximum tension. These facts indicate that the arrested crack in Fig. 3.8 is really a non-propagating crack. Similar phenomena were also recognized at the other elevated temperatures. Considering the result at room temperature (chapter 2, section 2.3.3), it can be concluded that although a fatigue crack in Inconel 718 initiated at the early stage of stress repetitions, it was arrested from further propagating and became a non-propagating crack after growing up to about 20~30 μm on the surface of specimen, signifying that the fatigue limit of plain specimen in Inconel 718, irrespective of temperature, is determined by the limiting stress for small crack growth.

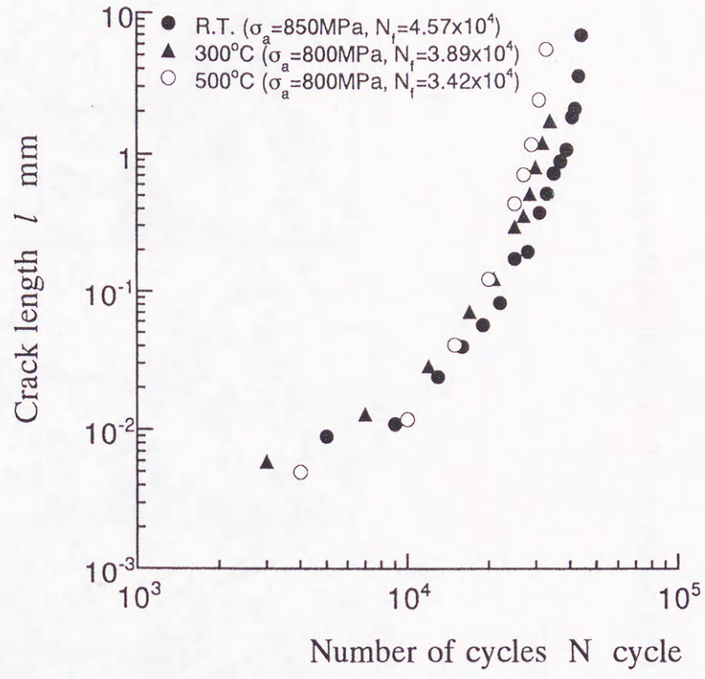

(a) $l-N$

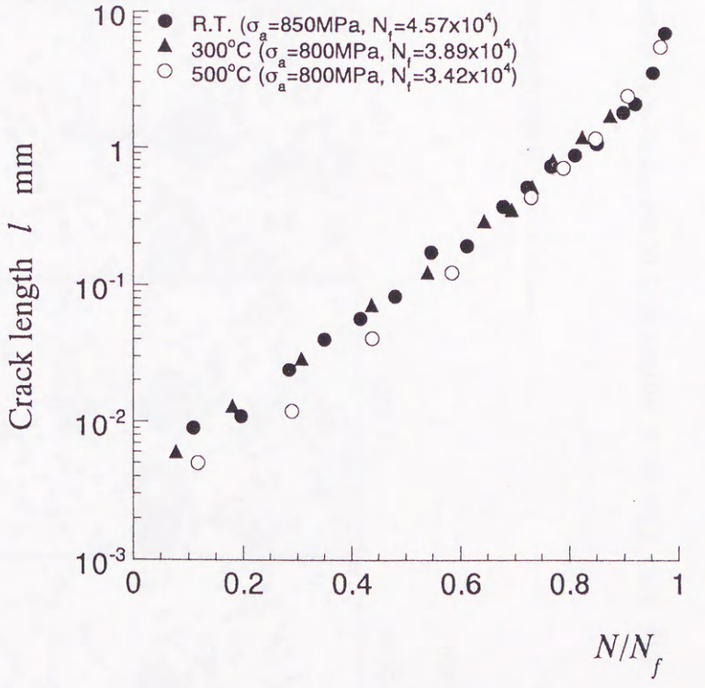

(b) $l-N/N_f$

Fig. 3.7 Crack growth curves near the fatigue life N_f = 4 x 10^4 cycles.

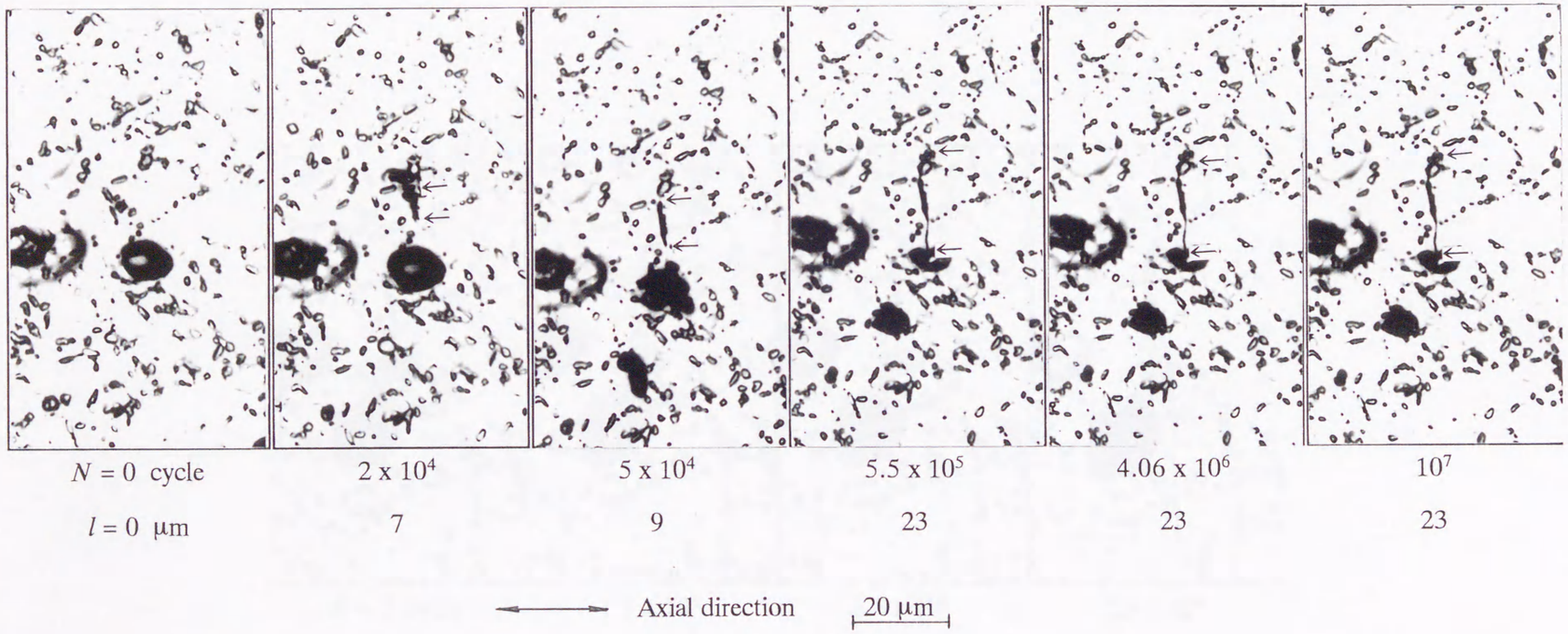

Fig. 3.8 Change in surface state of specimen with stress repetition at the fatigue limit (σ_{w0} = 680 MPa) at 500°C.

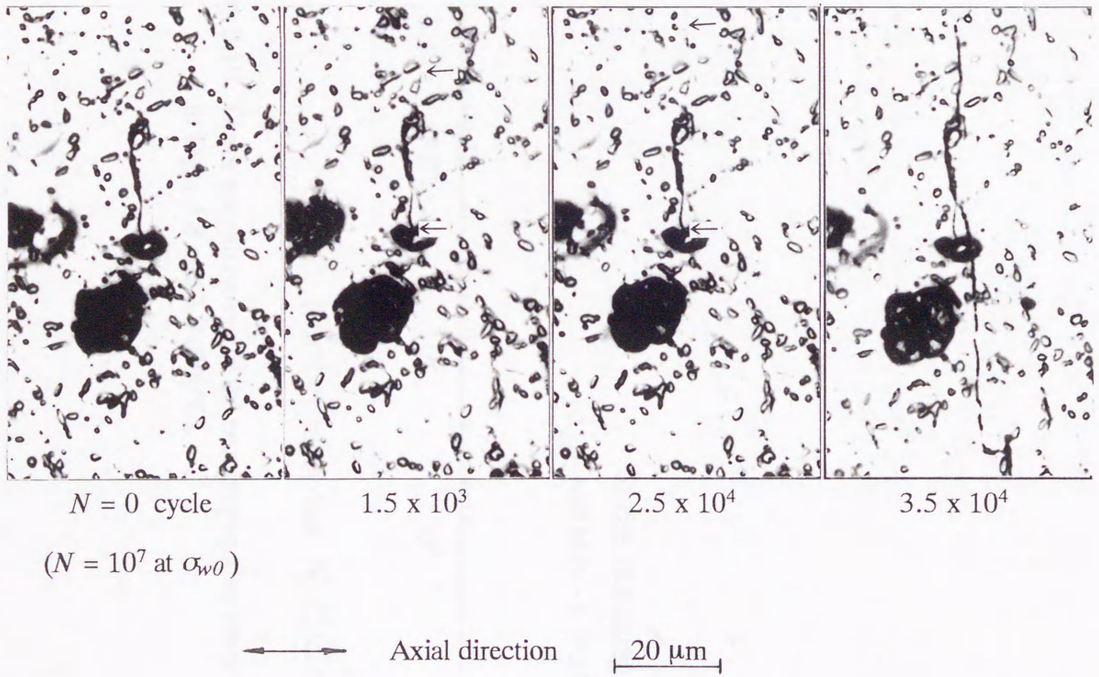

Fig. 3.9 Growth behavior of the arrested crack in Fig. 3.8 under high stress ($\sigma_{w0} \rightarrow 750$ MPa).

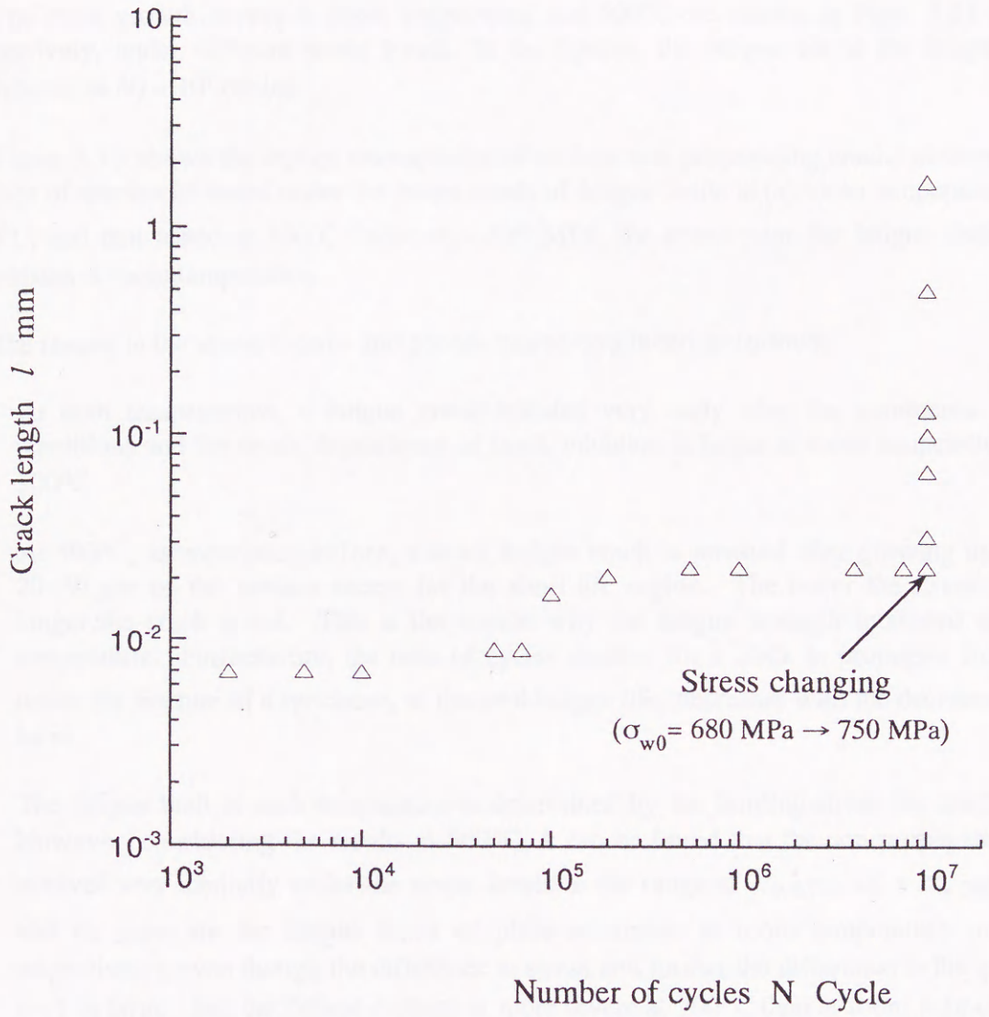

Fig. 3.10 Crack growth curves of the non-propagating crack in Figs. 3.8 and 3.9 (500°C).

3.3.4 Stress dependence of small crack initiation and its early growth

The crack growth curves at room temperature and 500°C are shown in Figs. 3.11 and 3.12 respectively, under different stress levels. In the figures, the fatigue life at the fatigue limit is designated as $N_f = 10^7$ cycles.

Figure 3.13 shows the replica microphotos of surface non-propagating cracks observed on the surface of specimens tested under the stress levels of fatigue limits at (a) room temperature and (b) 500°C, and that tested at 500°C under σ_a= 500 MPa, the stress near the fatigue limit of plain specimens at room temperature.

The results in the above figures and photos can be concluded as follows.

(1) At both temperatures, a fatigue crack initiated very early after the commence of stress repetitions and the stress dependence of crack initiation is larger at room temperature than at 500°C.

(2) At 500°C, as mentioned before, a small fatigue crack is arrested after growing up to about 20~30 μm on the surface except for the short life region. The lower the stress level, the longer the crack arrest. This is the reason why the fatigue strength increased at elevated temperature. Furthermore, the ratio of cycles number for a crack to propagate from 20~30 μm to the fracture of a specimen, to the total fatigue life, decreases with the decrease of stress level.

(3) The fatigue limit at each temperature is determined by the limiting stress for crack growth. However, considering the results at 500°C, it can be found that the non-propagating cracks behaved very similarly under the stress levels in the range of $\sigma_{w\ RT} < \sigma_a < \sigma_{w\ 500°C}$ ($\sigma_{w\ RT}$ and $\sigma_{w\ 500°C}$ are the fatigue limits of plain specimens at room temperature and 500°C, respectively), even though the difference in stress and further the difference in the quantity of $\sigma\sqrt{l}$ is large. But the fatigue damage is more severe at 500°C than at room temperature due to the softening of matrix. Moreover, in the case of 500°C, the fatigue damage is more severe under higher stress.

Consequently, the influence of temperature on the fatigue behavior of Inconel 718 is more remarked in the early growth process of small cracks than in the crack initiation process.

Figure 3.14 shows the relation of crack length with the life ratio, $(N-N_{0.05})/(N_f-N_{0.05})$, in the steady growth process of cracks larger than about 50 μm, at (a) 500°C and (b) all the temperatures. In Fig. 3.14, $N_{0.05}$ is the growth life for an initiated crack to grow to 50 μm. It can be seen that in the relation of l versus $(N-N_{0.05})/(N_f-N_{0.05})$, the effect of stress level as well as that of temperature are almost ignorable, a result corresponding to the fact that the stress dependence of crack growth rate is nearly the same and values about 5 at each temperature (chapter 4, Fig. 4.7). This means that for cracks larger than 50 μm, the growth life will approximately follow the linear cumulative law, irrespective of the changing of the stress and the temperature.

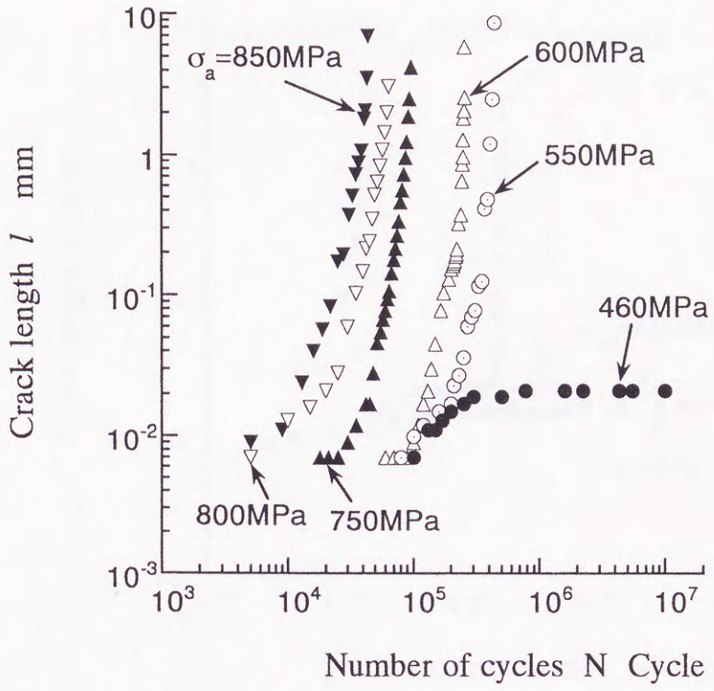

(a) l versus N

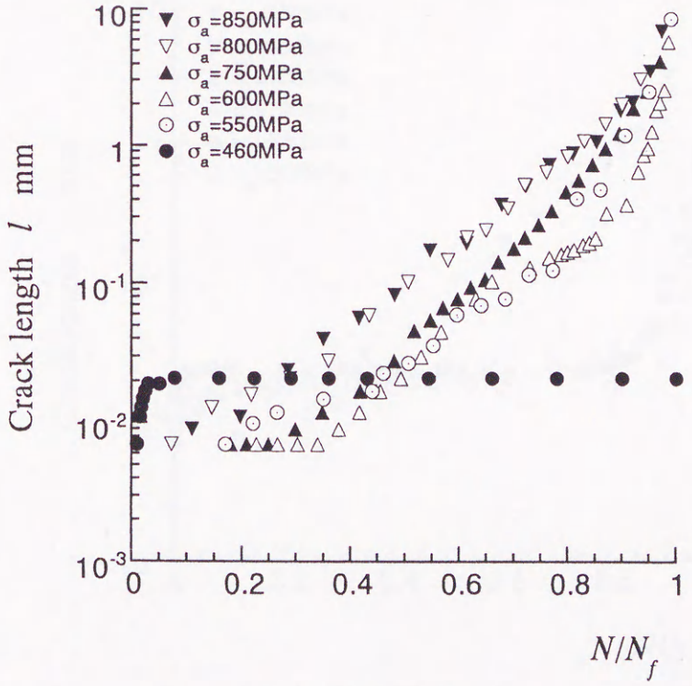

(b) l versus N/N_f

Fig. 3.11 Crack growth curves at room temperature.

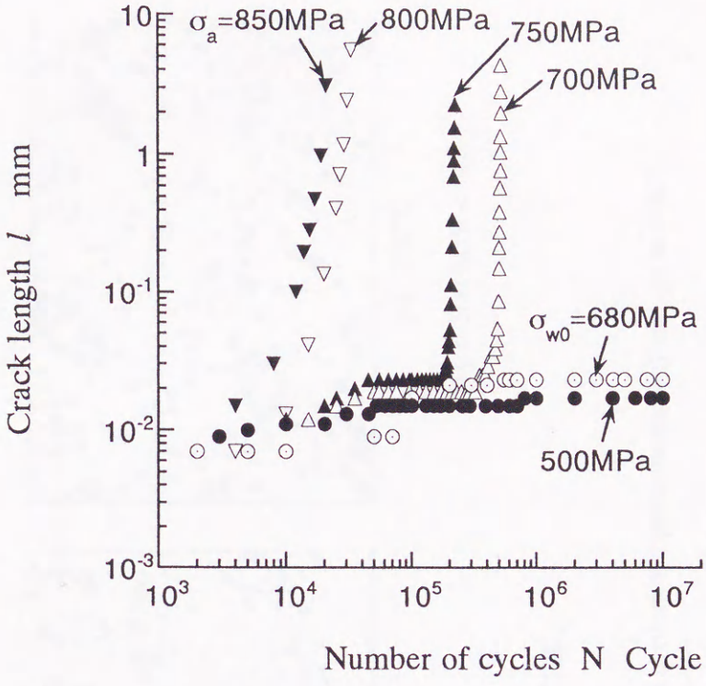

(a) l versus N

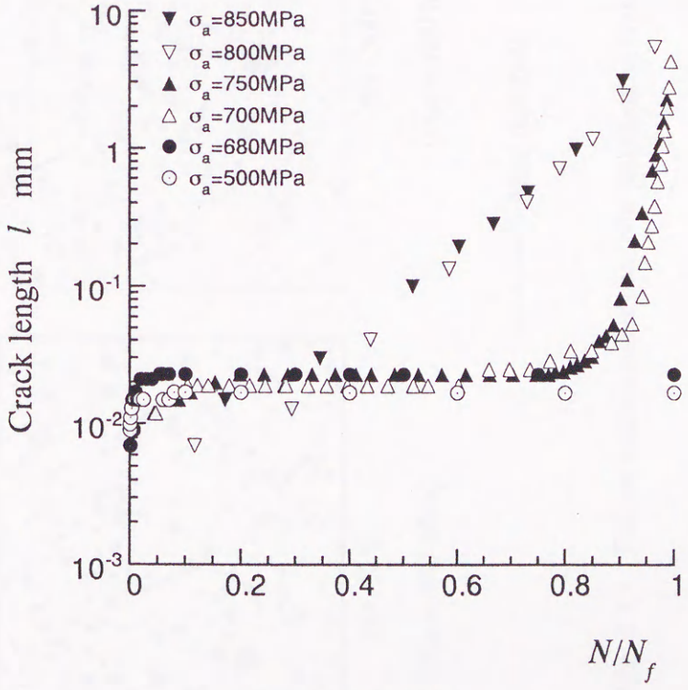

(b) l versus N/N_f

Fig. 3.12 Crack growth curves at 500°C.

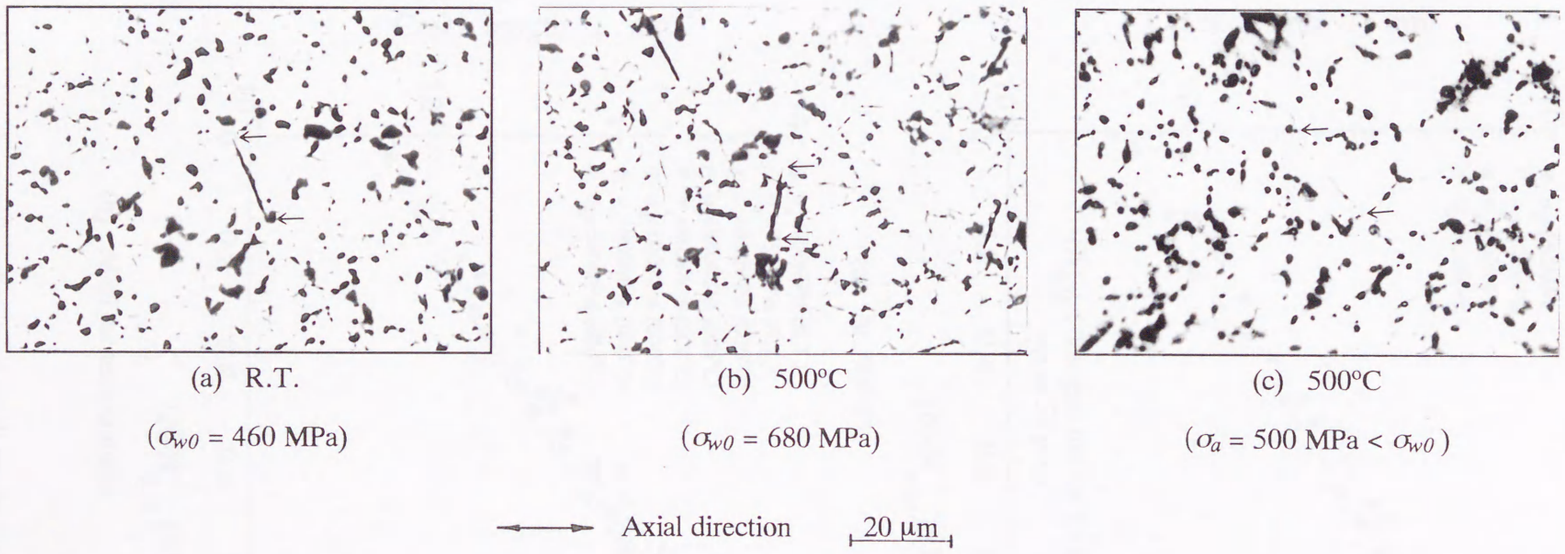

Fig. 3.13 Fatigue surface states near non-propagating cracks (a) at room temperature and (b) and (c) at 500°C.

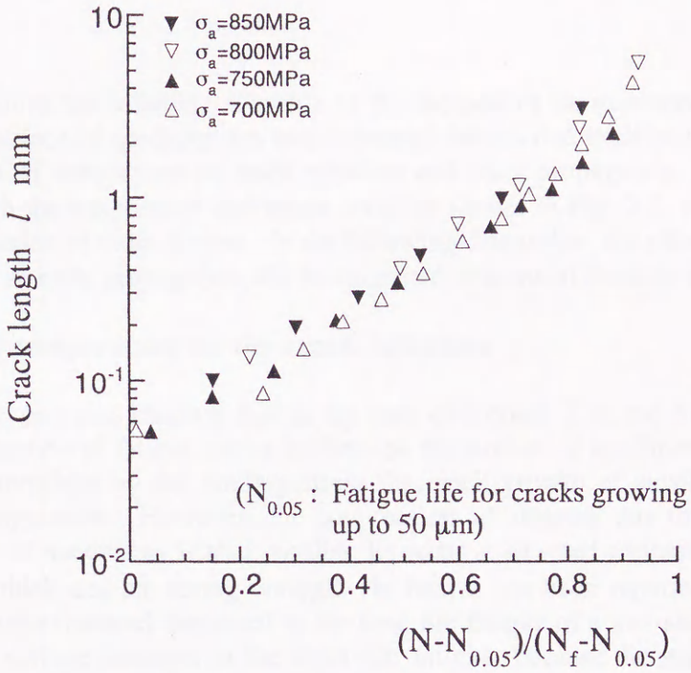

(a) At 500°C

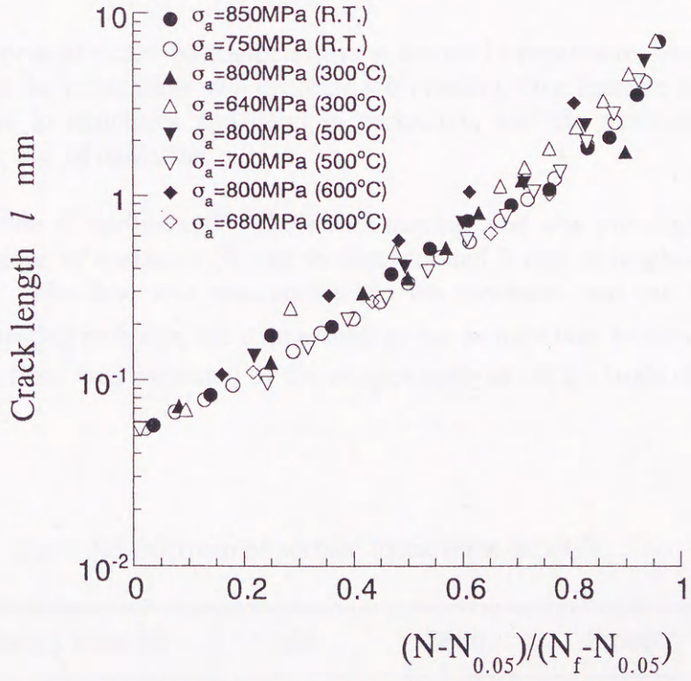

(b) At all the temperatures

Fig. 3.14 Crack growth behavior of small cracks larger than 50 μm.

3.4 Discussion

At elevated temperature, the softening of matrix or the decrease of the resistance to slipping and the oxidation on the surface of specimen are two important factors that must be considered in the research into the effect of temperature on crack initiation and crack propagation. And the change of fatigue strength with the temperature and stress level, as shown in Fig. 3.2, can be concerned as a result of the interaction of these factors. In the following discussion, the effect of temperature on crack initiation and its early propagation will be examined in terms of these two factors.

3.4.1 The effect of temperature on the crack initiation

As known from the previous chapters that in the case of Inconel 718, the fracture is usually caused from the propagation of fatigue cracks initiated on the surface of specimens (Fig. 3.3) and the fatigue limit is determined by the limiting stress for crack growth of small surface cracks, irrespective of the temperature. However, the suppression of slipping due to the oxide films formed on the surface of specimens is also possible to occur at elevated temperatures so long as the oxide films grow thick and are strong enough. In fact, it has been reported[16] that fisheye fracture (a kind of interior fracture) happened in the long life fatigue of a low-alloy steel SCMV2 which fractured from surface damages in the short life fatigue, because the surface slipping or surface crack initiation was suppressed by the oxide films thicker than 1 μm. Similar interior fracture was also observed in an dispersion-strengthened nickel-base superalloy MA758[11].

In the oxidation process of nickel-base superalloys at elevated temperature, however, the rate of increase in thickness of the oxide films will decrease with heating time because the oxides formed on the surface are fine in structures and good in protective, and the oxidation rate decreases following the parabolic law of oxidation.

The thickness variation of surface oxide films with heating time was investigated at 500°C by ESCA using a small piece of specimen (8 mm in diameter and 3 mm at height) under zero load condition (Table 3.3). The time was measured when the specimen was put into the attached furnace of the fatigue testing machine, the temperature in the furnace was preserved at 500 ±3°C. The thickness of oxide films was estimated by the oxygen analysis on the basis of Ar^+ etching rate (about 0.017 nm/s) [17].

Table 3.3 Growth of surface oxide films at 500°C

Heating Time (s)	180	3600	21600
Thickness (μm)	0.34	0.48	0.73

The thickness of oxide films increases rapidly to be about 0.34 μm in merely 3 minutes after the beginning of heating, but it is only about twice as much as that in the early heating even being heated continuously for 6 hours, the time corresponding to the repetitions of 10^6 cycles in the fatigue tests. However, the thickness of oxide films is estimated to be able to increase to about 1 μm when heated for about 60 hours, the time equal to the repetitions of 10^7 cycles.

Similar research has been carried out by Lenglet et al.[18] at high temperatures of 800°C, 900°C and 1000°C under zero load condition. It was found that oxide films formed quickly on the surface of Inconel 718 and then grew slowly, but the films became more thicker at higher temperature (e.g., about 1 μm when heating up to 1000°C).

The effect of oxide films on crack initiation was investigated for the specimen which was cyclically stressed for 10^7 cycles at the fatigue limit at 600°C. The oxide films was lightly removed by electro-polishing. The change of surface state of the specimen during the fatigue process and after electro-polishing are presented in Fig. 3.15.

It can be seen that besides the slip bands and the non-propagating crack (denoted as A in Fig. 3.15) observed before and after electro-polishing, a slip band or subcrack (denoted as B in Fig. 3.15) which is concealed by the oxide films during the fatigue process, appeares on the specimen surface after electro-polishing. This provides a evidence that the growth of slip bands or subcracks is suppressed by the oxide films.

On the other hand, because the oxides formed on the surface of Inconel 718 are chemically stable and easy to be reproduced when broken, therefore, it is possible that the initiated slip bands or cracks may be concealed from observing by the subsequently formed oxide films. However, no sign in Fig. 3.15 shows the disappearance or haziness of slip bands or cracks (e.g., crack A) which initiate in the early stage of stress repetitions. Similar phenomenon was observed at the other temperatures.

Figure 3.16 shows SEM photographs of fractured surfaces at 500°C and 600°C. At each temperature, the crack initiation occurs from the surface of specimens and the interior fracture is not observed even at 500°C. However, as the softening of matrix will proceed more seriously and the oxide films will grow more thicker at higher temperature, the possibility of interior fracture could not be negated.

Consequently, it can be concluded that the effect of temperature on the crack initiation in Inconel 718 can be evaluated from two contradictory ways, one is the suppression action due to the oxide films formed on the surface of specimens and the other is the promotion action owing to the softening of matrix.

The surface fracture and the earlier initiation of small fatigue cracks at the elevated temperatures, however, can be explained as a result that the oxide films formed on the surface of specimens was too thin to suppress the crack initiation efficiently.

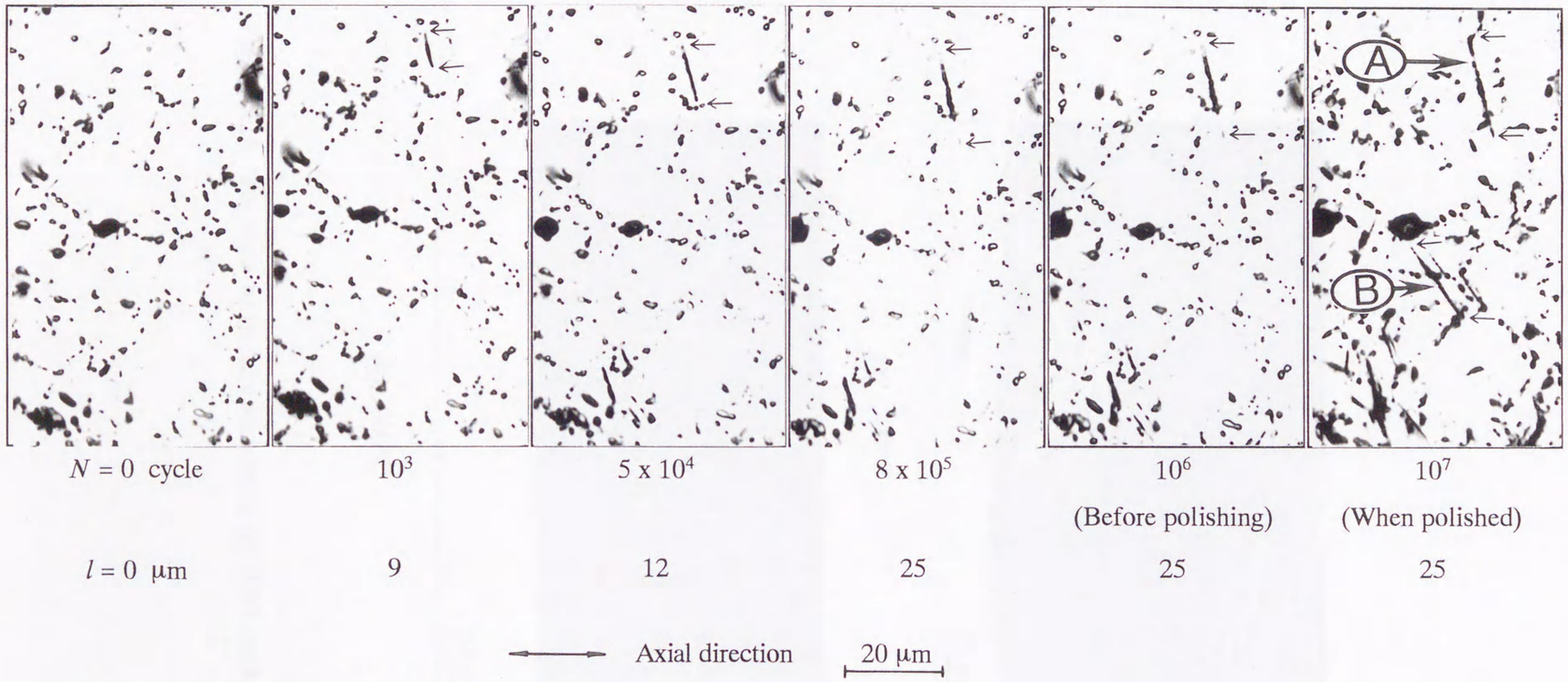

Fig. 3.15 Change in surface state of specimen with stress repetition at the fatigue limit (σ_{w0} = 610 MPa) at 600°C.

(a) 500°C

(b) 600°C

Figure 3.16 Top view of fracture surfaces at (a) 500°C and (b) 600°C.

3.4.2 The effect of temperature on the early crack growth

As above mentioned, the softening of matrix at elevated temperature leads to the reduction of fatigue crack growth resistance or the increase of crack growth rate (for details refer to chapter 4). Meanwhile, the growth of small cracks is remarkably suppressed in their early propagation process at elevated temperature and this is a fact contradicting with the softening of matrix and has to be explained by the decrease of crack propagating force.

Two important factors are considered to be responsible for the suppression of small crack growth. One is the crack closure caused by the oxidation on crack faces and the other will be the compressive residual stress generated on the surface of matrix due to the difference in the coefficient of thermal expansion between the oxides and the matrix. Regarding to the crack closure, it can be seen from Table 3.3 that the oxide films form rapidly in the early heating and can grow up to nearly 1 μm in thickness, a sufficient thickness for the crack closure of small cracks in the length of 20~30 μm growing at 10^{-9}~10^{-8} m/cycle, hence decrease the small crack growth rate.

However, the propagation after the small crack suppression at elevated temperatures can not be explained only by the phenomenon of crack closure. The action of compressive residual stress on the surface of matrix is necessary to be considered.

It has been reported [8], [18] that at elevated temperatures, the oxides on the surface of Inconel 718 are mainly composed of the oxides of Fe, Ni and Cr and the coefficient of thermal expansion of these oxides are smaller than that of matrix, so that a compressive residual stress creates on the surface of matrix. The combined suppressive effect of these two factors, therefore, hinder the early propagation of small cracks at elevated temperatures. But the compressive residual stress will release gradually with the stress repetitions at elevated temperature, hence the crack propagating force will increase. If the crack propagating force is great enough to overcome the suppressive force, then the suppressed small cracks will propagate again and become macro cracks and lead to final fracture. Otherwise, they will become the non-propagation cracks. The shorter stagnation at higher stress levels is then concerned to be relative to the faster releasing of the compressive residual stress.

Therefore, the phenomena of crack suppression in the early crack propagation at elevated temperature can be explained as a result of the formation of oxide films on the surface of specimen which promotes the crack closure and the generation of compressive residual stress and then reduces the crack growth rate.

To ascertain the above hypothesis, the following experiment was performed in which the effect of temperature can be evaluated from the effect due to the oxide films and the effect due to the softening of matrix, separately. The experiment was carried out at room temperature under the stress level of σ_a = 700 MPa using two pieces of electro-polished specimens: one was surface oxidized at room temperature and the other was surface oxidized at 500°C for 2 hours.

Figure 3.17 shows the crack growth curves for two specimens, in which the crack growth curve at 500°C is also included for comparison. As seen from the data at room temperature, the delation of crack initiation is observed in the case of specimen which was surface oxidized at

500°C but the difference is very small, indicating that the suppressive effect of the oxide films formed by heating at 500°C for 2 hours is too less to be mentioned. On the other hand, however, the steady crack growth behavior in the two specimens is almost the same no matter which kind of oxide films formed on their surfaces (if the experiment were performed under lower stress levels, the suppression of early crack growth due to the oxide films formed at elevated temperature would had happened).

That is, at room temperature, the remarked suppression of early crack growth observed in the fatigue tests at elevated temperatures will not happen because the compressive residual stress generated at room temperature can be nearly neglected. Similarly, the acceleration of steady state crack growth observed at elevated temperature will not occur because the matrix is not softened.

Although the above inquiry is half-quantitative because the results were obtained at room temperature and the influence of oxide films will be intensified at elevated temperature, there will not be any change in the tendency in general.

Consequently, it can be concluded that the elevated temperature affects the early growth of small cracks in two contradictory ways, one is the acceleration action due to the softening of matrix and the other is the suppression action due to the formation of oxide films on the surface of specimen. Which action is dominant will depend on the conditions of temperature and stress levels.

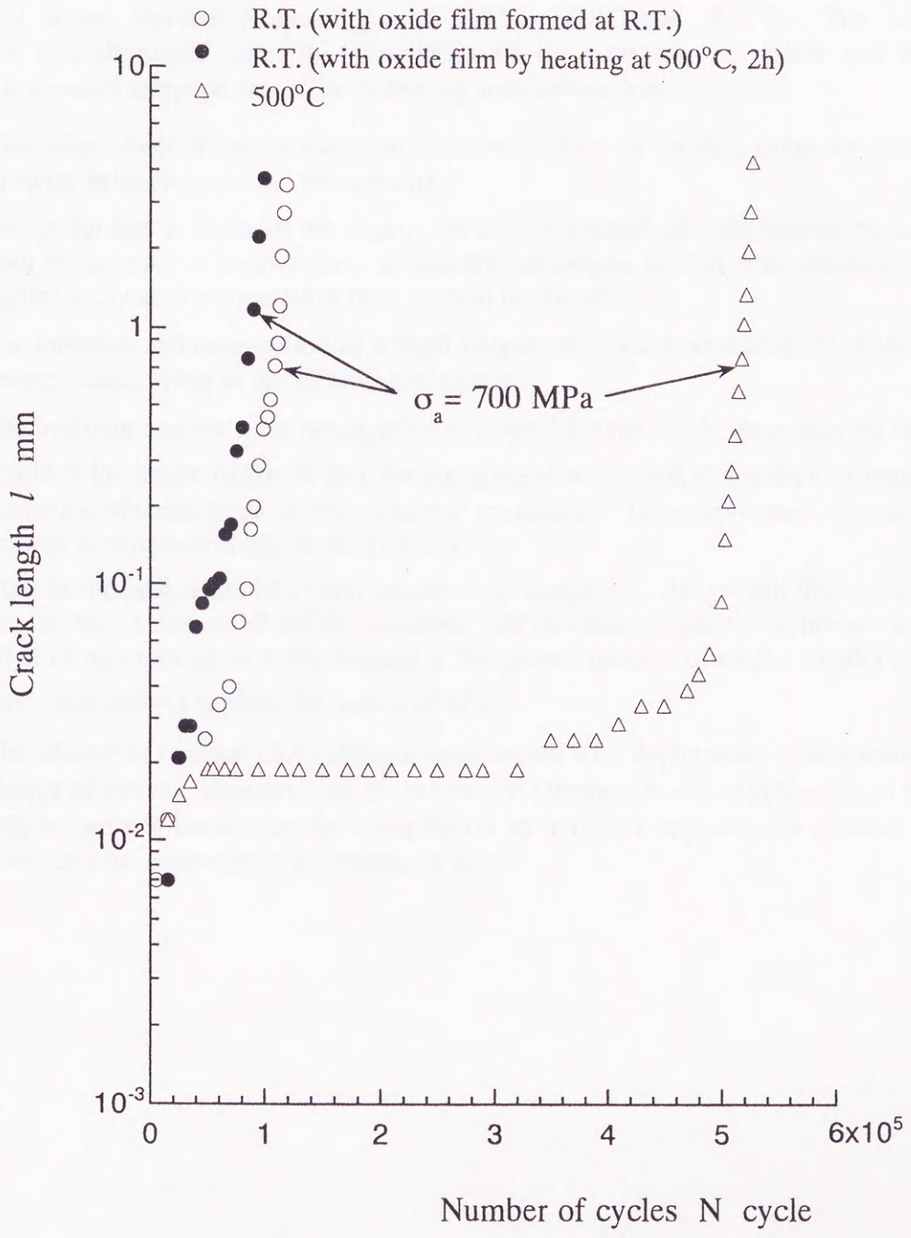

Figure 3.17 Effect of oxide films on the crack growth behavior under σ_a= 700 MPa.

3.4 Conclusions

The initiation and early growth behavior of a small fatigue crack in Inconel 718 was investigated at the elevated temperatures of 300°C, 500°C and 600°C. The influence of temperature was discussed from the viewpoints of the softening of matrix and the surface oxidation at elevated temperatures. The following conclusions were obtained.

(1) The fatigue limit of a plain specimen is determined by the limiting stress for small crack growth, irrespective of the temperature.

(2) Except for that in the short life region, the fatigue strength of plain specimens increases with the increase of temperature. Especially, the fatigue limit of plain specimens is much higher at elevated temperatures than at room temperature.

(3) The initiation and propagation of a small fatigue crack are promoted at the elevated temperatures owing to the softening of matrix.

(4) The initiation and the early propagation of a small fatigue crack, especially the small cracks at the length of 20~30 μm, are suppressed at elevated temperatures owing to the formation of oxide films on the surface of specimens. The suppression of small crack growth is remarked at higher temperature.

(5) Most of the fatigue life of a plain specimen is occupied by the growth life of cracks smaller than 1 mm, at all the temperatures. At elevated temperatures, however, about 90 % of the crack growth life is spent in the growth process of cracks smaller than 20~30 μm. This and (4) explain the reason of (2).

(6) The relation of l versus N/N_f changes enormously with the increase of temperature and the change of stress. However, on the relation of l versus $(N-N_{0.05})/(N_f-N_{0.05})$ in which only the growth lives of cracks larger than 0.05 mm are compared, the effect of both the stress and the temperature are extremely small.

References

(1) Maccagno, T.M., et al., *Metall. Trans. A*, **21**A (1990), pp. 3115-3125.

(2) Brown, C.W. & Hicks, M.A., *Int. J. Fatigue*, **4** (1982), pp. 73-81.

(3) Brown, C.W., et al., *Metal Science*, **18** (1984), pp. 374-380.

(4) Burke, M.A. & Beck, C.G., *Metall. Trans. A*, **15**A (1984), pp. 661-670.

(5) Nazmy, M.Y. & Singer, R.F., *Metall. Trans. A*, **16**A (1985), pp. 1437-1444.

(6) Singh, V., et al., *Metall.Trans. A*, **22**A (1991), pp. 499-505.

(7) Stephens, R.R., et al., *Int. J. Fatigue*, **15**-4 (1995), pp. 273-282.

(8) Yoshiba, M., et al., *Trans. Jpn Soc. Mech. Eng.*, (in Japanese), **50**-456, A (1974), pp. 1443-1452.

(9) Goto, M., et al., *Trans. Japan Society of Materials Science*, (in Japanese), **46**-12 (1997), pp. 1389-1395.

(10) Okazaki, M., et al., *Trans. Japan Society of Materials Science*, (in Japanese), **41**-467 (1992), pp. 1261-1267.

(11) Okazaki, M., et al., *Prepr of Jpn Soc. Mech. Eng.*, (in Japanese), No. **96**-1 (1996), pp. 444-445.

(12) Yuen, J.L., et al., *Metall. Trans. A*, **15**A (1984), pp. 1769-1775.

(13) Reger, M. & Remy, L., *Metall. Trans. A*, **19**A (1988), pp. 2259-2268.

(14) Hwang, S.K., et al., *Metall. Trans. A*, **20**A (1989), pp. 2793-2801.

(15) Kumazaki, S., et al., *Trans. Jpn Soc. Mech. Eng.*, (in Japanese), **63**-611, A (1997), pp. 1481-1488.

(16) Kanazawa, K. & Nishijima, S., *Trans. Jpn Soc. Mech. Eng.*, (in Japanese), **46**-12 (1997), pp. 1396-1401.

(17) Hamazaki, K., et al., *J. Japan Inst. Met.*, **60**-6 (1996), pp. 616-623.

(18) Lenglet, M., et al., *Mat. Res. Bull.*, **25** (1990), pp. 715 - 722.

Chapter 4 Fatigue crack growth resistance at elevated temperatures

4.1 Introduction

The significance of the estimation of small crack growth rate in the life assessment has been emphasized in many materials[1-3] by pointing out that the growth behavior of a small fatigue crack is a vital problem that must be aware of by the engineers in the fields of machine design, equipment maintenance and new material development.

However, in the case of nickel-base superalloys, it seems very confused about the effect of temperature on the crack growth behavior. For example, it has been reported that the crack growth resistance in nickel-base superalloys increased [4],[5], decreased [6] or almost did not change [7] at high temperature, and the united explanation has not been achieved yet. Furthermore, when a crack is small, the crack growth is easy to be influenced by the microstructure of materials and the estimation of crack growth rate will become more complicated, especially at elevated temperature.

In chapter 4, the fatigue behavior of small cracks in steady state growth process is investigated. The crack growth rate will be evaluated on the basis of Paris law under low stresses and the small crack growth law under high stresses, respectively. The effect of temperature on the fatigue crack growth resistance will be assessed by considering the strength degeneration at elevated temperature.

4.2 Experimental procedures

The specimen with a small blind hole (0.3 mm at diameter and in depth) at the center of specimen was used to estimate the fatigue crack growth resistance in Inconel 718. Figure 4.1 shows the shape and dimensions of specimen which will be mentioned as the drilled specimen hereinafter. The small blind hole was established for the convenience of crack measuring. The observation of fatigued surfaces and the measurement of crack length were conducted by an optical microscope using the plastic replica method. The crack length, l, is measured along the circumferential direction on the specimen surface including the 0.3 mm diameter of the hole. The stress amplitude, σ_a, is defined as a nominal stress on the net area of specimen by ignoring the existence of the hole. The tests were carried out at room temperature and the elevated temperatures of 300°C, 500°C and 600°C. The machine used and the experimental procedures conducted are the same as those mentioned in chapter 3.

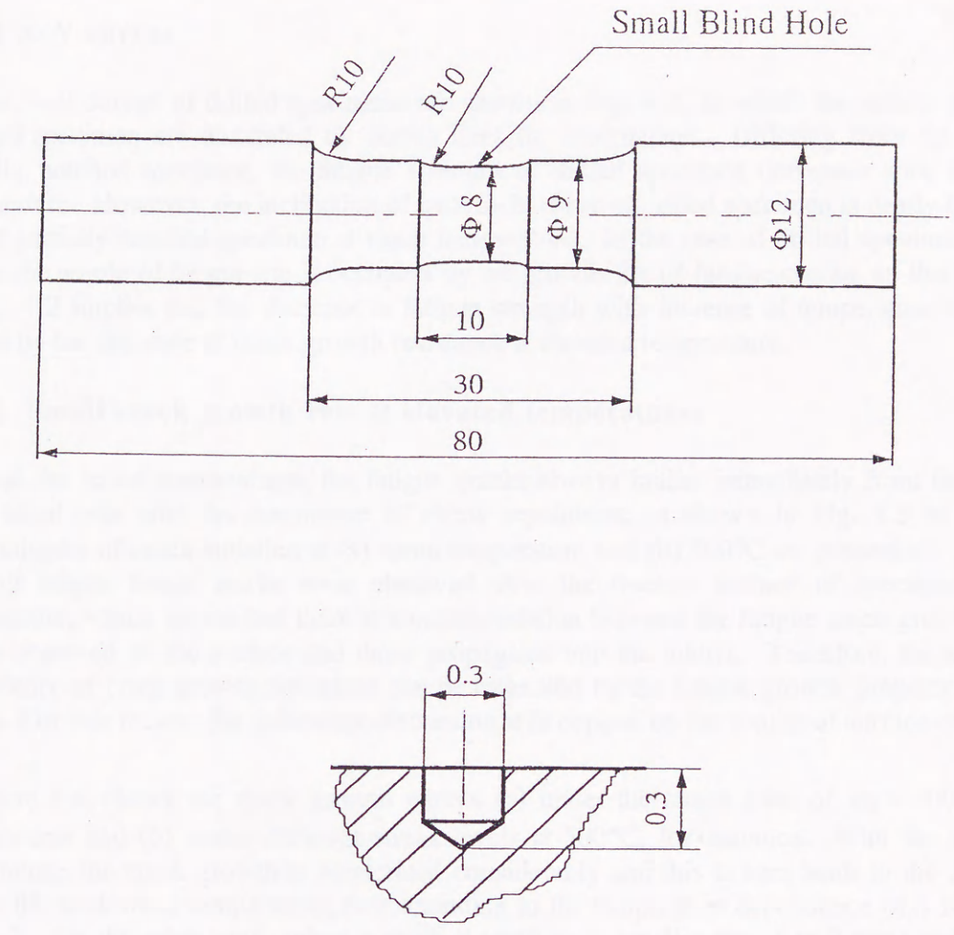

Figure 4.1 The shape and dimensions of drilled specimen (in mm).

4.3 Results and discussion

4.3.1 *S-N* curves

The *S–N* curves of drilled specimens are shown in Fig. 4.2, in which the results of partially notched specimen are illustrated by dotted lines for comparison. Differing from the results of partially notched specimen, the fatigue strength of drilled specimen decreases with increase of temperature. However, the inclination of each *S–N* curve of drilled specimen is nearly the same as that of partially notched specimen at room temperature. In the case of drilled specimen, because almost the whole of fatigue life is occupied by the growth life of fatigue cracks, so that the results in Fig. 4.2 implies that the decrease in fatigue strength with increase of temperature is probably caused by the decrease of crack growth resistance at elevated temperature.

4.3.2 Small crack growth rate at elevated temperatures

At all the tested temperatures, the fatigue cracks always initiate immediately from the edges of small blind hole after the commence of stress repetitions, as shown in Fig. 4.3 in which the morphologies of crack initiation at (a) room temperature and (b) 500°C are presented. Moreover, the half elliptic beach marks were observed over the fracture surface of specimens at each temperature, which means that there is a certain relation between the fatigue crack growth rates of cracks observed on the surface and those propagated into the matrix. Therefore, the temperature dependence of crack growth resistance can be estimated by the fatigue growth property of surface cracks. For this reason, the following discussion will depend on the results of surface cracks.

Figure 4.4 shows the crack growth curves (a) under the stress level of σ_a = 700 at all the temperatures and (b) under different stress levels at 500°C, for instance. With the increase of temperature, the crack growth is accelerated considerably and this in turn leads to the decrease of fatigue life at elevated temperature, corresponding to the temperature dependence of *S-N* curves in Fig. 4.2. On the other hand, when a crack is small (e.g. smaller than 1 to 2 mm) and the stress level is high (e.g. $\sigma_a/\sigma_{0.2} > 0.6$), the relation between the logarithm of crack length, *lnl*, with the number of cycles, *N*, can be approximated linearly. That is

$$ln\, l \propto N \tag{4-1}$$

By differentiating Eq. (4-1) with respect to *N*, the crack growth rate can be expressed as the following

$$dl/dN \propto l \tag{4-2}$$

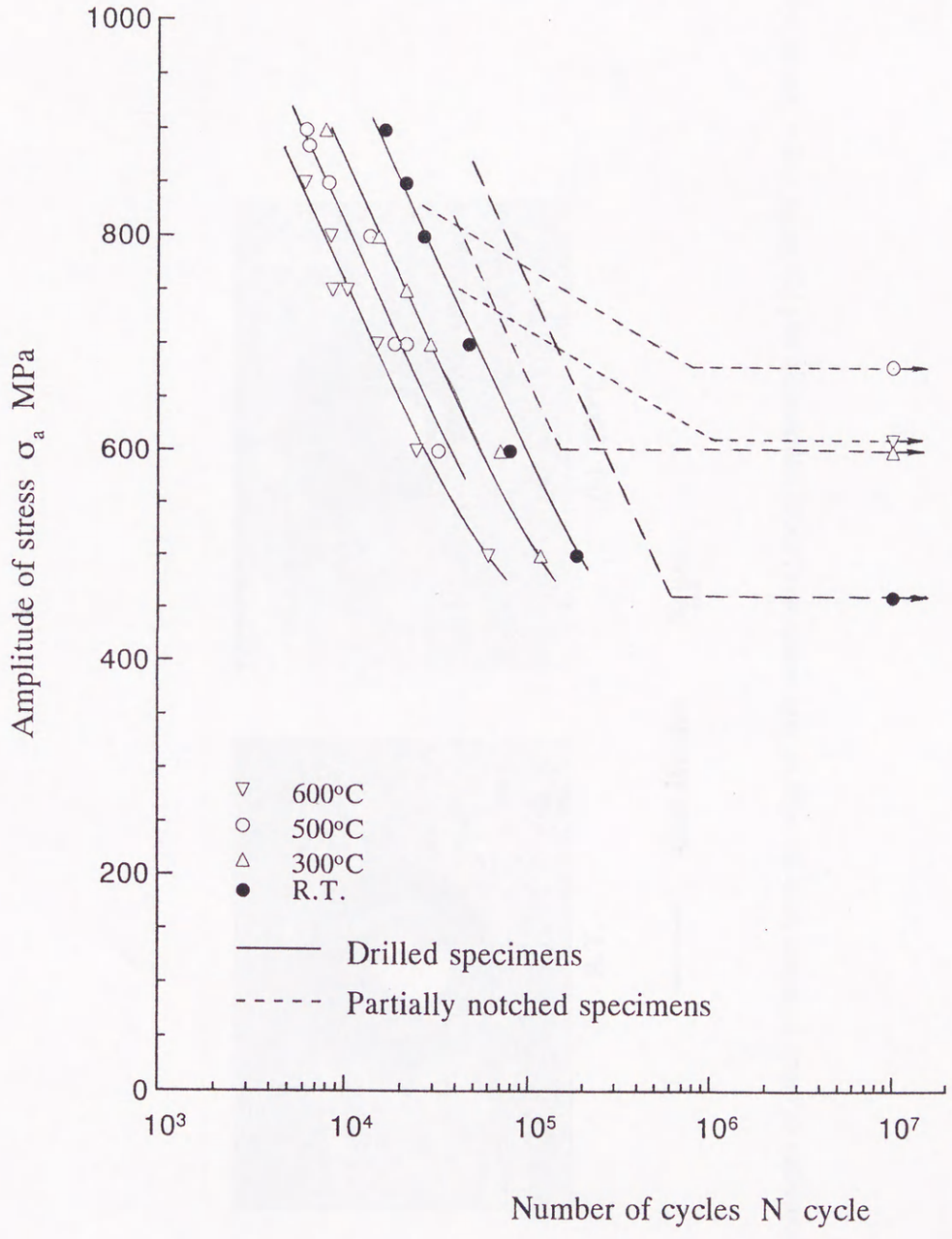

Fig. 4.2 *S–N* curves of drilled specimens.

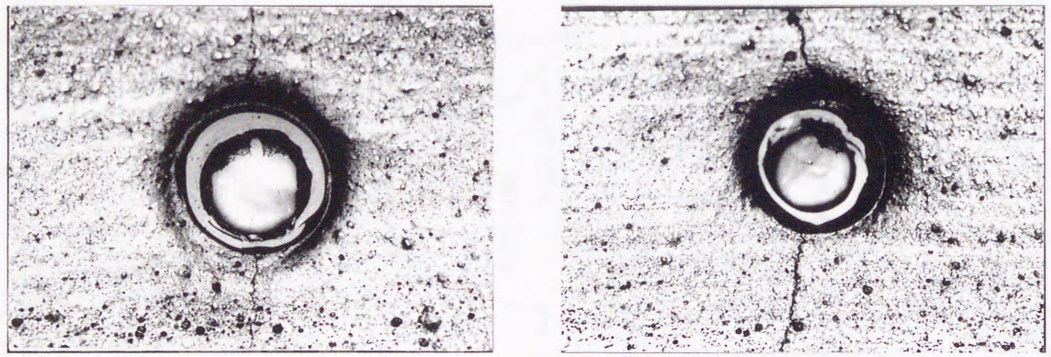

Fig. 4.3 Morphologies of crack initiation from the edge of hole notch at (a) room temperature and (b) 500°C (σ_a = 700 MPa).

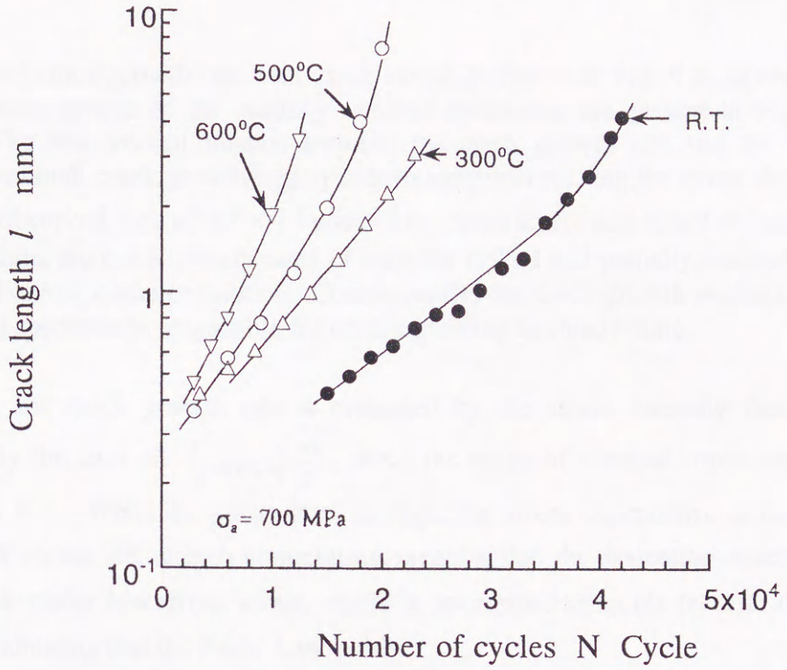

(a) At all the temperatures

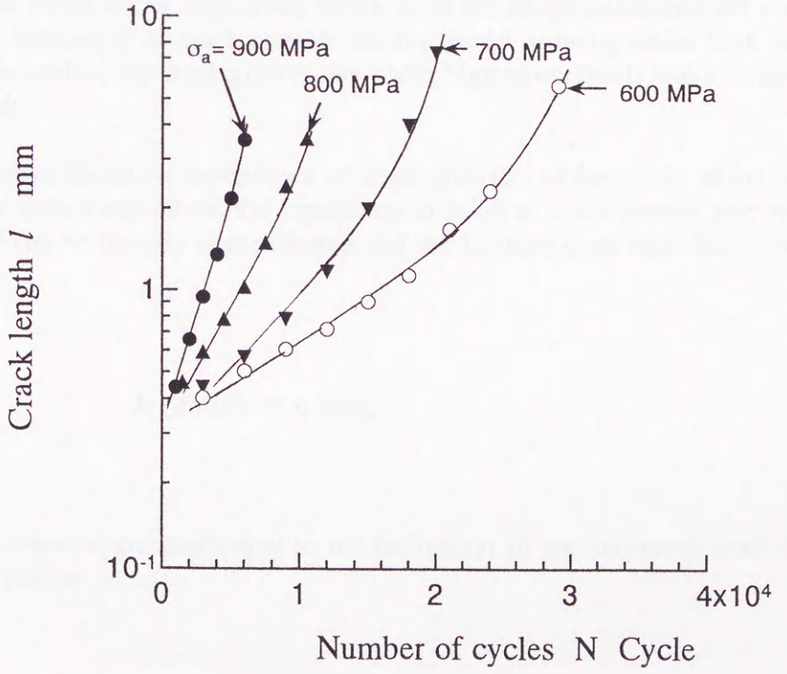

(b) At 500°C

Fig. 4.4 Crack growth curves (a) at all the temperatures and (b) at 500°C.

Equation (4-2) holds for all the small cracks growing under high stresses at all the tested temperatures.

The relation of crack growth rate with crack length is shown in Fig. 4.5, at room temperature and 500°C. Some results of the partially notched specimens are plotted in Fig. 4.5 too, for comparison. The proportional relation between the crack growth rate and the crack length is recognized in the small crack growth region at both temperatures, but the stress dependence of the relation is also observed, i.e. $dl/dN \propto l^2$ under low stress levels and $dl/dN \propto l$ under high stress levels. Meanwhile, the crack growth rates of both the drilled and partially notched specimens are found in a good correspondence relation. Consequently, the crack growth evaluation based on the results of drilled specimen is reasonable for cracks growing in steady-state.

In Fig. 4.6, the crack growth rate is evaluated by the stress intensity factor range, ΔK, (approximated by the term of $\frac{2}{\pi}\Delta\sigma_a\sqrt{\frac{\pi l}{2}}$, $\Delta\sigma_a$: the range of nominal stress amplitude), using the data in Fig. 4.5. When the stress level is high, the stress dependence is recognized in the relation of dl/dN versus ΔK at each temperature, meaning that the evaluation based on Paris' Law is invalid. While under low stress levels, dl/dN is determined uniquely by ΔK, that is, $dl/dN \propto \Delta K^m$ ($m \approx 4$), indicating that the Paris' Law holds.

Similar results were also obtained at 300°C and 600°C. Therefore, the stress dependence of crack growth rate exists under high stress levels at all the temperatures and the Paris' Law is not applicable to the evaluation of crack growth rate for cracks growing under high stress levels. In the following discussion, the crack growth rate under high stress levels was evaluated by the small crack growth law.

Figure 4.7 shows the stress dependence of crack growth rate for cracks in the length of 1 mm, for example. At each temperature, the logarithmic relation of crack growth rate with the nominal stress amplitude can be linearly approximated and the inclination of each line is nearly the same. That is

$$ln\ (dl/dN) \propto n\ ln\ \sigma_a \qquad (4\text{-}3)$$

in which n is a constant corresponding to the inclination of approximated lines in Fig. 4.7 and values about 5. Hence

$$dl/dN \propto \sigma_a^n \qquad (n \approx 5) \qquad (4\text{-}4)$$

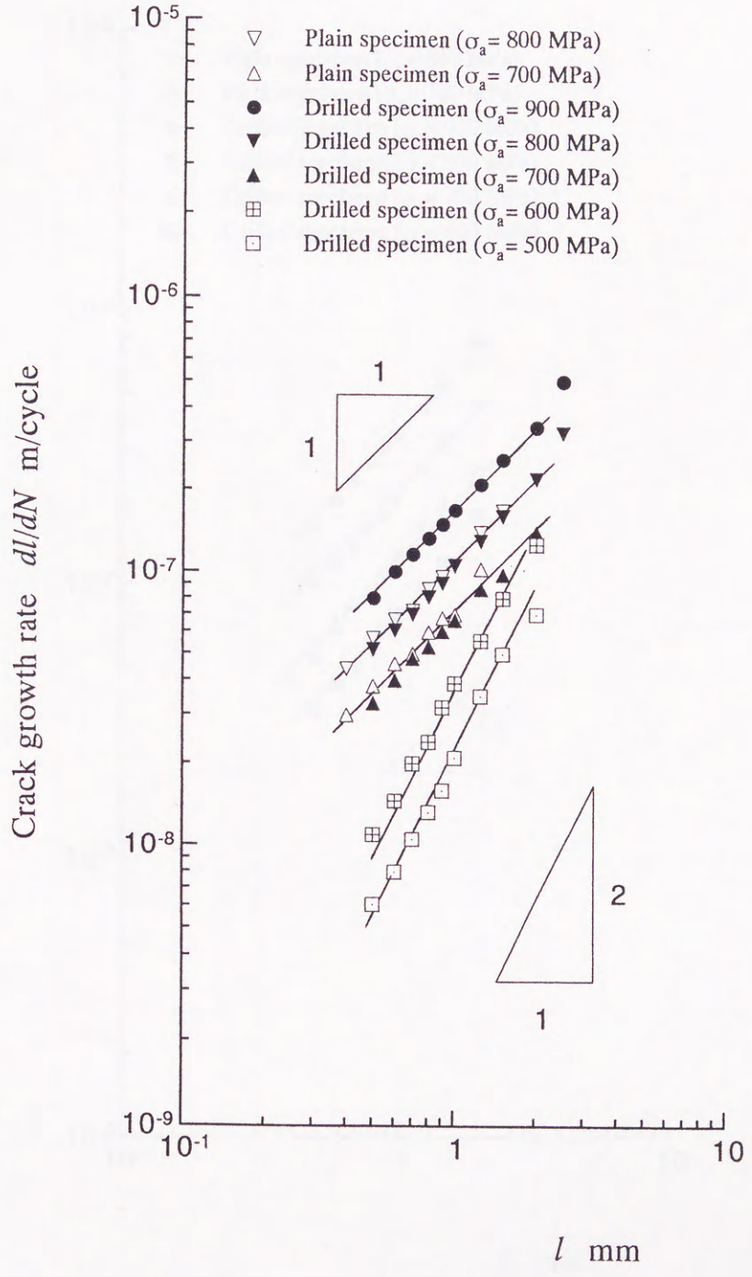

Fig. 4.5 (a) *dl/dN* versus *l* at room temperature.

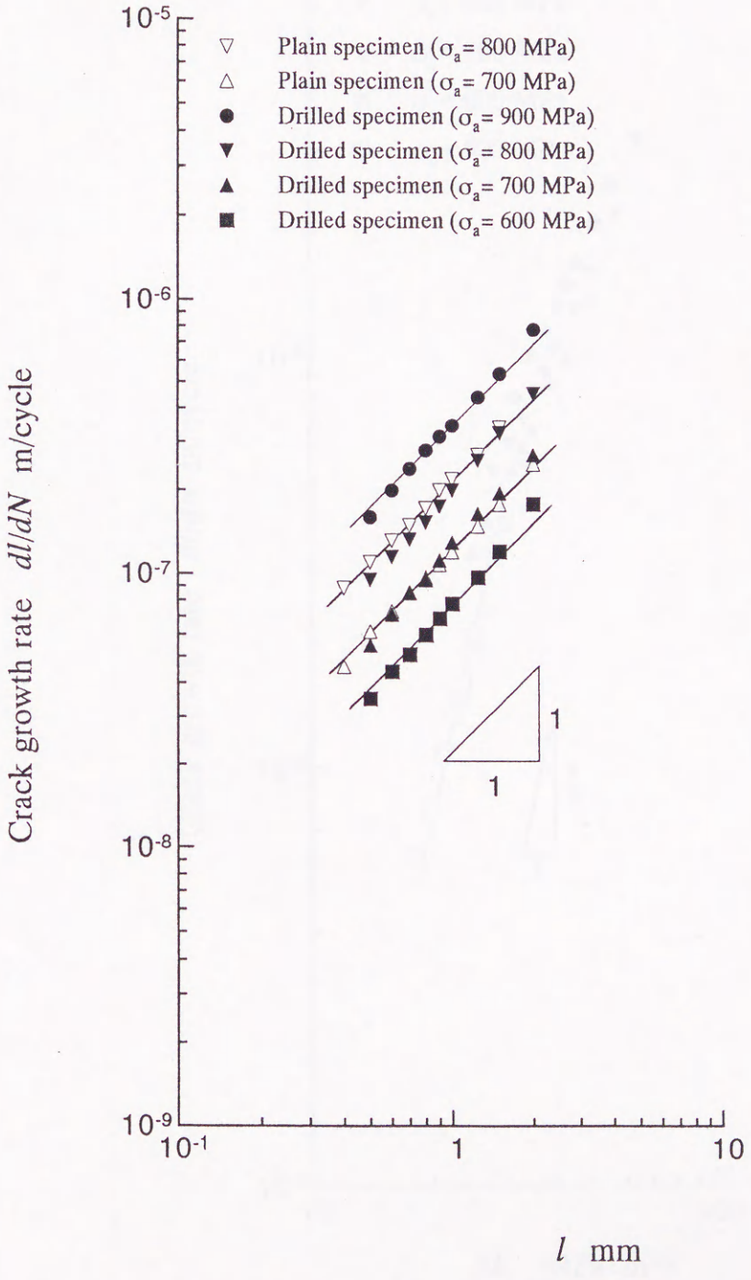

Fig. 4.5 (b) dl/dN versus l at 500°C.

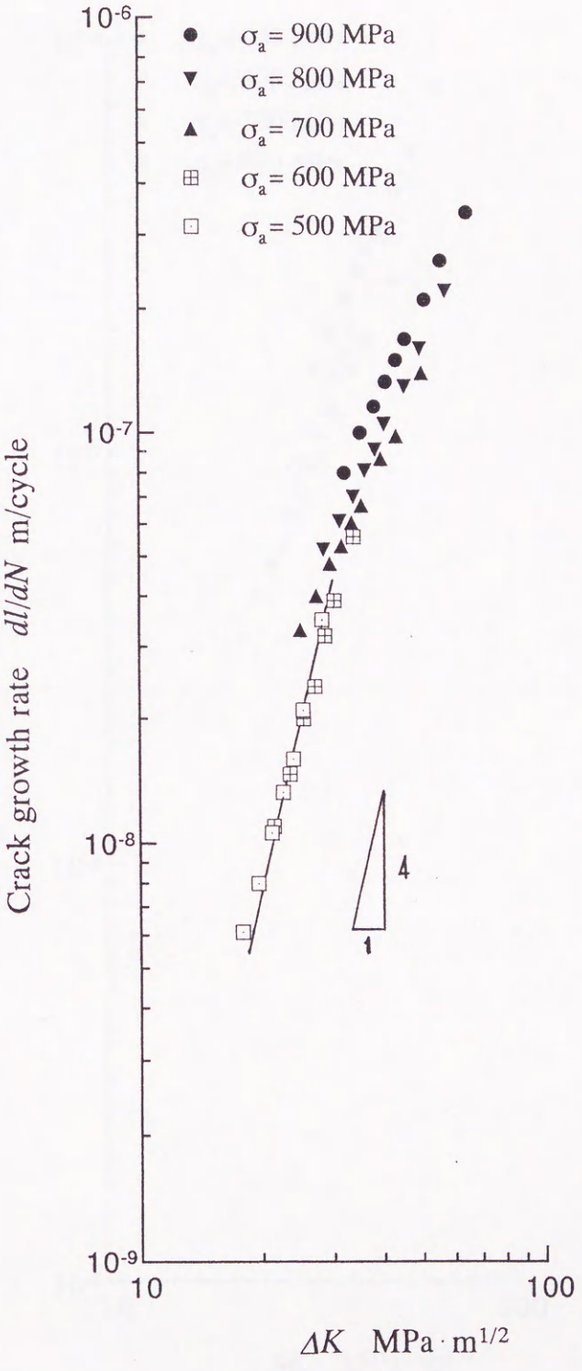

Fig. 4.6 (a) dl/dN versusΔK at room temperature.

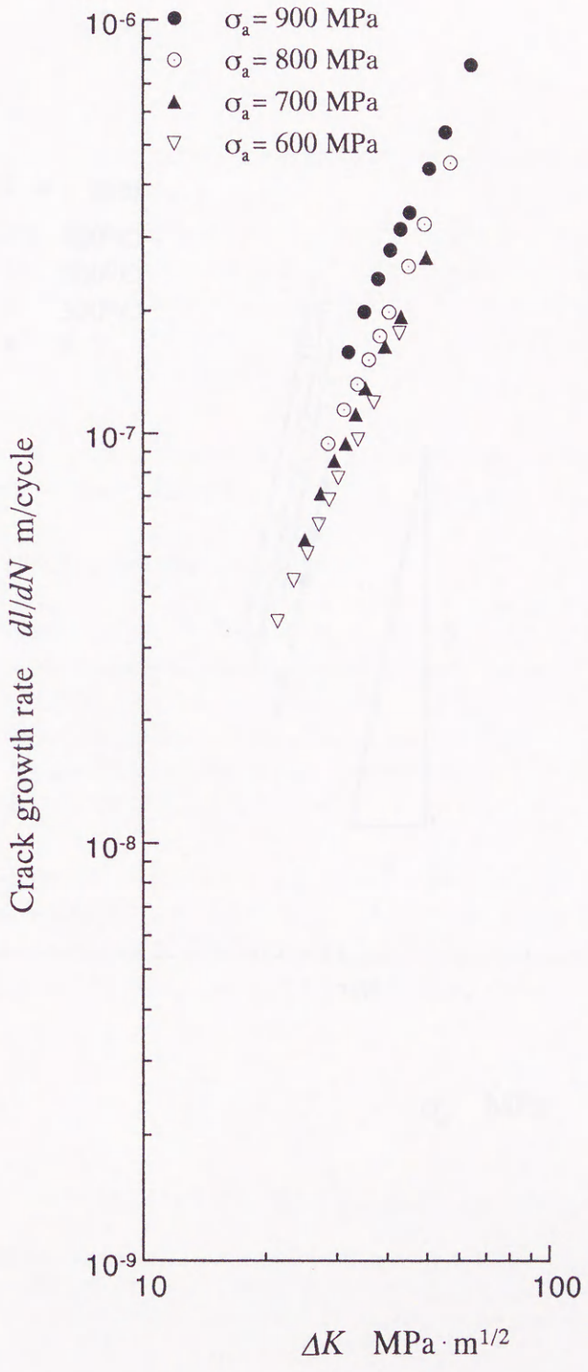

Fig. 4.6 (b) dl/dN versusΔK at 500°C.

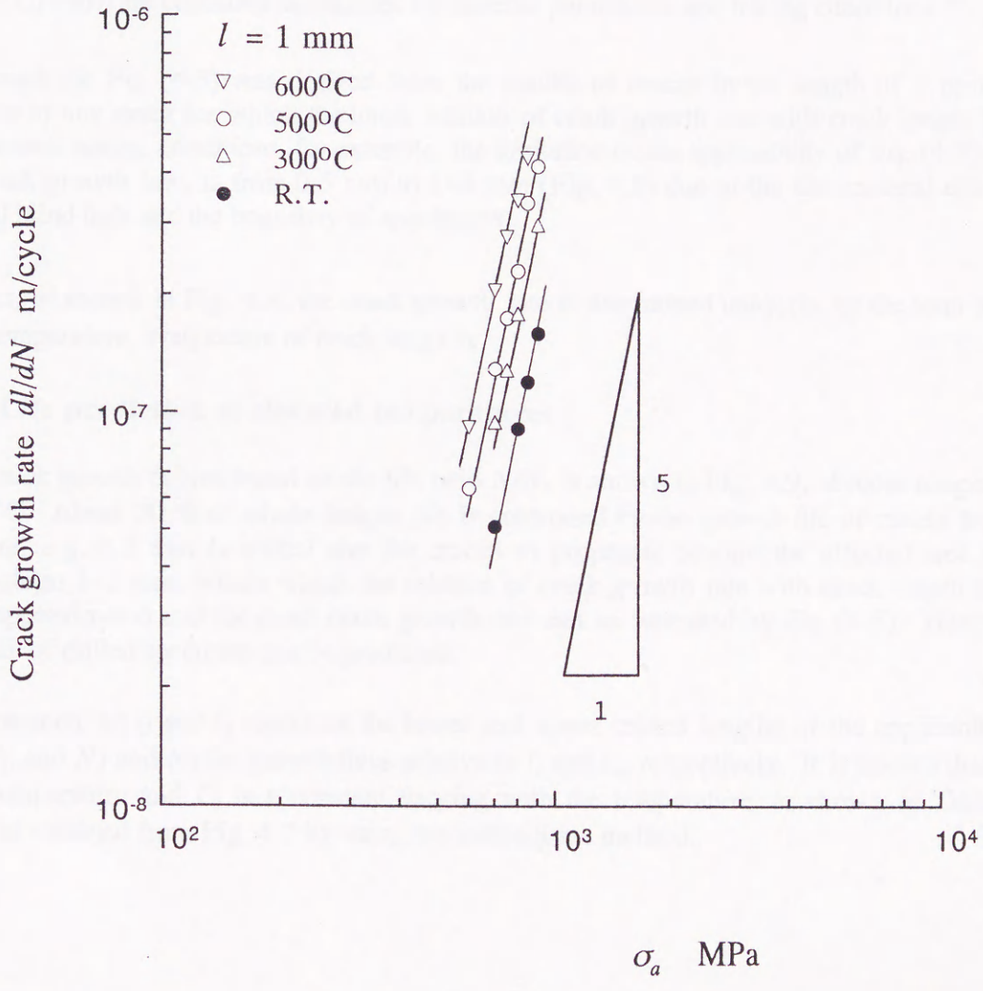

Fig. 4.7 Stress dependance of crack growth rate under high stress levels.

Combining Eqs. (4-2) and (4-4), Equation (4-5) can be derived.

$$dl/dN = C_1 \sigma_a^n l \tag{4-5}$$

in which C_1 and n are constants determined by material parameters and testing conditions [8].

Although the Eq. (4-5) was derived from the results of cracks in the length of 1 mm, it is applicable to any crack for which the linear relation of crack growth rate with crack length holds. In the present testing conditions, for example, the limitation of the applicability of Eq. (4-5) or the small crack growth law, is from 0.5 mm to 1~2 mm (Fig. 4.5) due to the dimensional effects of the small blind hole and the boundary of specimens.

In fact, as shown in Fig. 4.8, the crack growth rate is determined uniquely by the term of $\sigma_a^n l$ at each temperature, irrespective of crack leng+th.

4.3.3 Life prediction at elevated temperatures

The crack growth curves based on the life ratio N/N_f is shown in Fig. 4.9, at room temperature and 500°C. About 70 % of whole fatigue life is controlled by the growth life of cracks from an initial size, e.g. 0.5 mm (a critical size for cracks to propagate beyond the affected area of the drilled hole)to 1~2 mm, within which the relation of crack growth rate with crack length can be linearly approximated and the small crack growth rate can be estimated by Eq. (4-5). Hence, the fatigue life of drilled specimen can be predicted.

For instance, let l_1 *and* l_2 represent the lower and upper critical lengths of the applicability of Eq. (4-5), and N_1 and N_2 the growth lives relative to l_1 and l_2, respectively. It is known that n≈ 5 at each temperature and C_1 is a constant varying with the temperature, as shown in Table 4.1 which was obtained from Fig. 4.7 by using the least square method.

Table 4.1 The values of constant C_1 at all the temperatures

Temperature	R.T.	300°C	500°C	600°C
C_1	2.95×10^{-19}	5.56×10^{-19}	8.13×10^{-19}	1.09×10^{-18}

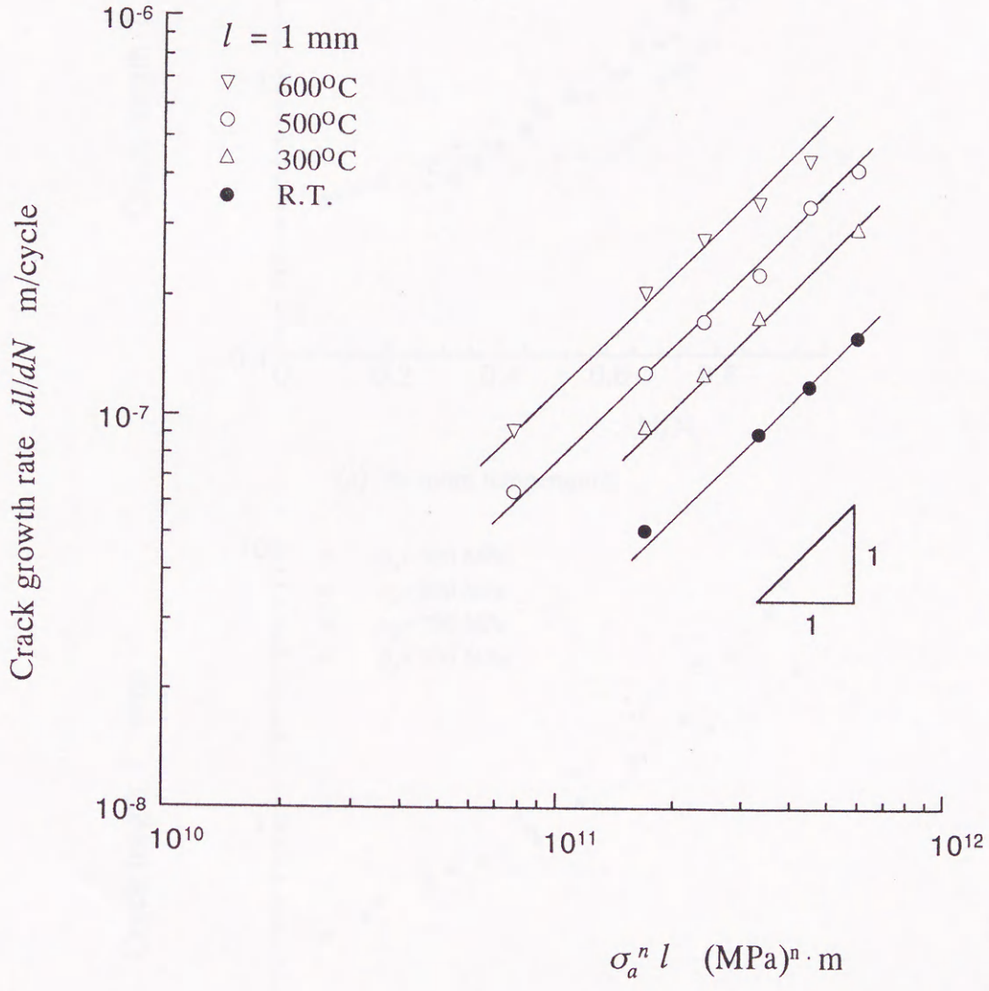

Fig. 4.8 Crack growth ratedl/dN as a function of$\sigma_a^n l$.

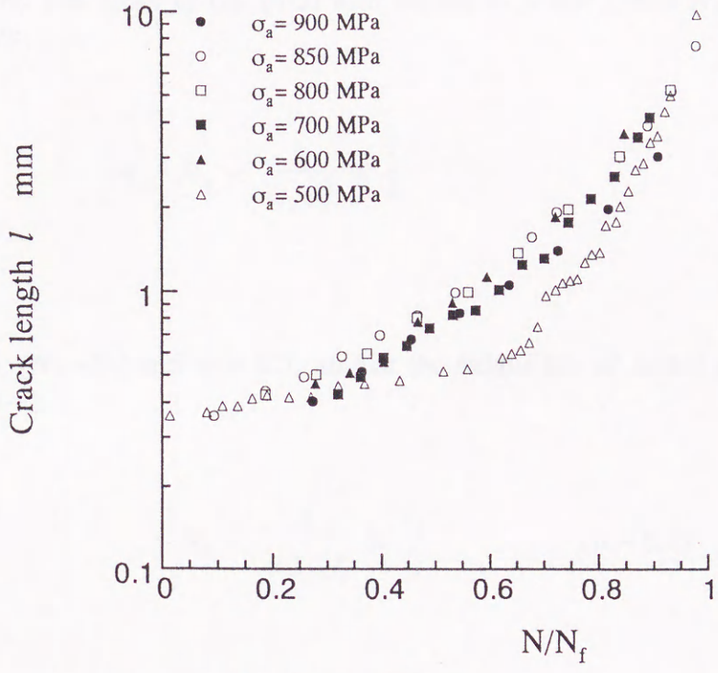

(a) At room temperature

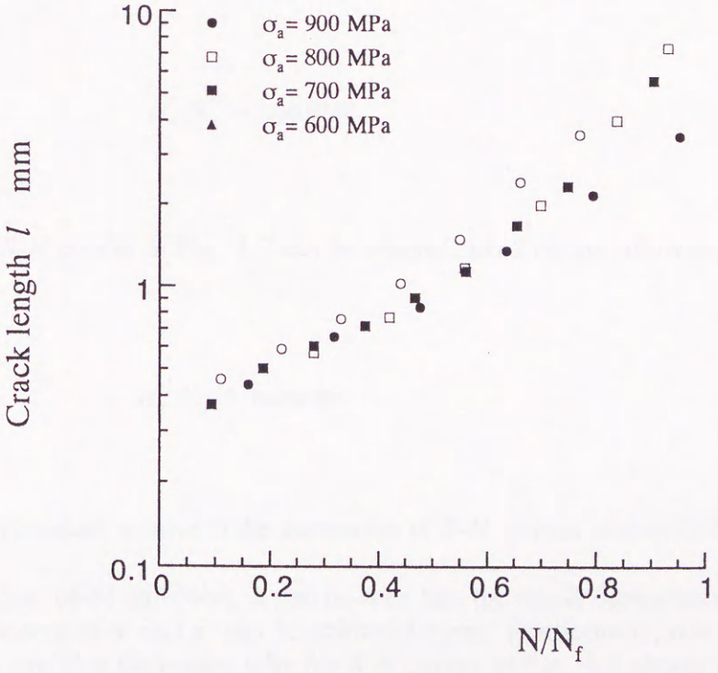

(b) At 500°C

Fig. 4.9 Crack length l versus life ratio N/N_f at (a) room temperature and (b) 500°C.

By integrating the both sides of Eq. (4-5) with respect to N and l from N_1 to N_2 or l_1 to l_2 respectively, it gives

$$N_2 - N_1 = \frac{1}{C_1 \sigma_a^n} ln \frac{l_2}{l_1} \tag{4-6}$$

Because $\alpha N_f = (N_2 - N_1)$ and $\alpha \approx 0.7$, so that the fatigue life of drilled specimens can be predicted by Eq. (4-7).

$$N_f = \frac{1}{\alpha C_1 \sigma_a^n} ln \frac{l_2}{l_1} \qquad (\alpha \approx 0.7) \tag{4-7}$$

In addition, Eq. (4-7) can be further written as

$$\sigma_a^n N_f = \text{constant} \tag{4-8}$$

Meanwhile, the S-N curves in Fig. 4.2 can be approximated by the following equation at each temperature.

$$\sigma_a^{n'} N_f = \text{constant} \tag{4-9}$$

In Eq. (4-9), n' is a constant relative to the inclination of S-N curves in their finite life regions.

Comparing the Eqs. (4-8) and (4-9), it can be seen that the stress dependence of fatigue life is reflected by the exponent of n' and n' can be estimated by n. Furthermore, n is the same at all the temperatures. This explains the reason why the S-N curves in Fig. 4.2 almost parallel each other in the short life region.

The temperature dependence of C_1 and N_f, standardized by the results at room temperature $C_{1\,RT}$ and N_{fRT} respectively, are shown in Fig. 4.10. The temperature dependence of C_1 is in a good correspondence with that of N_f.

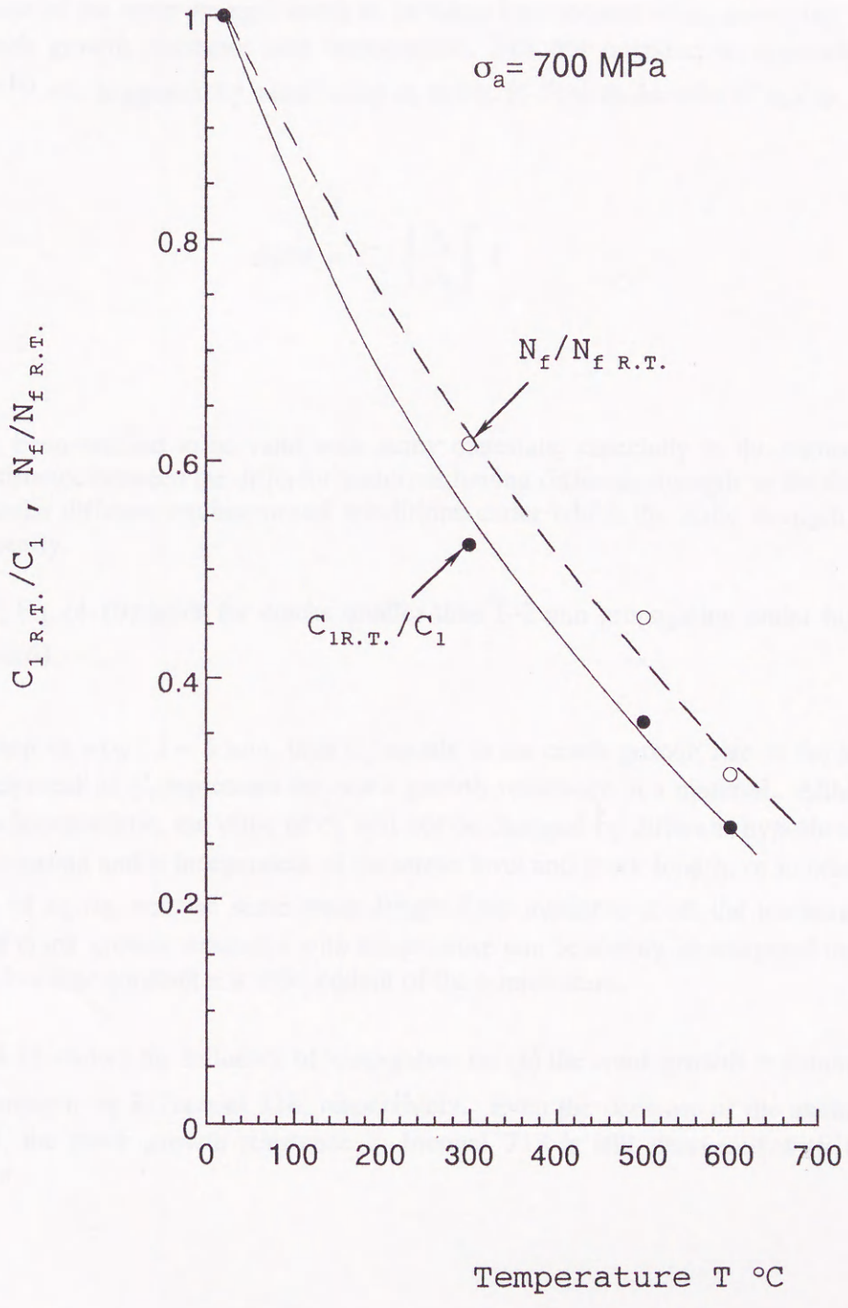

Fig. 4.10 C_{1RT}/C_1 and N_f/N_{fRT} versus T under σ_a= 700 MPa.

4.3.4 Fatigue crack growth resistance at elevated temperatures

In general, the static strength of metals decreases with the increase of temperature. Therefore, this decrease of the static strength needs to be taken into account when surveying the variation of fatigue crack growth resistance with temperature. For this purpose, an approximate evaluation method[9],[10] was suggested by substituting σ_a in Eq. (4-5) with the ratio of σ_a/σ_B.

$$dl/dN = C_2 \left(\frac{\sigma_a}{\sigma_B}\right)^n l \qquad (4\text{-}10)$$

which has been verified to be valid with many materials, especially in the comparison of crack growth resistance between the different materials having different strength or for the same material serviced under different environmental conditions under which the static strength of the material changes greatly.

Clearly, Eq. (4-10) holds for cracks smaller than 1~2 mm propagating under high stress levels ($\sigma_a/\sigma_{0.2} > 0.6$).

Supposing $\sigma_a = \sigma_B$, l = 1 mm, then C_2 equals to the crack growth rate in the length of 1 mm and the reciprocal of C_2 represents the crack growth resistance in a material. Although the above hypothesis is unrealistic, the value of C_2 will not be changed by different hypotheses because it is a material constant and is independent of the stress level and crack length, or in other words, if the same ratio of σ_a/σ_B and the same crack length l are available at all the temperatures, then the variation of crack growth resistance with temperature can be simply investigated using the term of $1/C_2$ or C_2 because constant n is independent of the temperature.

Figure 4.11 shows the influence of temperature on (b) the crack growth resistance $1/C_2$ and (a) the static strength σ_B in Inconel 718, respectively. Even the decrease of the static strength σ_B is considered, the crack growth resistance in Inconel 718 is still decreased with the increase of temperature.

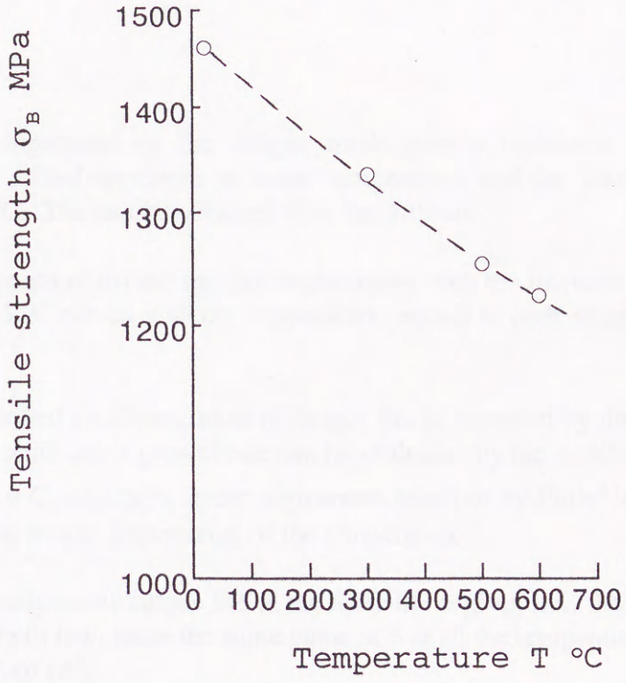

(a) σ_B versus T

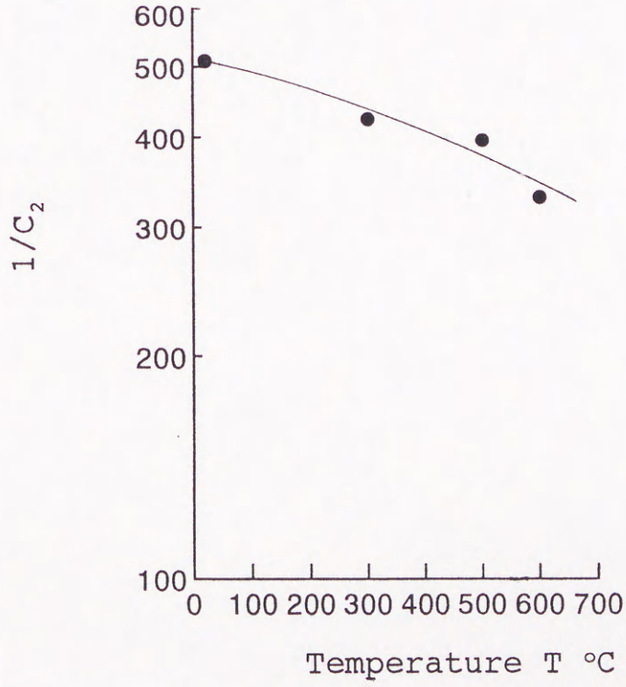

(b) $1/C_2$ versus T

Fig. 4.11 Changes of σ_B and $1/C_2$ with T.

4.4 Conclusions

The influence of temperature on the fatigue crack growth resistance in Inconel 718 was investigated using the drilled specimen at room temperature and the elevated temperatures of 300°C, 500°C and 600°C. The results obtained is as the follows.

(1) The fatigue strength of drilled specimens decreases with the increase of temperature. The inclinations of *S-N* curves at all the temperatures equals to each other in their finite life region.

(2) In the case of drilled specimen, most of fatigue life is occupied by the growth life of small cracks and the small crack growth rate can be evaluated by the small crack growth law, $dl/dN = C_1 \sigma_a^n l = C_2 (\sigma_a/\sigma_B)^n l$, under high stress levels or by Paris' law, $dl/dN = C\Delta K^m$, under low stress levels, irrespective of the temperature.

(3) The stress dependence of fatigue life in the finite life region, i.e., the exponent n in the small crack growth law, takes the same value of 5 at all the temperatures. This and (2) form the reason of (1).

(4) The crack growth resistance in Inconel 718 decreases with the increase of temperature, even though the degeneration of static strength is considered.

References

(1) Nisitani, H., *Mechanics of Fatigue-AMD*, *ASME*, **47** (1981), pp. 151-166.

(2) Nisitani, H. & Kawagoishi, N., *Trans. Jpn Soc. Mech. Eng.*, (in Japanese), **49**-440, A (1983), pp. 431-440.

(3) Nisitani, H. & Goto, M., *Trans. Jpn Soc. Mech. Eng.*, (in Japanese), **51**-462, A (1985), pp. 332-341.

(4) Leach, B.A. and Antolovich, S.D., *Met. Trans.*, A, **21**A (1990), pp. 2169-2177.

(5) Hoffelner,W., *Mater. Sci. Tech.*, 3 (1987), pp. 765-770.

(6) Crompton, J.S. and Martin, J.W., *Met. Trans.* A, **15**A (1984), pp. 1711-1719.

(7) Gell, M. and Leverant, G.R., *Proc.ICF-2*, (1969), pp. 565-575.

(8) Wang, X.S., Dr. Eng. Thesis, "Relation between the cyclic deformation properties in various kinds of materials and the small crack growth law", (in Japanese), Kagoshima University, 1997.

(9) Nisitani, H. and Kawagoishi, N., *JSME Int. J.*, **35**-1, A (1992), pp. 1-11.

(10) Kawagoishi, N., et al., *Fatigue 93*, **I** (Ed Bailon, J.PP. & Dickson, J.I., EMAS Ltd, Canada, 1993), pp. 409-414.

Chapter 5 Notch sensitivity at elevated temperatures

5.1 Introduction

It is well known that a fatigue crack is generally initiated from the stress concentrations such as defects induced in material processing, notches designed in structures and/or flaws after machining. The fatigue strength of a component will be reduced significantly due to the existence of stress concentrations. In fact, a recent fatigue damage[1] was reported in the critical component of H2 rocket engine caused by the stress concentrations. For this reason, many researches have been reported in and several methods have been suggested to estimate the fatigue strength of notched specimens, but none has been accepted widely because each of them was effective only in a narrow range of tested conditions.

Because Inconel 718 is frequently used as a chief structure material in the critical components of jet engines and gas turbines where heavy load must be suffered at high temperature and the fatigue reliability of components must be secured, the deterioration of fatigue strength due to stress concentration or the notch effect of the alloy is of great importance in practice. However, most of the previous researches were carried out at room temperature and the information at elevated temperature is almost not available[2]-[6].

In general, a material becomes notch sensitive with the increase of tensile strength. Furthermore, both the crack initiation and its early propagation in Inconel 718 are easily affected by the surface oxidation at elevated temperature (chapter 3). Therefore, the influence of temperature on the notch sensitivity of Inconel 718 needs to be clarified.

In the present chapter, the notch sensitivity of Inconel 718 is investigated by using 60 degree V-grooved specimens. The effect of temperature on the fatigue strength of notched specimens is examined from the effect on crack initiation and crack propagation. The notch sensitivity of the alloy is evaluated based on the Linear Notch Mechanics (LNM)[7] which has been verified with many kinds of metals at various loading conditions[8]-[10].

5.2 Material and experimental procedures

The material used was Inconel 718 whose chemical composition (Table 5.1) differes a little from that (Table 5.2) used in the previous chapters. Through the similar heat treatments described in chapter 2, the material was machined into the specimens. The mechanical properties after heat treatments are listed in Table 5.3.

Figure 5.1 shows the shape and dimensions of (a) plain specimen and (b) notched specimen. Prior to testing, the surface of specimen was electro-polished after machining by about 20 μm for plain specimens and 10 μm for notched specimens. The observation of fatigue damage was conducted directly under an optical microscope. The stress amplitude σ_a was determined by the nominal stress amplitude at the minimum cross section area.

The tests were carried out at room temperature and the elevated temperatures of 300°C, 500°C and 600°C using the same Ono-type rotating bending fatigue testing machine as described in chapter 3.

Table 5.1 Chemical composition of Inconel 718 used in chapter 5

(wt. %)

C	Si	Mn	P	S	Ni	Cr	Mo	Co	Cu	Al	Ti	Fe	B	Nb+Ta
0.02	0.11	0.12	0.009	0.001	52.64	18.67	3.09	0.09	0.01	0.66	0.90	Bal.	0.004	5.12

Table 5.2 Chemical composition of Inconel 718 used in chapters 2, 3 and 4.

(wt. %)

C	Si	Mn	P	S	Ni	Cr	Mo	Co	Cu	Al	Ti	Fe	B	Nb+Ta
0.03	0.05	0.06	0.008	0.002	52.26	18.5	3.08	0.27	0.02	0.55	0.96	Bal.	0.004	5.03

Table 5.3 Mechanical properties at all the temperatures

Temperature	0.2 % proof stress $\sigma_{0.2}$ (MPa)	Tensile strength σ_B (MPa)	True breaking stress σ_T (MPa)	Reduction of area ψ (%)
R.T.	1147	1372	2073	38.1
300°C	1089	1292	1956	39.7
500°C	1050	1236	1876	40.9
600°C	1008	1159	1858	44.0

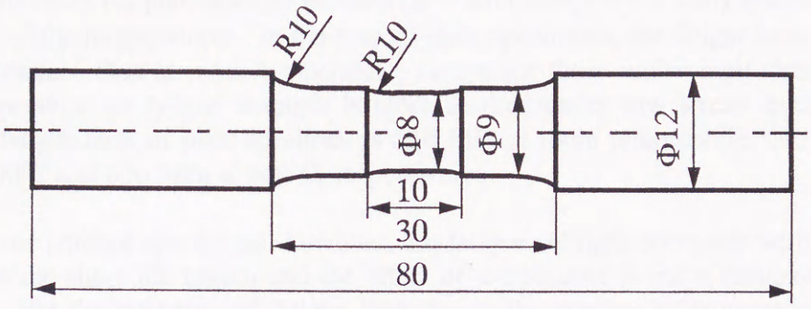

(a) Plain specimen

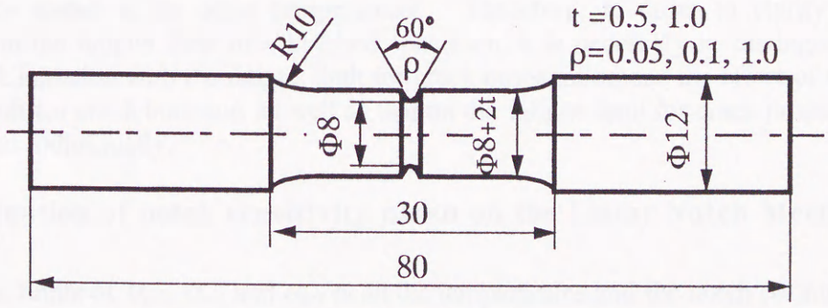

(b) Notched specimen

Fig. 5.1 The shape and dimensions of (a) plain and (b) notched specimens (in mm).

5.3 Results and discussion

5.3.1 *S-N* Curves

The *S-N* curves of (a) plain and (b) notched (ρ = 0.05 mm, t = 0.5 mm) specimens are shown in Fig. 5.2 at all the temperatures. In the case of plain specimens, the fatigue strength is higher at elevated temperature than at room temperature, except for those under high stress region. The effect of temperature on fatigue strength is more marked under low stress levels and long life region. The fatigue limit of plain specimen is 510 MPa at room temperature, 640 MPa at 300°C, 710MPa at 500°C and 630 MPa at 600°C, respectively.

In the case of notched specimens, however, the fatigue strength decreases with the increase of temperature in the short life region and the effect of temperature is more remarked under higher stress levels. But the reduction of fatigue limit due to the increase of temperature is so little as could be neglected if comparing with the great increase in plain specimen at elevated temperatures.

5.3.2 Significance of the fatigue limit in notched specimens

Figure 5.3 shows the optical micrographs of a non-propagating crack viewed over (a) the surface of notch root and (b) the cross section of a notched specimen (ρ = 0.05 mm, t = 0.5 mm). The notched specimen was cyclically stressed at 500°C for 10^7 cycles under the stress level of σ_{w2} = 370 MPa (σ_{w2}: the limiting stress for crack growth). A large mount of black powders which are considered to be the debris resulted from the "fretting" action during the crack growth process, are observed along the growth path of the non-propagating crack around the notch root. Similar non-propagating cracks were also recognized in the other notched specimens having different notch dimensions or tested at the other temperatures. Therefore, in order to clarify the effect of temperature on the fatigue limit of a notched specimen, it is necessary to distinguish the fatigue limit for crack initiation with the fatigue limit for crack propagation and the effect of temperature on the fatigue limit for crack initiation as well as that on the fatigue limit for crack propagation need to be investigated individually.

5.3.3 Evaluation of notch sensitivity based on the Linear Notch Mechanics

The fatigue limits of σ_{w0}, σ_{w1} and σ_{w2} at all the temperatures and the notch parameters of ρ and t are shown in Table 5.4, in which σ_{w0} is the fatigue limit of a plain specimen, σ_{w1} is the limiting stress for crack initiation and σ_{w2} is the limiting stress for crack growth. Since the judgement of crack initiation is not easy, σ_{w1} is defined as the limiting stress under which the same degree of fatigue damage (e.g. the existance of non-propagating cracks in the same surface length) as observed on the surface of a plain specimen at σ_{w0} occurs on the surface of notch root after the stress repetitions of 10^7 cycles. While, σ_{w2} is determined as the limiting stress for a specimen not to fracture after the stress repetition of 10^7 cycles. The stress concentration factor, K_t, is calculated using the Body force method[11].

Table 5.4 Fatigue limits of σ_{w0}, σ_{w1} and σ_{w2} at all the temperatures

Temperature	σ_B MPa	t mm	ρ mm	K_t	σ_{w1} MPa	σ_{w2} MPa	$K_t\sigma_{w1}/\sigma_{w0}$	$K_t\sigma_{w2}/\sigma_{w0}$
R.T.	1372	-	∞	1	510	-	1	-
		0.5	1.0	1.72	420	-	1.42	-
			0.1	4.16	230	390	1.88	3.18
			0.05	5.67	180	390	2.00	4.34
		1.0	1.0	1.85	380	-	1.38	-
			0.1	4.83	200	320	1.89	3.03
			0.05	6.65	150	320	1.96	4.17
300°C	1292	-	∞	1	640	-	1	-
		0.5	1.0	1.72	450	-	1.21	-
			0.1	4.16	250	350	1.63	2.28
			0.05	5.67	190	350	1.68	3.10
500°C	1236	-	∞	1	710	-	1	-
		0.5	1.0	1.72	460	-	1.11	-
			1.0	4.16	260	370	1.52	2.17
			0.05	5.67	200	370	1.60	2.96
		1.0	1.0	1.85	450	-	1.17	-
			0.1	4.83	220	310	1.50	2.11
			0.05	6.65	170	310	1.59	2.90
600°C	1159	-	∞	1	630	-	1	-
		0.5	1.0	1.72	410	-	1.12	-
			0.1	4.16	220	360	1.45	2.38
			0.05	5.67	170	360	1.53	3.24

($\sigma_{w0} = \sigma_{w1}$ at $\rho = \infty$)

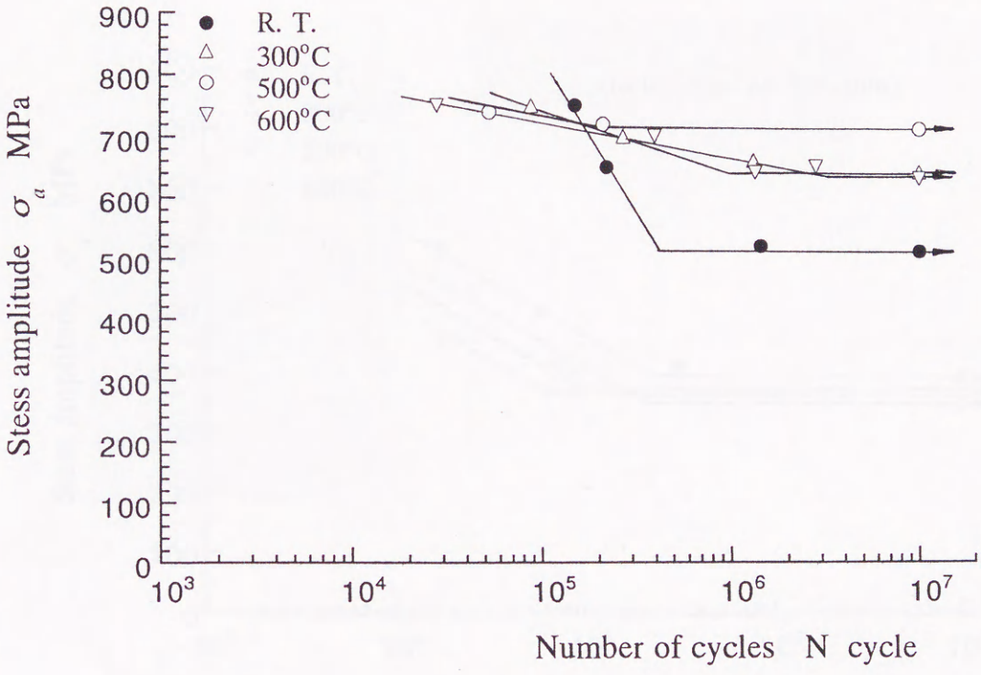

Fig. 5.2 *S-N* curves of plain specimens at all the temperatures.

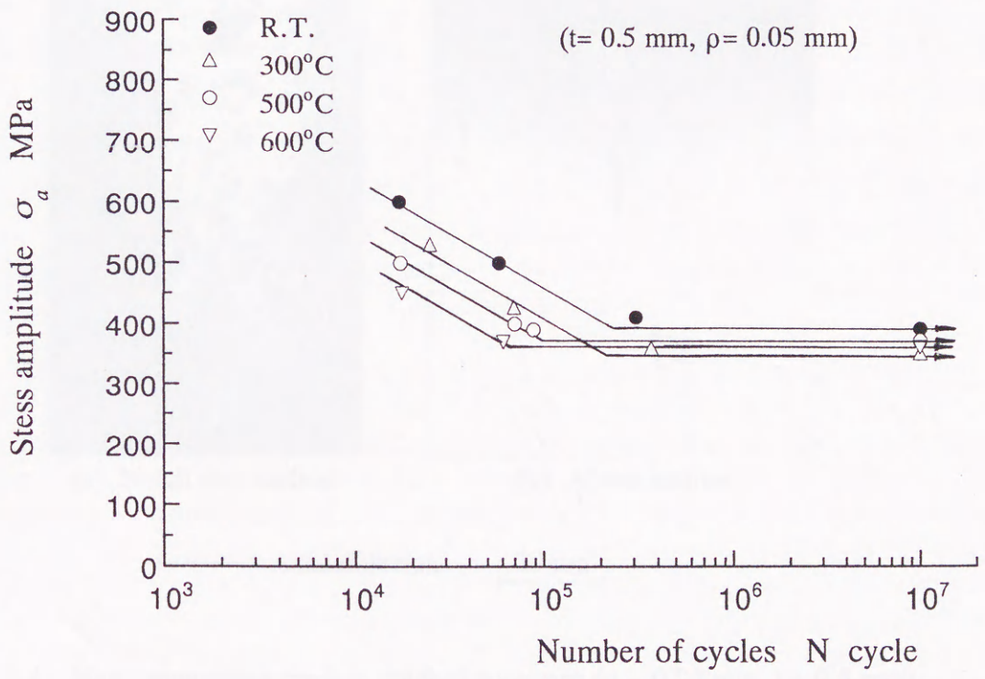

Fig. 5.3 *S-N* curves of notched (ρ = 0.05 mm, t = 0.5 mm) specimens at all the temperatures.

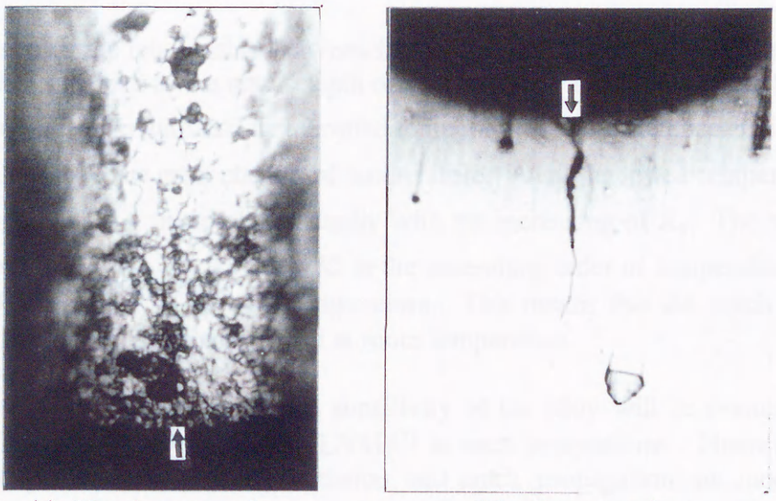

Fig. 5.4 Non-propagating crack in notched specimen (ρ = 0.05 mm, t = 0.5 mm) at the fatigue limit for crack growth (σ_{w2} = 370 MPa) at 500°C.

To give a example, the dependance of fatigue limits on the temperature is shown in Fig. 5.5 by using the data of plain specimen and a notched specimen (ρ= 0.1 mm, t = 0.5 mm). As mentioned before that σ_{w0} increases significantly with increase of temperature. This is correlated with the facts that the fatigue strength at each temperature is determined by the limiting stress for crack growth and that the crack growth of microstructural small cracks is suppressed remarkably at elevated temperatures (chapter 3). Similar increasing tendency can be found in the relation of σ_{w1} versus T, though the increase is quite small compared with that in σ_{w0}. But σ_{w2} decreases a little at elevated temperatures and this may be explained as a result of the interaction of (1) the softening of matrix at elevated temperature which causes the decrease of crack growth resistance[12] and then the decrease of σ_{w2}, and (2) the oxide-induced crack closure which is reinforced at higher temperature and promotes the crack arresting action[2], then checks the decrease of σ_{w2}.

Figure 5.6 shows the relationship between the fatigue limits and the stress concentration factor based on the data obtained in the notch depth of t = 0.5 mm. Compared to the large difference at σ_{w0} between room temperature and the elevated temperatures, the difference at either σ_{w1} or σ_{w2} is extremely small despite the great change of temperature. At all the tested temperatures, σ_{w2} keeps almost unchanged but σ_{w1} decreases gradually with the increasing of K_t. The notch radius at the branch point of curves σ_{w1}–K_t and σ_{w2}–K_t in the ascending order of temperature are 0.50, 0.30, 0.40 and 0.45 mm, lower at elevated temperature. This means that the notch sensitivity of the alloy is higher at elevated temperature than at room temperature.

In the following discussion, the notch sensitivity of the alloy will be evaluated quantitatively based on the Linear Notch Mechanics (LNM)[7] at each temperature. However, as discussed previously, the phenomena of crack initiation and crack propagation are more complicated at elevated temperature than at room temperature. For instance, the oxide films formed on the surface of specimen will suppress the surface slipping or crack initiation at elevated temperature[13] and the oxidation on the cracked surfaces will reinforce the crack growth arresting of small cracks or crack closure effect[2]. That is, the applicability of LNM to the evaluation of fatigue limits of a notched specimen is questioned at elevated temperature. In fact, the study based on LNM has not been reported at elevated temperature until now. But, as can be comprehended from the physical signifivance of LNM, the fatigue limits of a notched specimen is determined uniquely by the maximum stress at the notch root, σ_{max} ($=K_t \sigma_a$), and the notch radius ρ so long as the small scale yielding condition is satisfied, irrespective of the temperature.

To testify the above description, the data in Table 5.4 at both room temperature and 500°C are chosen and rearranged depending on the LNM. In Fig. 5.7, the stress ratios of $K_t\sigma_{w1}/\sigma_{w0}$ and $K_t \sigma_{w1}/\sigma_{w0}$, representing the notch sensitivities to crack initiation and crack growth respectively, are correlated to the reciprocal of notch radius, $1/\rho$. The maximum stresses at the notch root $K_t\sigma_{w1}$ and $K_t\sigma_{w2}$, are standardized with the fatigue limit of plain specimens, σ_{w0}, in order to compare the notch sensitivity between different materials and the notch sensitivity of a material at different temperatures.

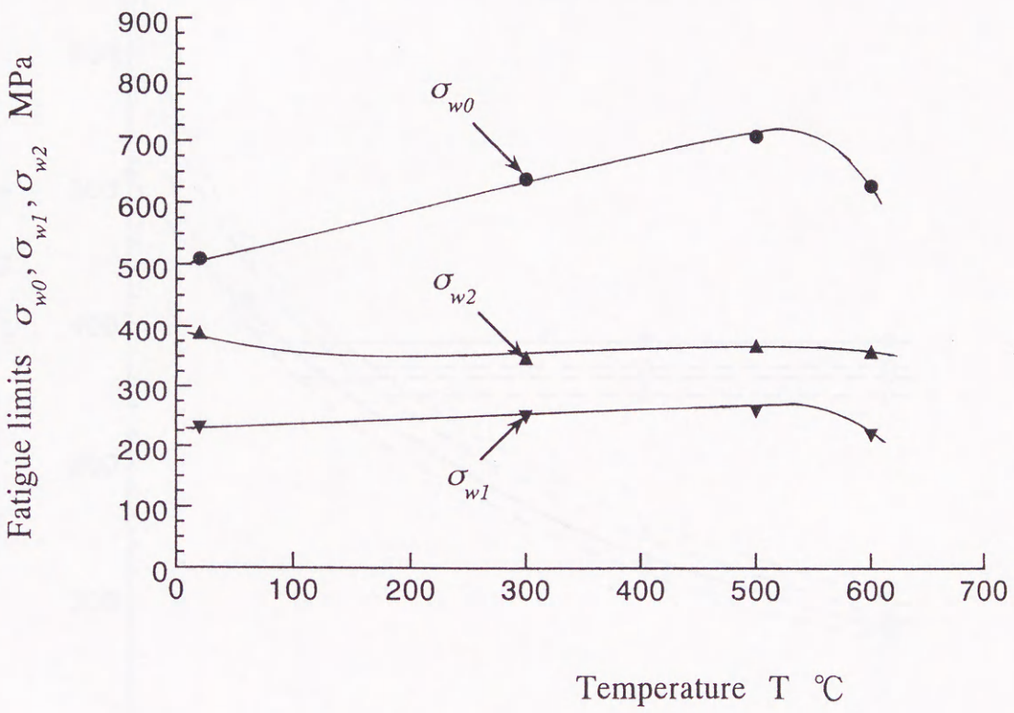

Fig. 5.5 Dependance of fatigue limits on the temperature.

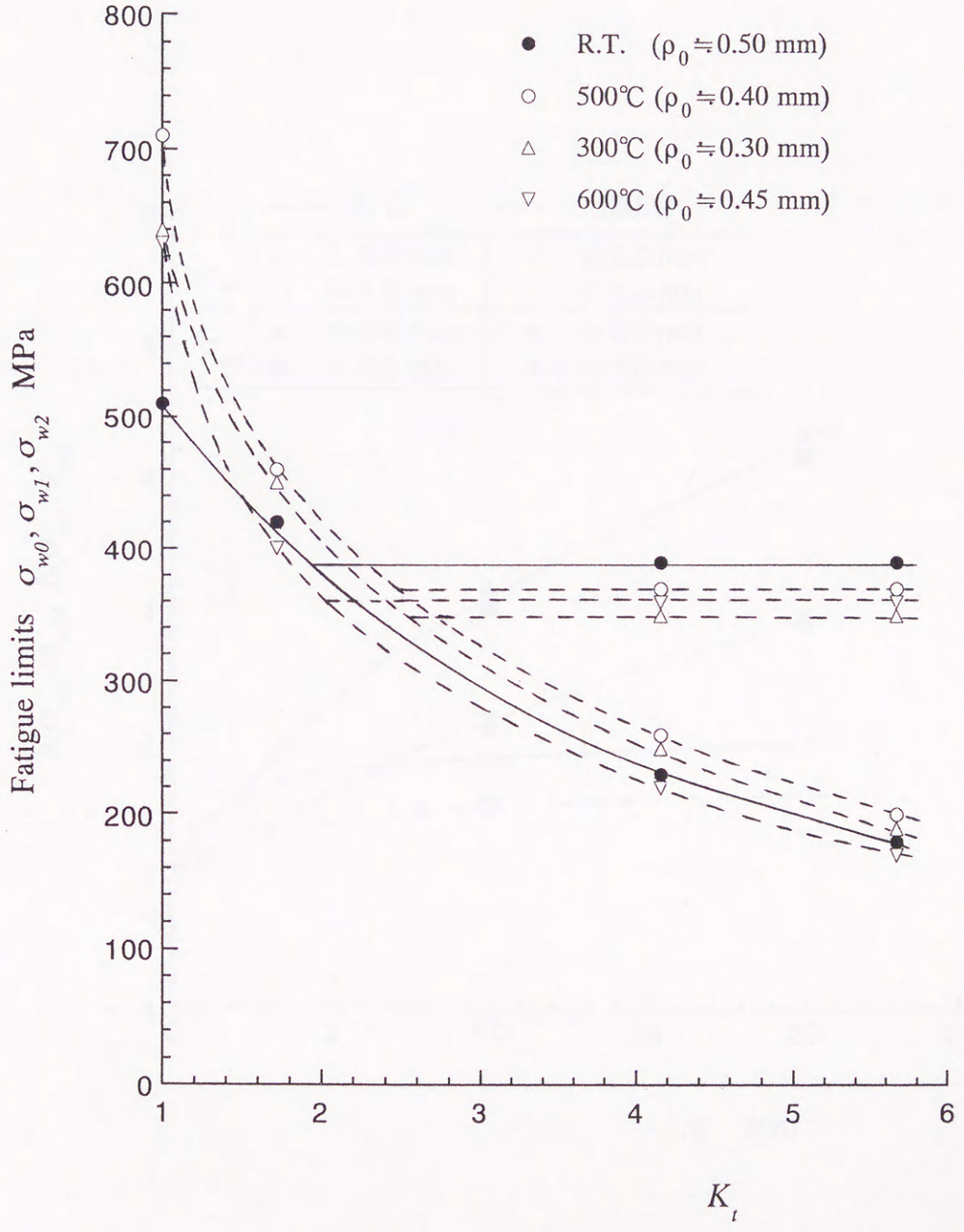

Fig. 5.6 Relation between the fatigue limits and the stress concentration factor (t = 0.5 mm).

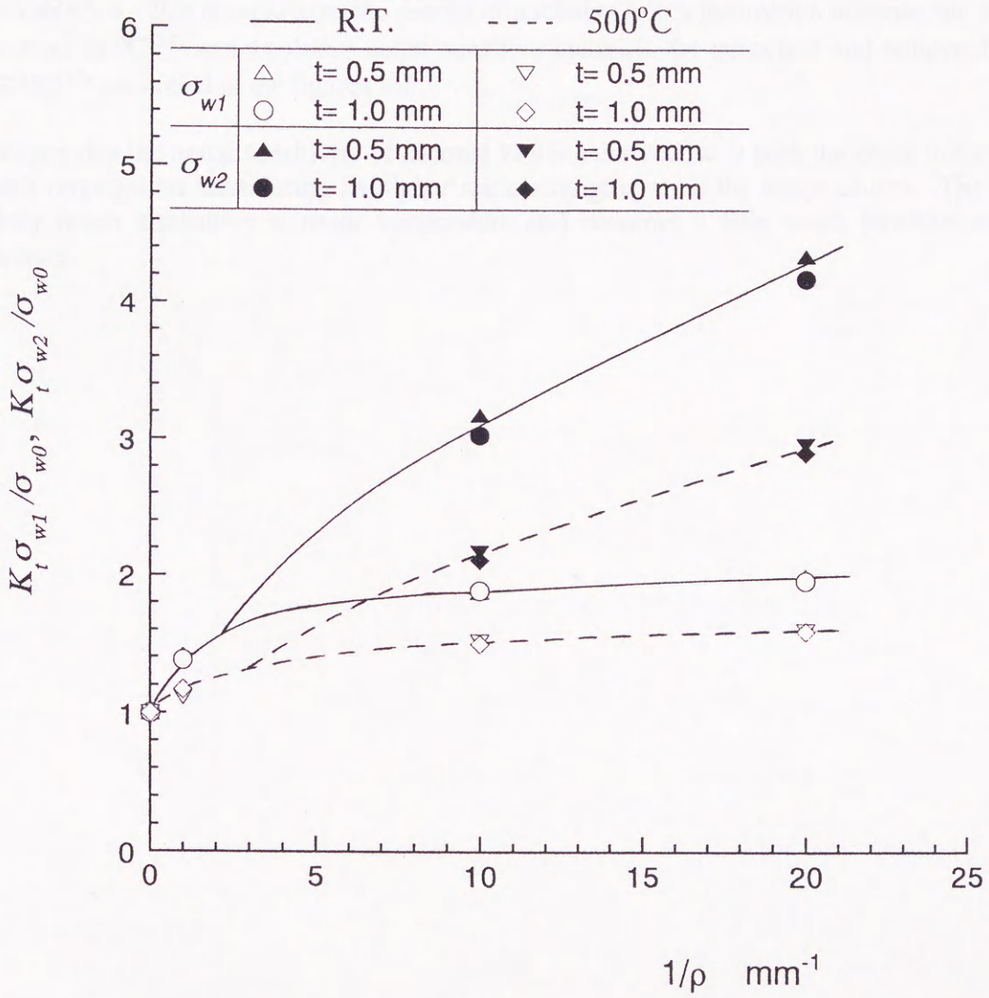

Fig. 5.7 Applicablity of LNM at room temperature and 500°C.

It is clear that the fatigue limits of notched specimens can be evaluated uniquely by the maximum stress σ_{max} (= $K_t\sigma_{w1}$ or $K_t\sigma_{w2}$) and the notch radius of ρ at each temperature, independent of the notch depth, t. This confirms the validity of LNM at elevated temperature.

By the way, in Fig. 5.7 and the Figures those follow, a lower value in the stress ratio of $K_t\sigma_{w1}/\sigma_{w0}$ or $K_t\sigma_{w1}/\sigma_{w0}$ means a higher notch sensitivity and the reverse is the same.

Figures 5.8 and 5.9 show the notch sensitivities at crack initiation and crack propagation in Inconel 718 at all the temperatures respectively, depending on the data at the notch depth of t = 0.5 mm in Table 5.4. For comparison, the results of a relative notch insensitive material: the annealed carbon steel S10C[14] and a relative notch sensitive material: the quenched and tempered carbon steel S50C[15] are dotted in the figures too.

It is seen that the notch sensitivity of Inconel 718 is relative low at both the crack initiation and the crack propagation considering its higher static strengths at all the temperatures. The alloy is especially notch insensitive at room temperature and becomes a little notch sensitive at higher temperature.

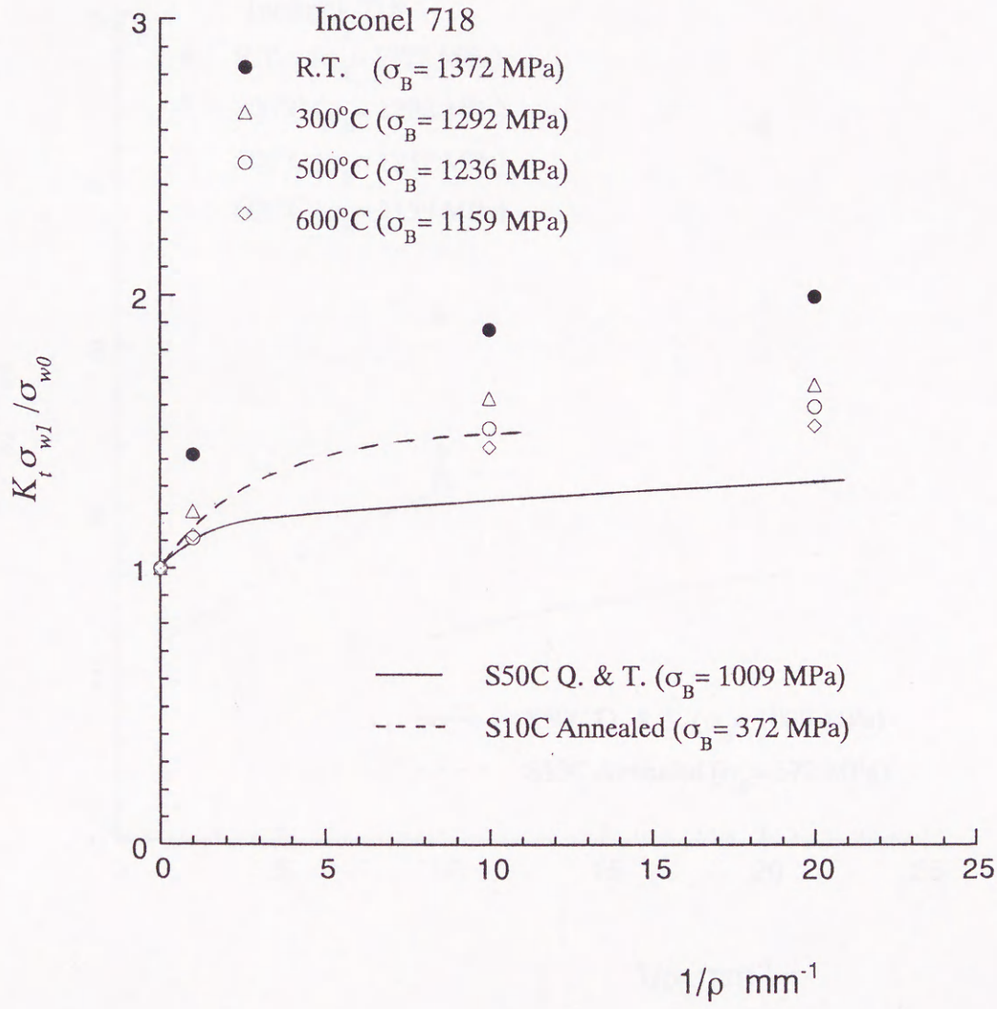

Fig. 5.8 Evaluation of notch sensitivity to crack initiation based on LNM at all the temperatures.

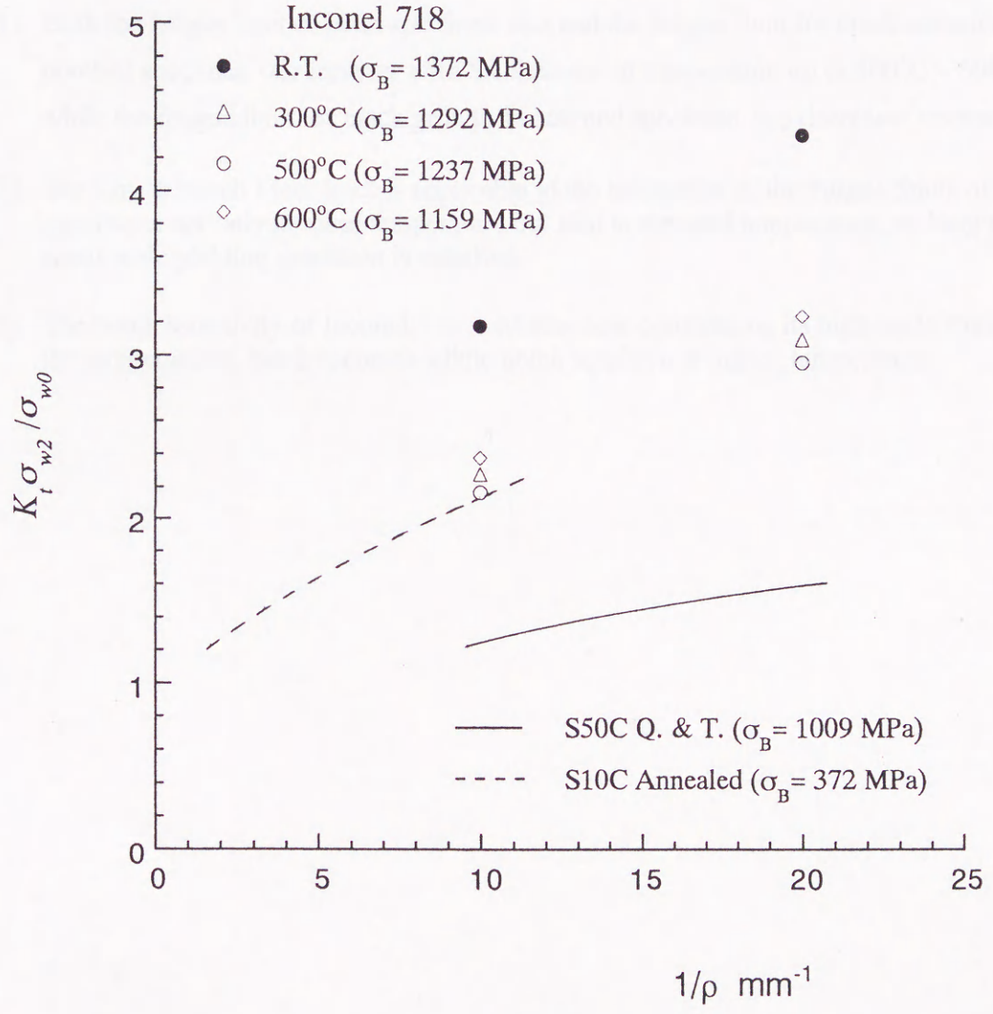

Fig. 5.9 Evaluation of notch sensitivity to crack growth based on LNM at all the temperatures.

5.4 Conclusions

The fatigue strength of notched specimen and the influence of temperature on the notch sensitivity of Inconel 718 was investigated at room temperature and the elevated temperatures. Following results are concluded.

(1) Both the fatigue limit of plain specimen σ_{w0} and the fatigue limit for crack initiation in notched specimen σ_{w1} increase with the increase of temperature up to 500°C ~ 600°C while the fatigue limit for crack growth in notched specimen σ_{w2} decreases reversely.

(2) The Linear Notch Mechanics is applicable to the estimation of the fatigue limits of notched specimens not only at room temperature but also at elevated temperature, so long as the small scale yielding condition is satisfied.

(3) The notch sensitivity of Inconel 718 is relative low considering its high static strength at all the temperatures, but it becomes a little notch sensitive at higher temperature.

References

(1) Hasegawa, E., *Trans. Jpn Soc. Mech. Eng.*, (in Japanese), **61**-588, A (1995), pp. 1707-1712.

(2) Yoshiba, M., *Trans. Jpn Soc. Mech. Eng.*, (in Japanese), **50**-456, A (1984), pp. 1443-1452.

(3) Korth, G.E. and Smolic, G.R., "Status of physical and mechanical test data of Alloy 718", *TREE*-**1254**, March 1978, pp. 1-81.

(4) Van Stone, R.H., *Mater. Sci. Eng.*, A**130** (1988), pp. 49-61,

(5) Kawagoishi, N., et al., *Trans. Jpn Soc. Mech. Eng.*, (in Japanese), **62**-596, A (1996), pp. 960-965.

(6) Kawagoishi, N., et al., *Proc. of 1996 Annual Meetings of JSME/MMD*, Vol. B, pp. 21-22.

(7) Nisitani, H., *Trans. Jpn Soc. Mech. Eng.*, (in Japanese), **48**-447, A (1983), pp. 1353-1359.

(8) Kawagoishi, N., et al., *Trans. Jpn Soc. Mech. Eng.*, (in Japanese), **56**-521, A (1990), pp. 10-14.

(9) Nisitani, H., et al., *Trans. Jpn Soc. Mech. Eng.*, (in Japanese), **55**-520, A (1989), pp. 2382-2387.

(10) Nisitani, H., et al., *Trans. Jpn Soc. Mech. Eng.*, (in Japanese), **54**-503, A (1988), pp. 1293-1297.

(11) Nisitani, N. & Noda, N., *Engng Fracture Mech.*, Vol.**20**, No.5, 1984, pp. 743-766.

(12) Kawagoishi, N., et al., *Trans. Jpn Soc. Mech. Eng.*, (in Japanese), **63**-615, A (1997), pp. 2298-2302.

(13) Kanazawa, K. & Nishijima, S., *Trans. Japan Society of Materials Science*, **46**-531 (1997), pp. 1396-1401.

(14) Nisitani, H. & Nishida, S., *Trans. Jpn Soc. Mech. Eng.*, (in Japanese), **35**-280, A (1969), pp. 2310-2315.

(15) Nisitani, H. & Chishiro, I., *Trans. Jpn Soc. Mech. Eng.*, (in Japanese), **40**-329, A (1974), pp. 41-52.

Chapter 6 Influence of CBN grinding on the fatigue strength

6.1 Introduction

Recently, Cubic Boron Nitride (CBN) grinding technology has been extensively applied for the machining of high strength alloys including Inconel 718 which is known as one of such difficult-to-machine materials because of its high hardenability, less thermal conductivity, high chemical reactivity with tools and the containment of hard carbides. CBN abrasive has many excellent properties such as the extremely high hardness that is second to the diamond, the high heat resistance and the inactivity with Ferrite, and most of all it can be manufactured at a moderate price. Many studies indicated that CBN wheel is superior to the general abrasive wheels in many ways: machinability, grinding efficiency, tool life as well as surface integrity of workpieces, the latter is considered to affect the fatigue property of materials[(1)-(3)].

On the other hand, CBN grinding generally induces a compressive residual stress in the worked surface region, which is considered to be contributive to the increase of fatigue strength, so that CBN grinding could be an excellent machining process even from the viewpoint of material strength. Nevertheless, the study of the influence of CBN grinding on the fatigue strength of Inconel 718, especially its fatigue strength at elevated temperature, was rarely reported[(4)].

In chapter 6, rotating bending fatigue tests are carried out at both room temperature and 500°C. The results of CBN ground specimens are compared with those of electro-polished and emery paper polished specimens. The influence of CBN grinding on the fatigue strength of Inconel 718, especially the fatigue strength at elevated temperature, is investigated from the viewpoints of residual stress, surface roughness and hardness in the ground layer.

6.2 Material and experimental procedures

The material used was Inconel 718 whose chemical composition and the mechanical properties at room and the elevated temperatures are the same as shown in Tables 2.1 and 3.1, respectively.

Figure 6.1 shows the shape and dimensions of specimen. A dull circumferential notch of 5 mm radius was made at the center of specimen. The notch was CBN ground directely or cut with a bite of 5 mm at radius, followed by electro-polishing to remove about 10 μm from surface.

CBN grinding was performed at 31 m/s of wheel velocity and 0.1 m/s of feed speed using a

CBN wheel CB170N75VN5GP (CB: CBN abrasive, 170: mesh size, N: grade, 75: concentration, V: vitrified bond, N5GP: symbol of specific bond, manufacturer: NORITAKE Co., Ltd) with an emulsion type coolant supplied. For some specimens, the notch was lightly scratched by two kinds of emery papers (120 and 600 mesh sizes) after electro-polishing in order to assess the effect of surface roughness on the fatigue strength.

The observation of fatigue damage in the CBN ground specimens was conducted directly under an optical microscope. The residual stress in the ground layers was detected using a X-ray diffraction device (XRD-6000 SHIMADZ, Cu-Kα ray, the wavelength λ = 1.54178Å, the angle of diffraction 2θ = 155.6° and the area of irradiation = 1x10 mm^2). The surface hardness was measured by a Vickers' micro durometer (AKASHI, load w = 50 g). The distributions of residual stress and hardness under the surface of specimens were investigated by removing off the surface layer at several μm after each measurement. The stress, σ_a, was defined as the nominal stress amplitude of net area.

The tests were carried out using the Ono-type rotating bending fatigue testing machines with a capacity of 15N·m operating at about 50 Hz for the tests at room temperature and 100N·m, 55 Hz at 500°C.

6.3 Results and discussion

6.3.1 Fatigue strength at room temperature

Figure 6.2 shows the *S–N* curves of both the electro-polished and CBN ground specimens at room temperature. The fatigue strength of CBN ground specimen is much higher than that of electro-polished specimen. For instance, the fatigue limit of CBN ground specimen is 650 MPa while that of electro-polished specimen is 500 MPa, about 30 % up in the fatigue strength through CBN grinding. Therefore, CBN grinding is really an excellent machining process for Inconel 718 not only because the superior performance in machining but also from the viewpoint of the fatigue strength of the alloy.

6.3.2 Fatigue strength at elevated temperature

Figure 6.3 shows the *S–N* curves of electro-polished and CBN ground specimens at 500°C. The fatigue strength of CBN ground specimens is a little lower than that of electro-polished specimens under all the stress levels except near the fatigue limit, the fatigue limit of CBN ground specimen is nearly equal to or a little higher than that of electro-polished specimen.

6.3.3 Significance of fatigue limit in CBN ground specimens

Figure 6.4 shows the surface state of CBN ground specimen after the stress repetitions of 10^7 cycles at the fatigue limit of CBN ground specimen (σ_{w0} = 650 MPa). Non-propagating cracks are recognized among the ground flaws.

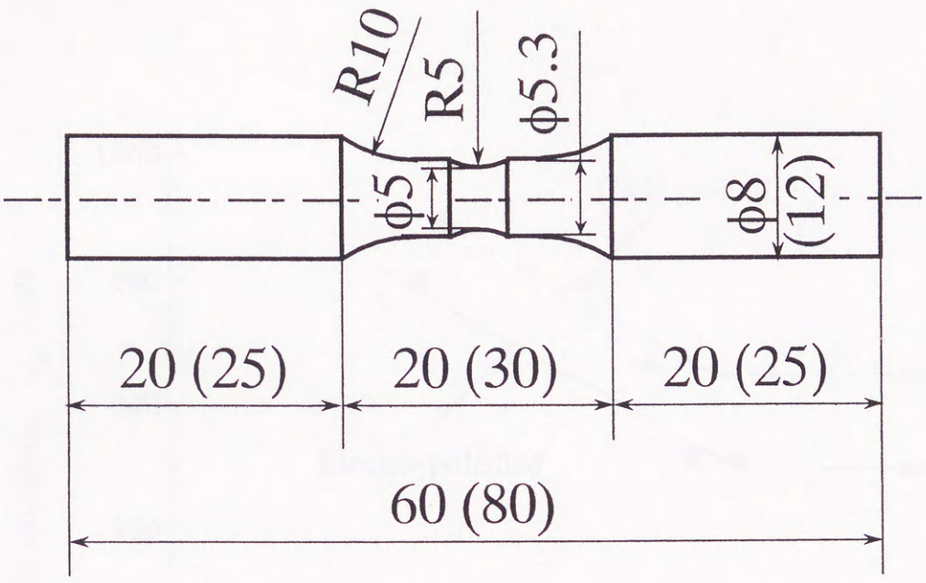

( ): For tests at elevated temperature

Fig. 6.1 Shape and dimensions of specimen (in mm).

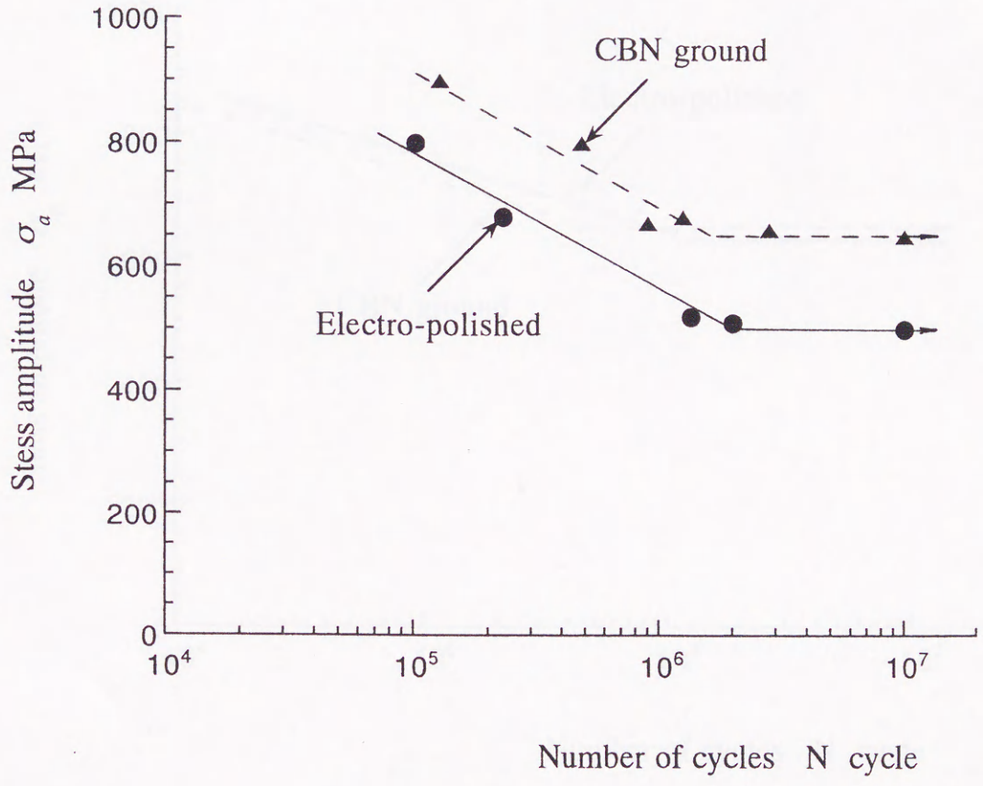

Fig. 6.2 *S–N* curves at room temperature.

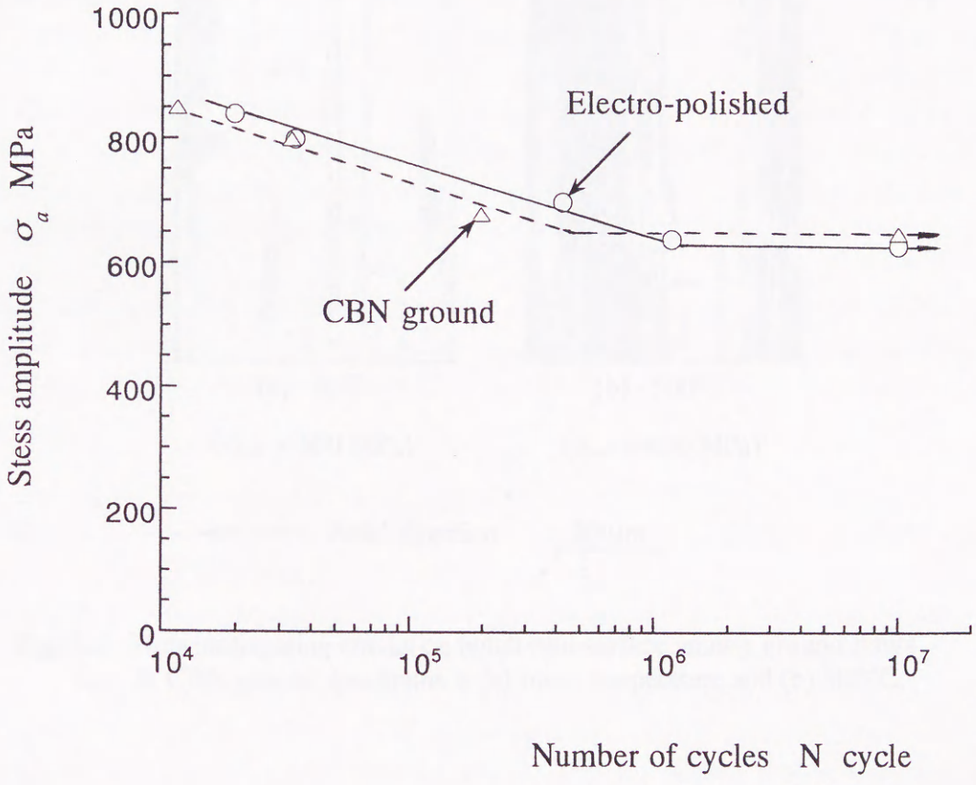

Fig. 6.3 *S–N* curves at 500°C.

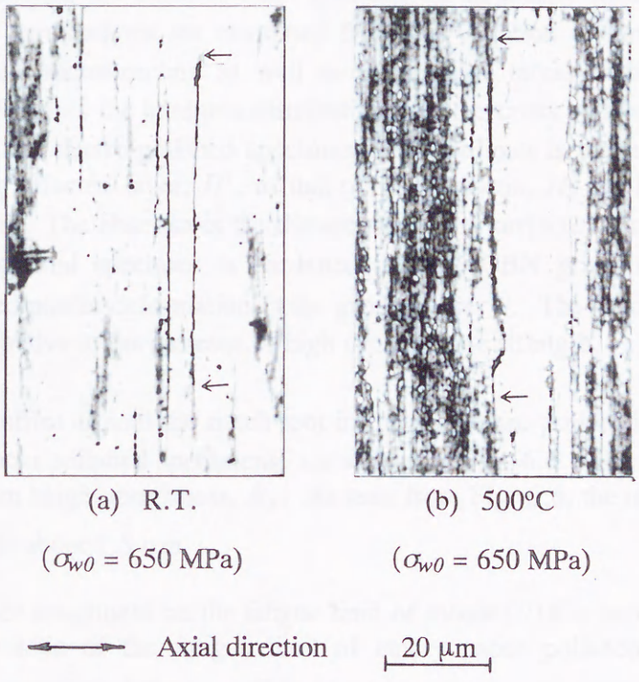

Fig. 6.4 Non-propagating cracks on notch root surface among ground flaws in CBN ground specimens at (a) room temperature and (b) 500°C.

Although the detailed observation is necessary for the crack initiation and crack propagation in CBN ground specimens, it may be concluded that the fatigue limit of CBN ground specimen is similarly determined by the limiting stress for crack growth as that of electro-polished specimen (chapter 3), considering the fact that non-propagating cracks was recognized in the emery paper polished specimens[5].

6.3.4 Discussion

In the following discussion, the effect of CBN grinding on the fatigue strength of the alloy at both room and elevated temperatures are examined from the variation of hardness and surface roughness, the change of microstructure as well as the residual stress generated in the CBN ground layer. Figure 6.5 shows the hardness distribution over the cross section beneath the notch root in the CBN ground and electro-polished specimens. The ordinate is the ratio of the hardness measured in the grinding affected layer, H', to that of inner matrix, H, the latter is almost not affected by CBN grinding. The abscissa is the distance from the surface. It can be seen that the surface layer of CBN ground specimen is hardened through CBN grinding, which may be explained by the remarked plastic deformation in the ground layer[6]. The hardened surface layer is considered to be contributive to the increase of high cycle fatigue strength.

The typical surface profiles around the notch root in the (a) electro-polished, (b) CBN ground and (c) and (d) emery paper polished specimens, are shown in Fig. 6.6. The surface roughness referred to is the maximum height roughness, R_y. As seen from Fig. 6.6, the mean value of R_y in CBN ground specimens is about 1.5 μm.

The influence of surface roughness on the fatigue limit of Inconel 718 is shown in Fig. 6.7, in which m designates the ratio of the fatigue limit of emery paper polished or CBN ground specimens (σ_{wPP} or σ_{wCBN}) to that of electro-polished specimens ($\sigma_{w\,EP}$). As can be seen from the results of emery paper polished specimens in which the machining effect was extremely eliminated and can be overlooked except for the effect of surface roughness, that the decrease of fatigue limit caused by surface flaws is too little to be mentioned within the range of $R_y < 2$ μm. This means that the influence of surface roughness on the fatigue strength of CBN ground specimens is very small at the present CBN grinding condition, i.e. ($R_y \approx 1.5$ μm). Similar results[7] were obtained for Inconel 718 at elevated temperature as well, though the chemical composition of the alloy is a little different.

It is known that a tensile residual stress is usually resulted in the conventional abrasive grinding, while reversely in CBN grinding, a compressive residual stress is usually generated in the ground surface layer[3],[4],[6]. Figure 6.8 shows the change of residual stress distribution over the cross section beneath the notch root of CBN ground specimen (a) before and (b) after heating at 500°C for one hour under zero load condition are illustrated. The compressive residual stress is generated in the surface layer of CBN ground specimen, with the minimum compressive residual stress appears on the outer side.

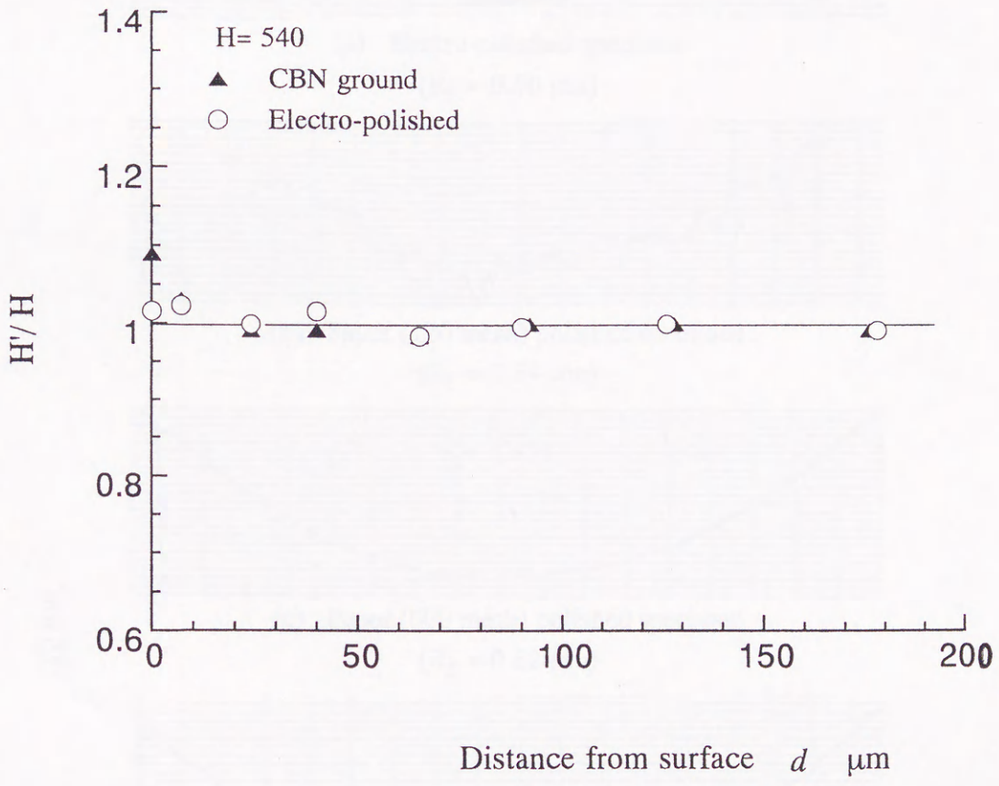

Fig. 6.5 Distribution of hardness over the cross section beneath the notch root in CBN ground and electro-polished specimens.

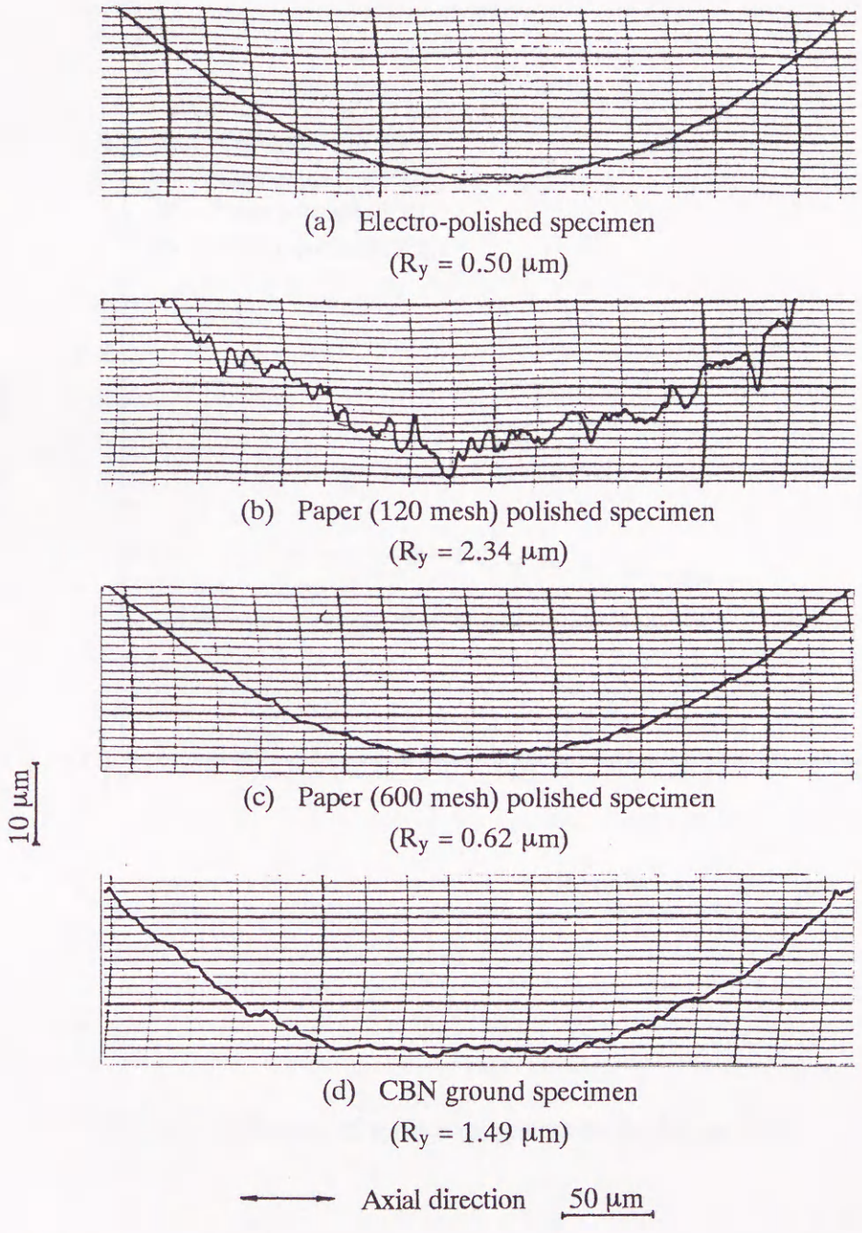

Fig. 6.6 Typical surface profiles around the notch root in (a) electro-polished, (b) and (c) emery paper polished and (d) CBN ground specimens.

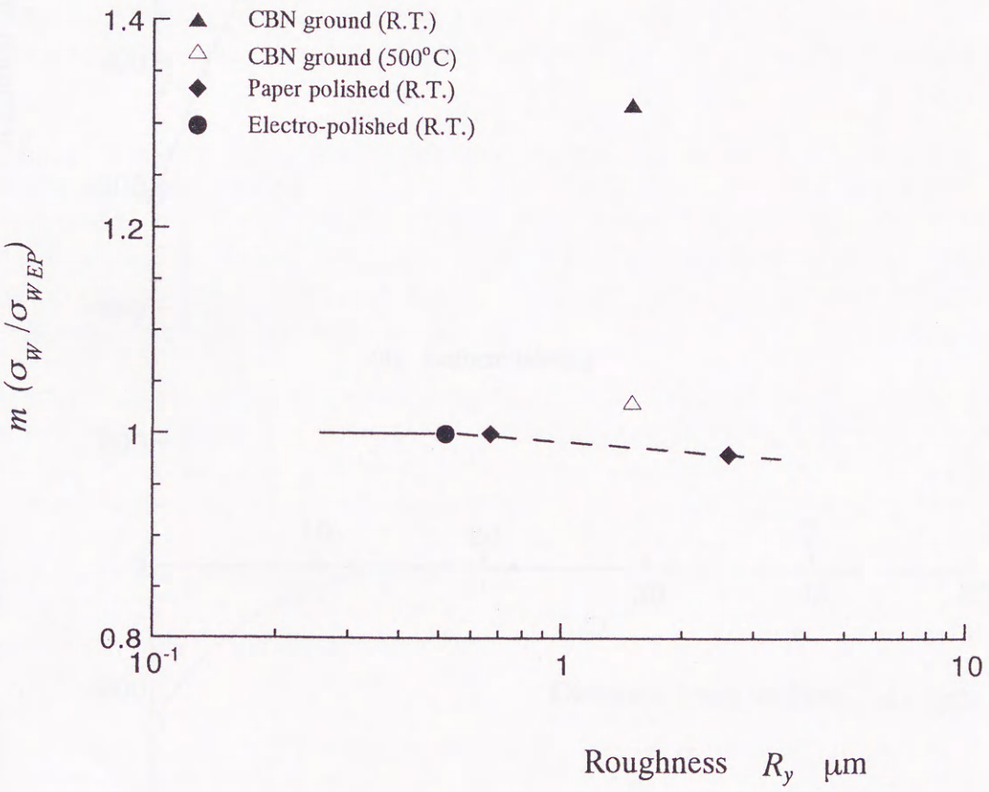

Fig. 6.7 Influence of surface roughness on the fatigue limit.

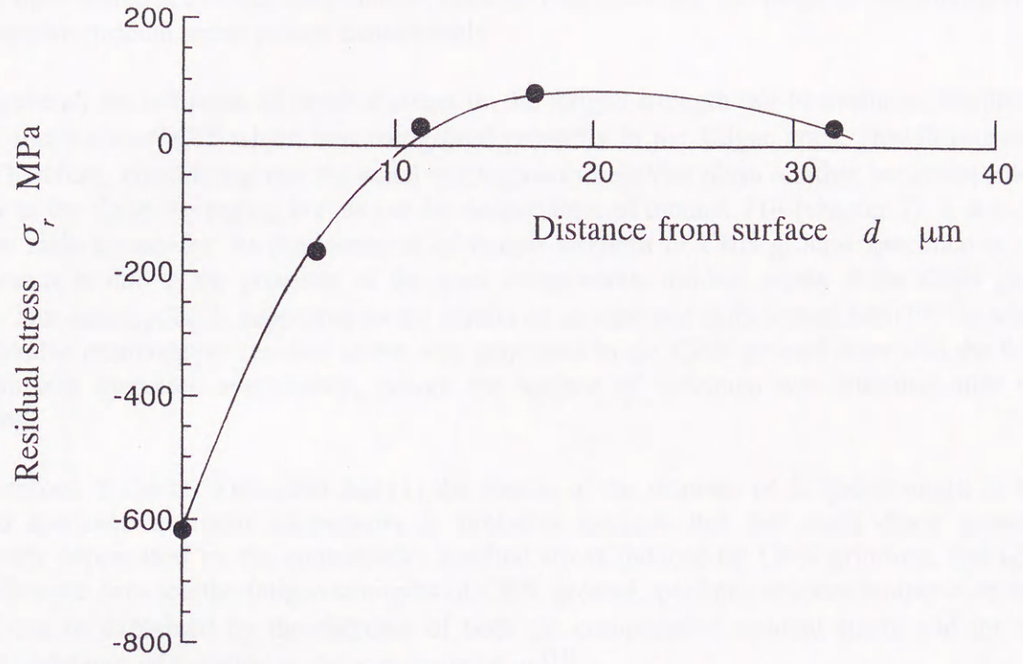

(a) Beforre heating

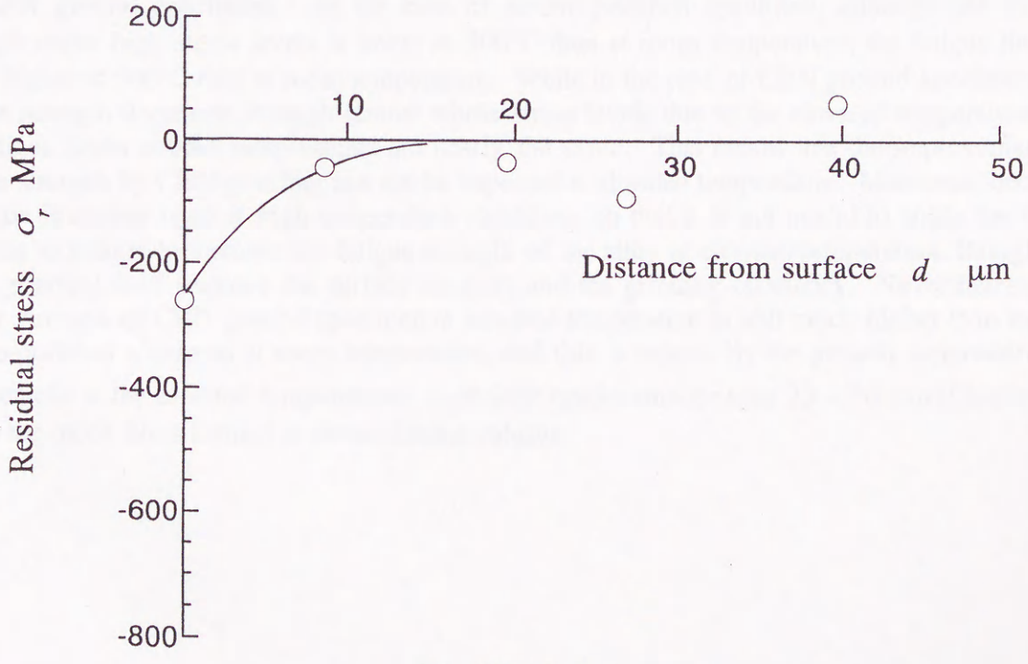

(b) After heating

Fig. 6.8 Change of residual stress distribution over the cross section beneath the notch root (a) before and (b) after heating at 500°C (CBN ground specimen).

But once heated at elevated temperature, both the magnitude and the range of distribution of the compressive residual stress reduce considerably.

In general, the influence of residual stress on the fatigue strength can be evaluated similarly as that of mean stress[8]~[10] which was recognized primarily in the fatigue crack growth process[11], [12]. Therefore, considering that the small crack growth behavior plays a rather important role not merely in the finite life region but also at the fatigue limit of Inconel 718 (chapter 3), it is evident that the main reason for the improvement of fatigue strength of CBN ground specimen at room temperature is due to the presence of the great compressive residual stress in the CBN ground layer. This assumption is supported by the results of an annealed carbon steel S45C[13] in which a considerable compressive residual stress was generated in the CBN ground layer and the fatigue strength was increased remarkably, though the surface of specimen was softened after CBN grinding.

Therefore, it can be concluded that (1) the reason of the increase of fatigue strength in CBN ground specimen at room temperature is probably because that the small crack growth is effectively suppressed by the compressive residual stress induced by CBN grinding, and (2) the big difference between the fatigue strengths of CBN ground specimen at room temperature and at 500°C can be explained by the decrease of both the compressive residual stress and the crack growth resistance of the alloy at elevated temperature[14].

Figure 6.9 shows the effect of temperature on the fatigue strength of (a) electro-polished and (b) CBN ground specimens. In the case of electro-polished specimen, although the fatigue strength under high stress levels is lower at 500°C than at room temperature, the fatigue limit is much higher at 500°C than at room temperature. While in the case of CBN ground specimen, the fatigue strength decreases through almost whole stress levels due to the elevated temperature and the fatigue limits at both temperatures are nearly the same. This means that the improvement of fatigue strength by CBN grinding can not be expected at elevated temperature. Moreover, because the alloy is mainly used at high temperature condition, so that it is not useful to apply the CBN grinding technique to increase the fatigue strength of the alloy at elevated temperature, though the CBN grinding does improve the surface integrity and the grinding efficiency. Nevertheless, the fatigue strength of CBN ground specimen at elevated temperature is still much higher than that of electro-polished specimen at room temperature, and this is caused by the growth suppression of small cracks at the elevated temperatures, especially cracks smaller than 20 ~ 30 μm (Chapter 3), due to the oxide films formed at elevated temperatures.

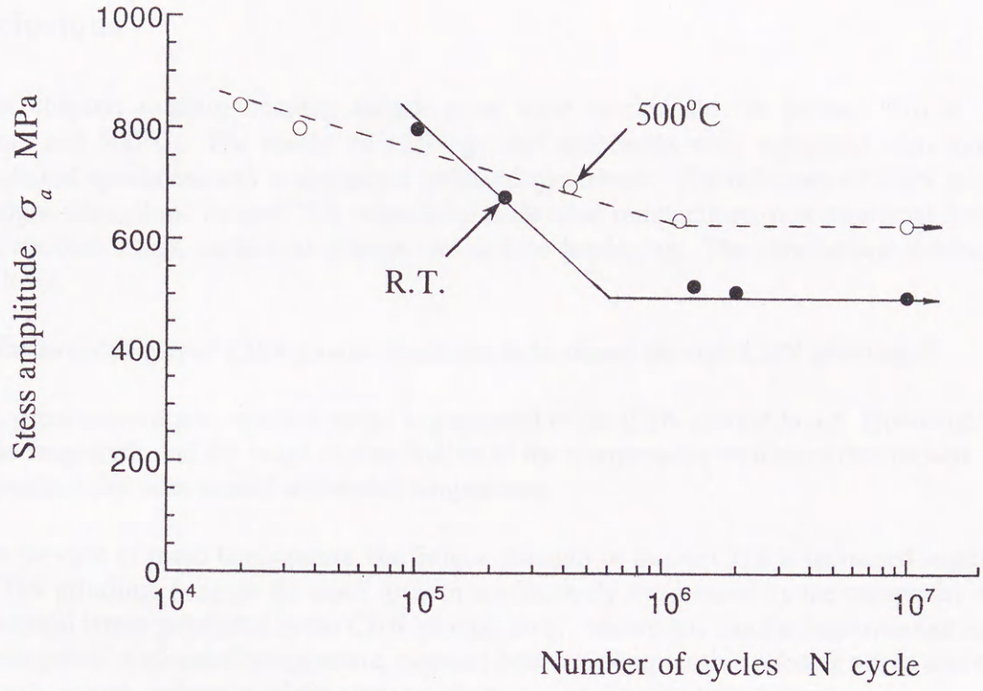

(a) Electro-polished specimen

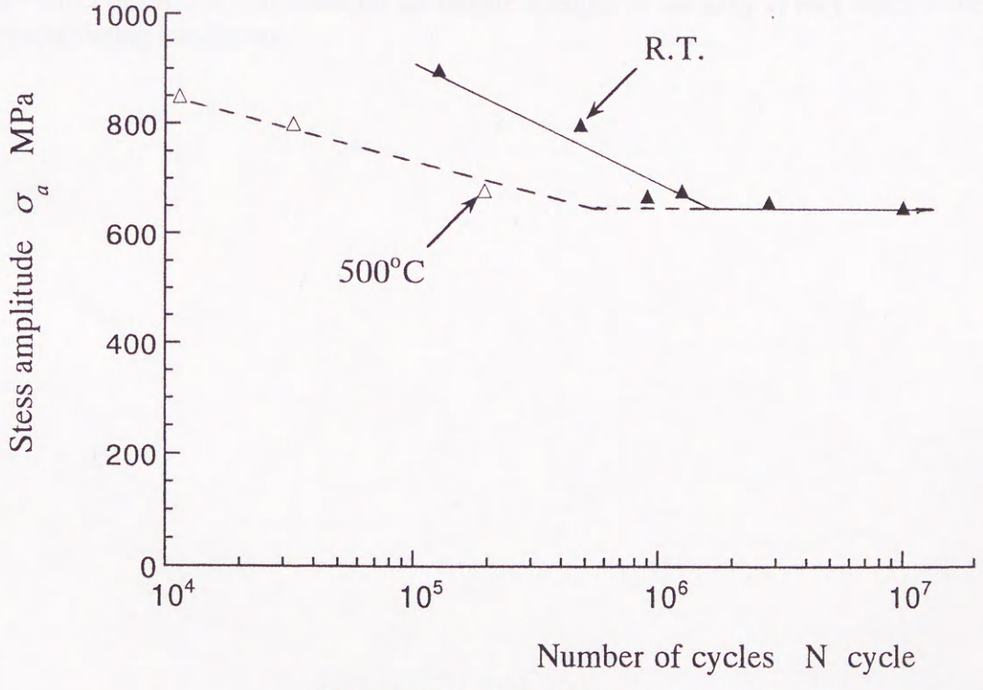

(b) CBN ground specimen

Fig. 6.9 *S–N* curves of (a) electro-polished and (b) CBN ground specimens.

4 Conclusions

In this chapter, rotating bending fatigue tests were carried out on Inconel 718 at room temperature and 500°C. The results of CBN ground specimens were compared with those of electro-polished specimens and emery paper polished specimens. The influence of CBN grinding on the fatigue strength of Inconel 718, especially at elevated temperature, was examined from the effects of residual stress, surface roughness and surface hardening. The conclusions obtained are in the follows.

(1) The surface layer of CBN ground specimen is hardened through CBN grinding.

(2) A great compressive residual stress is generated in the CBN ground layer. However, both the magnitude and the range of distribution of the compressive residual stress reduce considerably after heated at elevated temperature.

(3) In the case of room temperature, the fatigue strength of Inconel 718 is increased largely by CBN grinding, because the crack growth is effectively suppressed by the compressive residual stress generated in the CBN ground layer. However, similar improvement is not recognized at elevated temperature, because both the compressive residual stress and the crack growth resistance of the alloy are decreased at elevated temperature.

(4) The effect of surface roughness on the fatigue strength of the alloy is very small in the present testing conditions.

References

(1) Tonshoff, H. K., & Hetz, F., Influence of the abrasive on fatigue in precision grinding, *ASME PED*, 1985, **16**, pp. 20-25.

(2) Kumagai, N., *J. Jpn Soc. Mech. Eng.*, (in Japanese), **58** (1992), pp. 12-15.

(3) Ishikawa, T. & Kumar, K. V., *J. Japan Society of Precision Engineering*, (in Japanese), **58** (1992), pp. 597-600.

(4) Yokogawa, M. & Yokogawa, K., *J. Japan Society of Precision Engineering*, (in Japanese), **58** (1988), pp. 909-914.

(5) Nisitani, H. & Imai, R., *Trans. Jpn Soc. Mech. Eng.*, (in Japanese), **49**-442, A (1983), pp. 693-698.

(6) Kumagai, N., *Publications of the 14th Special Committee for the grinding of difficult-to-cut materials*, (Edited by Japan Society of Precision Engineering), (in Japanese), 1993, pp. 1-10.

(7) Kawagoishi, N., et al., *Prepr. Jpn Soc. Mech. Eng.*, (in Japanese), No. **978**-2 (1997), pp. 43-45.

(8) Taira, S. & Murakami, H., *J. Japan Society for Testing Materials,* (in Japanese), **10** (1961), pp. 610-615.

(9) Kodama, S., *J. Jpn Soc. Mech. Eng.*, (in Japanese), **75** (1972), pp. 1026-1033.

(10) Kodama, S., *J. Japan Society of materials Science*, (in Japanese), **26** (1977), pp. 56-61.

(11) Nisitani, H. & Yamashita, N., *Trans. Jpn Soc. Mech. Eng.*, (in Japanese), **32** (1966), pp. 1456-1461.

(12) Nisitani, H. & Goto, *Trans. Jpn Soc. Mech. Eng.*, (in Japanese), **50**-460, A (1984), pp. 1926-1935.

(13) Kawagoishi, N., et al., *Trans. Jpn Soc. Mech. Eng.*, (in Japanese), **62**-596, A (1996), pp. 960-965.

(14) Kawagoishi, N., et al., *Trans. Jpn Soc. Mech. Eng.*, (in Japanese), **63**-615, A (1997), pp. 2298-2302.

Chapter 7 Summary

Rotating bending fatigue tests were carried out at room temperature and the elevated temperatures of 300°C, 500°C and 600°C in order to investigate the high cycle fatigue properties of nickel-base superalloy Inconel 718 at elevated temperatures.

The behavior of small fatigue cracks and the fatigue damage on the surface of specimens were observed successively under an optical microscope using the plastic replica method or directly under scanning electron microscope. The influence of temperature on the fatigue properties of Inconel 718 was examined in terms of the initiation and propagation behavior of small fatigue cracks, the fatigue strength including the fatigue limit, the resistance to small crack growth as well as the notch sensitivity by comparing the results at elevated temperatures with those at room temperature. The results were discussed from the competition between the softening of matrix and the surface oxidation of specimens at elevated temperatures.

Because Inconel 718 is difficult to machine using conventional machining tools and CBN grinding is proved to be useful for the machining of Inconel 718, so that the effect of CBN grinding on the fatigue strength of Inconel 718, especially the fatigue strength at elevated temperatures, was also investigated from the viewpoints of residual stress, surface roughness and work-hardening in the surface region of specimens through the comparison of the fatigue strength of CBN ground specimens with those of electro-polished specimens and emery paper polished specimens.

The conclusions obtained can be drawn as the follows.

(1) At all the temperatures, a small fatigue crack in a plain specimen usually initiates from slip bands near a grain boundary in the early stage of stress repetitions, then propagates transgranularly accompanied with the formation of striations. Most of fatigue life in a plain specimen is occupied by the growth life of cracks smaller than 1 mm. However, the influence of temperature on the mechanism of both small fatigue crack initiation and its propagation is not recognized.

(2) At the fatigue limit of plain specimens, the major small fatigue crack in a plain specimen is arrested from further propagating and becomes a non-propagating crack after growing up to about 20~30 μm on the specimen surface, irrespective of the temperature. This means that the fatigue limit of a plain specimen is determined by the limiting stress for small crack growth instead of that for small crack initiation, at all the temperatures.

(3) Owing to the oxide films formed on the surface of specimens at elevated temperatures, the

initiation and the early propagation of the small fatigue crack, especially at the length of 20~30 μm, are suppressed at elevated temperatures. The suppression of small fatigue crack growth is more remarked at high temperature and under low stress level. For this reason and the fact that most of fatigue life in a plain specimen is occupied by the growth life of small cracks, especially at elevated temperatures about 90 % of the growth life of small cracks is spent in the growth process for a initiated small fatigue crack to grow up to 20~30 μm, the fatigue strength of plain specimens, except for that in the short life region, increases with the increase of temperature. This increase of fatigue strength can be seen more clearly at the fatigue limit of plain specimens, at which the fatigue limit of plain specimens is much higher at elevated temperatures than at room temperature with the peak value of fatigue limit appears between 500°C~600°C.

The suppression of small fatigue crack growth can be explained as a result of the intensified oxide-induced crack closure effect and the compressive residual stress generated on the surface of matrix due to the big difference in coefficient of thermal expansion between the matrix and the oxides formed on the specimen surfaces.

(4) On the other hand, owing to the softening of matrix, the initiation and propagation of the small fatigue crack are promoted at the elevated temperatures. For this reason, at high temperature, the small fatigue crack tends to initiate earlier and grows faster after growing longer than 50 μm. The fatigue strength of all the specimens including plain, drilled and notched specimens decreases monotonously with the increase of temperature in their short life regions. The fatigue crack growth resistance decreases with the increase of temperature too, even the degeneration of static strength of the alloy at elevated temperatures is considered.

(5) Consequently, it can be concluded that the elevated temperature affects the initiation and propagation of the small fatigue crack in two contradictory ways, one is the acceleration action due to the softening of matrix and the other is the suppression action due to the formation of oxide films on the surface of specimen. Which action is dominant will depend on the temperature and the stress levels.

(6) At all the temperatures, the crack growth rate of the small fatigue crack can be evaluated by Paris' law, $dl/dN = C\Delta K^m$ (C and m: constants), under low stress levels (e.g. $\sigma_a/\sigma_{0.2} < 0.5$) or by small crack growth law, $dl/dN = C_1\sigma_a{}^n l$ (C_1 and n: constants), under high stress levels (e.g. $\sigma_a/\sigma_{0.2} > 0.6$). In the present study, constant n takes almost the same value of 5 at all the temperatures, indicating that the stress dependence of fatigue crack growth rate under high stress levels at each temperature is similar to each other. Considering that nearly all of the fatigue life of a specimen was occupied by the growth life of the small fatigue crack, these consist the reason why the inclinations of *S–N* curves of drilled specimens at all the temperatures and that of plain specimens at room temperature are almost the same, in the short life region.

(7) Both the fatigue limit of plain specimen σ_{w0} and the fatigue limit for crack initiation in notched specimens σ_{w1} increases with the increase of temperature up to 500°C~ 600°C, however, the fatigue limit for crack growth in notched specimens σ_{w2} decreases slightly at elevated temperatures. The fatigue limits of notched specimens, i.e. σ_{w1}, σ_{w2}, can be estimated by the

Linear Notch Mechanics not only at room temperature but also at elevated temperatures, so long as the small scale yielding condition is satisfied. The notch sensitivity of Inconel 718 is relative low considering its high static strength at all the temperatures, but it becomes a little more notch sensitive at elevated temperatures than at room temperature.

(8) The fatigue strength of Inconel 718 was increased largely at room temperature by means of CBN grinding because the small fatigue crack growth is effectively suppressed by the compressive residual stress generated in the CBN ground layer. However, similar improvement in fatigue strength is not recognized at elevated temperatures because both the compressive residual stress and the fatigue crack growth resistance decreases at elevated temperatures. The effect of surface roughness on the fatigue strength of Inconel 718 is very small in the present testing conditions.

Acknowledgments

I would like to express my gratitude to Dr. Norio KAWAGOISHI, professor with the Department of Mechanical Engineering, Faculty of Engineering, Kagoshima University, who kindly accepted me as his doctoral candidate in 1993 and has supervised me for almost 7 years with much patience. I am gratefully acknowledge to him not only for providing a number of sagacious and valuable instructions, offering many useful suggestions for the improvement of the dissertation, but also for giving always strict disciplines, and most importantly, encouragements that helped me to overcome many difficulties throughout the preparation of the dissertation. Without his tremendous helps, I could have never finished the dissertation before the end of 1999. Meanwhile, he is also a very good teacher and a cordial colleague, if I would be permitted, who affectted me in numerous ways through his every word and deed, from which I shall benefit all of my life. I am also thankful to him and to the Department of Mechanical Engineering, Faculty of Engineering, Kagoshima University, for having offered me the opportunity to prepare the dissertation while working as a research associate.

The grateful acknowledgements would be extended to Professors Hidekazu SUEYOSHI, Masayuki TOYA and Eiji KONDO, in the Department of Mechanical Engineering, Faculty of Engineering, Kagoshima University, for reviewing the entire manuscript and offering many valuable suggestions and constructive criticisms, which greatly assisted the technical accuracy and completeness of the dissertation. I am also thankful to Dr. Hironobu NISITANI, professor with the Department of Mechanical Engineering, Faculty of Engineering, Kyushu Sangyou University, for supervising me throughout the preparation of the dissertation and offering many valuable suggestions. Thanks are due to Messrs. Ichiro MAENO, chief-researcher, and Junichi KIYOFUJI, the head of Kagoshima Prefectural Institute of Industrial Technology, and to Mr. Yoshihisa OZONO, technician with the Department of Electric and Electronic Engineering, for granting the permission to include the results of tests conducted on a number of co-authored papers. I am indebted to Dr. Hiroshi OKADA, associated professor, Mr. Simon Szeman CHAN, doctoral candidate, both with the Department of Mechanical Engineering, and to Dr. Katta VENKATARAMANA, associated professor with the Department of Ocean Civil Engineering, Kagoshima University, who read portion of the dissertation and offered recommendations for its improvement. Dr. Yuzo NAKAMURA, associated professor with the Department of Mechanical Engineering, Kagoshima University, and Dr. Toshinobu TOYOHIRO, associated professor with the Department of Mechanical Engineering, Miyakonojyo National College of Industrial Technology, are much appreciated for providing helpful discussions.

I would like to take this opportunity to extend thanks to my former teacher and research supervisor, Dr. Hideo TANAKA, professor emeritus of Kagoshima University, now president of Sendai Polytech College, who provided me the 1992-1994 MONBUSHO Scholarship for foreign research students and introduced me to Professor KAWAGOISHI before his early retirement in 1996. I am grateful to him and his virtuous wife, Mrs. Sumiko TANAKA, for offering much concern and useful advises in all ways from child education to daily life, which secured me and my family a very pleasant and memorial abroad lives at Kagoshima.

Most of enlightened researches were contributed through the patient effort of many students who sojourned in the Laboratory of Machining and Strength of Materials, Department of Mechanical Engineering, Kagoshima University, and who searched with me in hot summer and cold winter for critical experiments and suffered a lot of defeats, or who laboriously accumulated

decisive data. I am gratefully acknowledged to them, particularly to Mr. Kenji SHIMANA, doctoral candidate, to Messrs. Tadahiko HIRAKAWA, Masaru ARIKAWA, Ryuji TAKADO and Youishi SETO, former postgraduates, and to Messrs. Hiroshi KAEDA, Shouzou MATSUNOSHITA, Hiroki TOMONAGA, Gou OHYAMA, Hideyou MORI, Masaki NAKANO, and Masato NOMURA, former graduates, for their assistance in conducting fatigue tests and preparing results in Chapters 2 to 6. Appreciation is expressed to my colleagues at the Faculty of Engineering, Kagoshima University, especially to Mr. Haruhisa TOMONO, technician with our laboratory, who provided many valuable suggestions and technical assistance through these years. I am also grateful to Messrs. Katsuo KIZUSHI, Mitsuhiro KURAUCHI, Akio KAMEDA, and Yoshikazu MAEDA, technicians with the Department of Mechanical Engineering, to Messrs. Hajime TAKAHASHI, Takeji ARIMA, Kenji YOSHINAGA, Shunichi YAMASHITA, Technicians with the Central Training Factory of the Faculty, to Mr. Wataru SAKAMOTO, technician with the Department of Bioscience Engineering, and to Mr. Terumi KAKOI, technician with the Laboratory of Electrical Microscopy, for their technical assistance in numerous ways.

Thanks are also due to the reviewers of the journals which published a number of my papers related to the dissertation. Special acknowledgements would be extended to Dr. Kentaro KOMAI, Associate editor for the Journal of International Journal of Fatigue, Dr. Masahiro KOIWA, Associate editor for the Journal of Materials Science and Technology A, and Dr. Yukitake MURAKAMI, Associate editor-in-Chief for the Journal of Fatigue and Fracture of Engineering Materials and Structures, and to the editors for the Transactions of Japan Society of Mechanical Engineers.

My wife, Fangping Wang, contributed much in companionship over a long period of years and helped in numerous ways in completing the dissertation, particularly offered great encouragements and much patience in the final preparation of the dissertation besides doing most of housework. I am thankful to her and our daughter, Jessie Chen, for many hours that should have been spent with them but were required in the preparation of the dissertation.

Qiang Chen

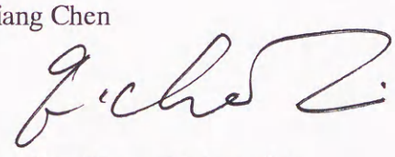

Eng. D., Research Associate
Kagoshima University
Faculty of Engineering
Department of Mechanical Engineering
Kagoshima
Japan

December 20, 1999

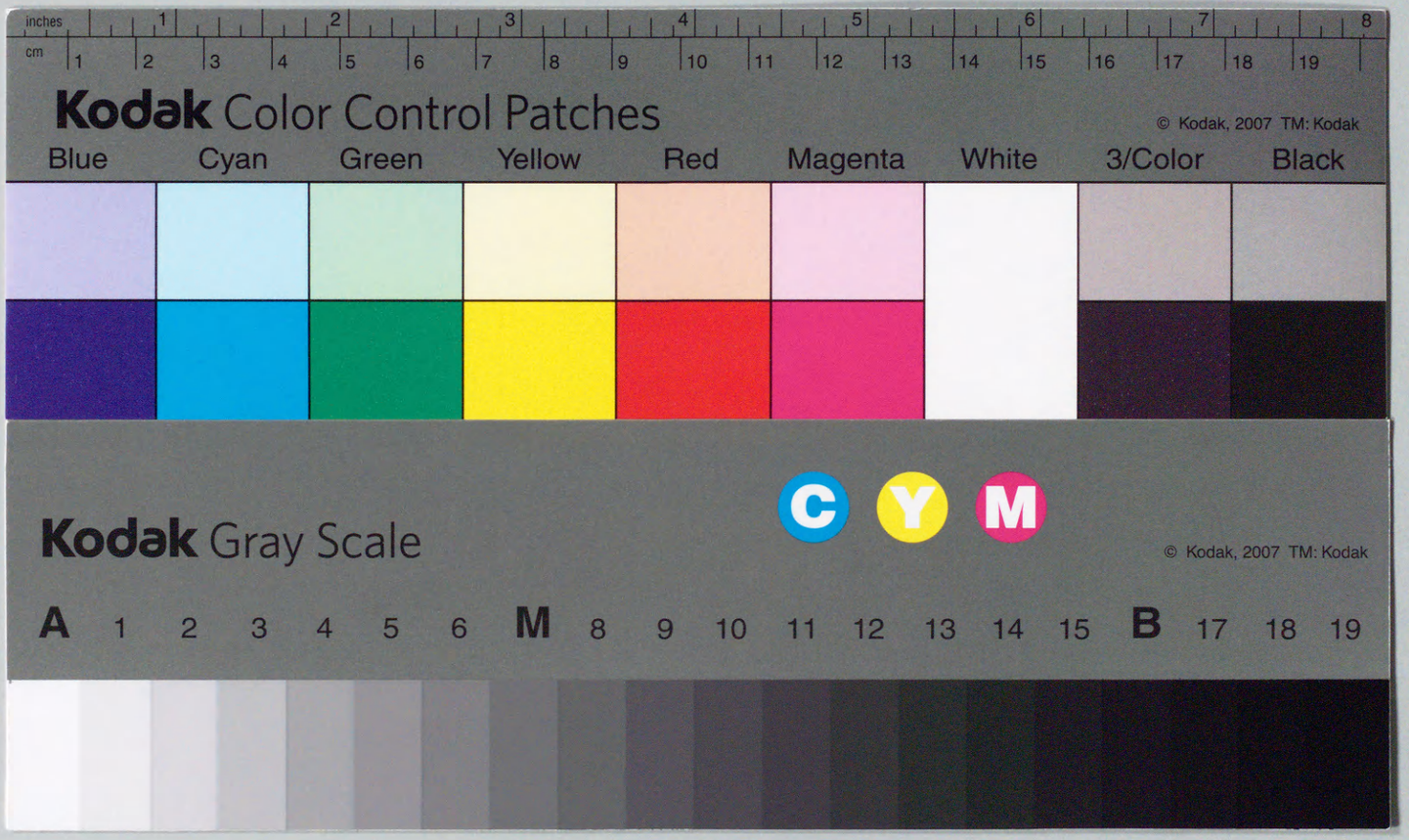
inches
cm
Kodak Color Control Patches
© Kodak, 2007 TM: Kodak
Blue
Cyan
Green
Yellow
Red
Magenta
White
3/Color
Black
Kodak Gray Scale
C
Y
M
© Kodak, 2007 TM: Kodak
A 1 2 3 4 5 6 M 8 9 10 11 12 13 14 15 B 17 18 19